Single-molecule Dynamics in Protein Interactions: Characterization of RarA and RecD2 of *Bacillus subtilis*

Fachbereich Chemie, Philipps Universität Marburg

Promotion dissertation

Doktoranden: Hector Romero Gonzalez
Geburtsort: Madrid (Spain)
Akademischer Titel: Master in Biochemistry, Molecular Biology and Biomedicine

Gutachter: Prof. Dr. Peter L. Graumann Dr. Juan C. Alonso Navarro
Prüfungkomission: Dr. Georg Fritz Prof. Dr. Norbert Hampp
Angenommen: 26.02.2018
Einreichungtermin: 12.03.2018
Prüfungtermin: 29.03.2018
Erscheinungsort Marburg **Erscheinungjahr:** 2018
Hochschulkenziffer 1180

Summary

Maintenance of genome integrity is one of the crucial functions in life, to preserve the appropriate genetic information, being homologous recombination a key process in the DNA repair. I have used a novel technique, using slim-field microscopy to obtain single-molecule dynamics of two poorly described proteins, RarA and RecD2, in different recombination deficient mutants and conditions to characterize them. Single-molecule microscopy has been shown as a powerful method for in vivo characterization of proteins and its interactions. Together with genetics, I have added a new level of complexity in the regulation of homologous recombination as a multiway process in which many factors are involved in different avenues with partially overlapping functions depending on the kind of DNA damage generated.

I have characterized RarA and RecD2 as factors involved in recombination, but also in replication of the DNA, being part of both RecA-independent and RecA-dependent replication progression, and antagonistic regulators of RecA filamentation. RarA plays its role in replication through interactions with DnaB, and in recombination as a RecA positive regulator through its interactions with RecA, RecO, RecR, RecD2 and RecU. RarA is regulated by the RecQ-like helicases RecQ and RecS. RecD2 plays a role in chromosomal segregation that becomes essential in the absence of RecG or RuvAB, and is a negative regulator in homologous recombination that interacts with RecA, RarA, RecX, RecF and PcrA.

Inhalt

Die Erhaltung der Genomintegrität ist eine sehr bedeutende Funktion des Lebens, um genetische Information zu bewahren. Die homologe Rekombination nimmt in diesem Zusammenhang eine Schlüsselfunktionen ein, da diese der Reparatur von DNA dient. Ich verwendete eine neue Technik, die es ermöglicht Einzelmolekül-Dynamiken über slim-field Mikroskopie von zwei bisher kaum verstandenen Proteinen, RarA und RecD2, zu beobachten. Zur Analyse ihrer Funktion wurden verschiedene rekombination-defiziente Mutanten getestet. Einzelmolekül-Mikroskopie erwies sich als eine gute Methode um in vivo Proteine und deren Interaktionen zu untersuchen. Unter Verwendung von genetischen Methoden konnte ich zu der Aufklärung eines komplexen Prozesses, der Regulation von homologer Rekombination, in welchem mehrere Faktoren auf verschiedene Art beteiligt sind, beitragen. Hierfür wurden teilweise überlappende Funktionen von Proteinen abhängig von der Art der DNA-Schädigung analysiert.

RarA und RecD2 wurden als zwei Faktoren charakterisiert, welche in die Rekombination und Replikation von DNA involviert sind. Es zeigte sich, dass die Proteine am Verlauf der RecA-unabhängigen und RecA-abhängigen Replikation beteiligt sind und als antagonistische Regulatoren der RecA-Filamentierung wirken. RarA interagiert während der Replikation mit DnaB. Desweiteren fungiert es durch die Interaktion mit RecA, RecO, RecR, RecD2 und RecU bei der Rekombination als positiver Regulator von RecA. RarA wird durch die RecQ-ähnlichen Helikasen RecQ und RecS reguliert. RecD2 spielt eine Rolle bei der chromosomalen Segregation, die unter Abwesenheit von RecG oder RuvAB essentiell ist. Als negativer Regulator interagiert RecD2 mit RecA, RarA, RecX, RecF und PcrA.

Index

I. INTRODUCTION

Maintenance of genome integrity is one of the crucial functions in life, to preserve the appropriate genetic information. Genome integrity is very often challenged as a result of natural functions of the cell or by exogenous agents, and multiple choices are available for the cells to repair the damage. Election of one or another pathway has to occur in consequence with the damage generated, offering different possibilities considering survivability and integrity. Because of this, a tight regulation and overlay between pathways has been developed during evolution. In *Bacillus subtilis*, there are at least seven characterized pathways for DNA repair and genome maintenance: homologous recombination (HR), non-homologous end joining (NHEJ), nucleotide excision repair (NER), base excision repair (BER), mismatch repair (MMR), translesion synthesis and alkylation damage response (reviewed in Alonso *et al.*, 2013; Lenhart *et al.*, 2012). Some of these pathways are meant to repair DNA with a high fidelity, as HR, while others are thought as a mechanism to improve survivability prior to fidelity on DNA sequence, as the translesion synthesis. Altogether, the ability of the cell to select the correct pathway will determine its fate for every challenge to come. Therefore, it is necessary to have a tight regulation between different pathways, but indeed there is not much information about all these regulation pathways, probably due to their complexity.

I.1- DNA replication

The main source of genomic stress in absence of drugs is replication. To ensure genomic stability and higher speed, bacteria have developed a factory composed of different proteins working together to create a stable complex with DNA known as replication fork. In *B. subtilis*, there are 13 proteins needed to fully replicate a plasmid *in vitro* (Sanders *et al.*, 2010): DnaB, DnaC, DnaD, DnaE, DnaG (Primase), DnaI, DnaN (β), DnaX (τ and γ), HolA (δ), HolB (δ'), PolC, PriA and Ssb. From all these 13, all except of DnaE and DnaG are needed for leading strand synthesis, while all 13 are needed for lagging strand synthesis. DnaC is a helicase that opens double strand DNA (ds-DNA) into two single strand DNA (ssDNA). DnaB, DnaD and DnaI are needed to load DnaC into DNA (Bruand *et al.*, 2001; Smits *et al.*, 2010) in concert with PriA, that recognizes the origin region and recruits the rest of the factors (Jameson & Wilkinson, 2017). DnaN is acting as a clamp, increasing the processivity of the polymerases PolC (in leading and lagging strand) and DnaE (in lagging strand), and the clamp loader

complex (composed by (τ/γ)3 δδ') is loading DnaN to DNA. DnaG creates RNA primers that are firstly elongated by DnaE and then by PolC in the lagging strand. Finally, Ssb proteins stabilizes ssDNA.

At this point, it is necessary to mention several issues that complicate the comparison between *B. subtilis* and *E. coli* replication forks:

i) Replication proteins are named different even in the case of the same function, leading to confusion; best examples are DnaB and DnaC: $DnaB_{EC}$ is the main helicase of the replication process in *E. coli* (corresponding to $DnaC_{BS}$), while $DnaC_{EC}$ is one of the components of the helicase-loader and its equivalent function is developed by both DnaI or $DnaB_{BS}$. To avoid confusions, in this work every *E. coli* replication protein will be named with "EC", while *B. subtilis* will not have any tag.

ii) Although both *E. coli* and *B. subtilis* have an equivalent DnaA as a replication initiator, the *ori* region is completely different: while *E. coli* is considered to have an unusual continuous *ori* region flanked by *gidA* and *mioC* genes and 44 kb away from the *rnpA-rpmH-dnaA-dnaN-recF-gyrB-gyrA* cluster, *B. subtilis* have a primitive one with two *ori* boxes that are separated by the *dnaA* gene in the cluster, and thus closer to eukaryotic (Jameson & Wilkinson, 2017).

iii) As mentioned above, the helicase-loader function of $DnaC_{EC}$ is depictured in at least two different proteins, DnaI and DnaB, acting together with a third factor, DnaI, normally in collaboration with DnaA in the *ori* (Smits *et al.*, 2010) and PriA in stalled replication fork, but also in a PriA-independent mechanism (Bruand *et al.*, 2001).

iv) Regulation of the replication initiation is completely different in *E. coli* and *B. subtilis*. In *E. coli*, DnaA-ATP is considered the limiting factor. Thus, there are several regulators (Had, IHF, Fis and SeqA) and DNA sequences that control replication initiation by modifying DnaA dynamics (Jameson & Wilkinson, 2017). In contrast, in *B. subtilis*, regulators act probably by blocking DnaA binding or oligomerization to *ori*, either tethering DnaA to the replication fork (YabA, which also binds DnaN), or by modifying oligomerization of DnaA (as Soj/Spo0J) (Jameson & Wilkinson, 2017).

I.2- Homologous recombination

Homologous recombination is the main response to double strand breaks (DSB), but also involved in other lesions that produces the block of the replication fork. HR happens as a cascade of events (Alonso *et al.*, 2013; Ayora *et al.*, 2011): recognition of damage, by RecN, PNPase, SbcE; DSB-end processing by AddAB or RecJ-RecQ/S; RecA loading and filamentation, regulated by accessory factors as RecO, RecR, RecF or RecX. After homologous search, there is a formation of Holliday junction (HJ) structures that are processed by RecG, RuvAB or RecQ-TopoIII and resolved by RecU. Although the general process is well understood, there are still several questions to address, especially in the specificity of some factors or the regulation among them.

The main regulation pathway known in bacteria is called SOS response and is based in regulation of more than 60 genes by the transcription factor LexA (Au *et al.*, 2005; Lenhart *et al.*, 2012). LexA is a repressor bound to the SOS boxes presented in many genes. When RecA filaments reach a certain size, RecA promotes the autocleavage of LexA and release the repression in the SOS-regulated genes, promoting its expression (Lenhart *et al.*, 2012).

I.2.1- DSB-end processing enzymes

RecA needs an ssDNA platform to be loaded. In *Bacillus subtilis*, there are two known possibilities to generate a ssDNA long enough for RecA loading: AddAB (counterpart of *E. coli* RecBCD in *B. subtilis*) and the combination of RecJ with one of the RecQ-like helicases: RecQ and RecS (Alonso *et al.*, 2013; Ayora *et al.*, 2011; Yeeles & Dillingham, 2010).

AddAB is a heterodimer composed of AddA, a SF1(3'-5')-helicase/RecB-like nuclease, and AddB, which contains a RecB-like nuclease C-terminal domain. The complex binds to blunt DNA ends, and separate and degrade single-strand nascent DNA with a similar rate until it recognizes Chi (crossover hotspot instigator) sequences that blocks AddA nuclease activity in the 3'→5' single-strand, while AddB is still active and promote a 3'-ssDNA end. There is controversy about the capacity of AddAB of actively load RecA into DNA as it happens with RecBCD (Yeeles & Dillingham, 2010) or if it requires RecO for the RecA loading (Carrasco *et al.*, 2015). AddAB has been characterized to play a role in protection to oxidative damage (ROS and NO), in DNA

repair when DNA is cross-linked with proteins, and promoting viability in a recombinational-independent manner, maybe by degradation of toxic intermediates for replication or reset reversed replication forks (Yeeles & Dillingham, 2010).

RecJ, in combination with either RecQ or RecS, represents an alternative pathway in *Bacillus subtilis* to AddAB in the previous step needed for RecA loading. Thus, Δ*addAB* Δ*recJ* double mutant behaves as Δ*recA* in growth impairment and sensitivity to DNA damage agents (Sanchez *et al.*, 2005), and impedes GFP-RecA threads formation (Kidane & Graumann, 2005). In this case, RecQ or RecS unwinds DNA due to its 3'→5' helicase activity while RecJ degrade 5'→3' ssDNA. Altogether, the result is a 3'-ssDNA end.

I.2.2- RecA and its accessory factors

Once the end-processing enzymes create a suitable 3'-ssDNA end, Ssb proteins stabilizes this ssDNA, but also interfere with RecA loading due to its higher affinity for ssDNA (Carrasco *et al.*, 2015). RecO is sufficient to displace Ssb *in vitro* and furthermore combination of both factors enhances RecA ATPase activity (Carrasco *et al.*, 2015), but *in vivo* it also requires RecR in both *B. subtilis* (Lenhart *et al.*, 2014) and *E. coli* (Lusetti *et al.*, 2006), with the only difference that in *E. coli* RecO and RecR are forming a complex (Lusetti *et al.*, 2006).

RecF is known to interact with RecR and RecX in *E. coli* (Lusetti *et al.*, 2006) and thus its considered that its function in *B. subtilis* is accelerate RecA filament formation (Carrasco *et al.*, 2015), probably by inhibiting RecX block of the RecA filamentation (Cárdenas *et al.*, 2012; Ragone *et al.*, 2008), therefore producing a longer RecA filament that is able to properly induce SOS response (Cárdenas *et al.*, 2012).

PcrA is an essential helicase of *Bacillus subtilis*, part of the UvrD-like helicases, as RecD2. However, they move in different ssDNA strands, as PcrA does in the 3'-5' strand while RecD2 does in the 5'-3'. It has been demonstrated that PcrA is able to compensate for UvrD- but not Rep-activities in *E. coli* (Petit *et al.*, 1998), which, together with the finding that mutations in *recF*, *recO* or *recR* suppressed is lethality (Petit & Ehrlich, 2002), suggesting a role in concert with recombination proteins rather than involvement in the normal replication fork displacement, although DNA synthesis is slightly compromised in absence of PcrA (Petit *et al.*, 1998). Nevertheless, the clear role of PcrA is yet undetermined and has been suggested to help in replication-

transcription conflicts (Merrikh *et al.*, 2012) and also as a RecA cofactor involved in the displacement of RecA filaments from the ssDNA (Thickman *et al.*, 2002).

I.2.3- Holliday Junction-processing enzymes

In most of the cases, homologous recombination pathway end in a four-strands DNA structure called Holliday Junction (HJ). This structure can move in a process known as branch migration, which is associated with RecG and RuvAB in *Bacillus subtilis*. RecG and RuvB are 3'→5' helicases (**Figure 2**), being RuvB part of a complex with RuvA, which is responsible of the loading of RuvB to the DNA (West, 1997). Finally, RecU is resolvase that can compensate the absence of the *E. coli* RuvC, resolvase and part of the complex RuvABC (Sanchez *et al.*, 2005). Double mutants are only possible in presence of suppression mutations such as *subA* (for *ΔrecG ΔruvAB*) or *radA* (when combine *ΔrecU* with either *ΔruvAB* or *ΔrecG*) indicating that HJ-processing is essential for life (Sanchez *et al.*, 2007; Sanchez *et al.*, 2005).

I.2.4- Differences between B. subtilis *and* E. coli *in homologous recombination*

Although HR in *B. subtilis* and *E. coli* share some orthologues, the recombinational process is not really equivalent and it present several differences:

i) In *B. subtilis*, DSB repair is condensed in one repair centre (RC) that is able to process more than one DSB at once, and even is able to be formed eventually with a single copy of the genome (Kidane & Graumann, 2005; Lenhart *et al.*, 2012). The presence of these RCs is extremely dependent on RecN (Kidane *et al.*, 2004), but other factors as RecO or RecF are also recruited to the RCs (Kidane *et al.*, 2004), which are located far from the replication fork (Kidane & Graumann, 2005). In *E. coli*, there are no evidences of RCs, and thus RecA-GFP are located in positions where is expected to be the replication fork (Renzette *et al.*, 2005) and is even suggested that replication fork is needed for RecA focus formation (Simmons *et al.*, 2006).

ii) Although the main factors of the SOS response, RecA and LexA, are highly conserved, only eight *B. subtilis* SOS-regulated orthologues genes are also SOS-regulated in *E. coli*, being three of them genes related with DSB response (Simmons *et al.*, 2009).

I.3- Interplay between recombination factors and replication

Many of the proteins initially described as homologous recombination factors have been also described as replication-related proteins. First, several recombination factors are part of the Ssb interactome (Costes *et al.*, 2010), which require a certain size of ssDNA to be formed. Replication fork progression involves the unwinding of ds-DNA into two strands allowing the binding of Ssb. However, the presence of these factor is not casual, as some recombination-deficient mutants show impaired growth in absence of external DNA damage, accumulation of unsegregated chromosomes and form anucleate cells (Carrasco *et al.*, 2004). Moreover, the number of RecA-GFP foci is increased after replication arrest by TetR binding to large *tetO* arrays (Bernard *et al.*, 2010). In *E. coli*, there are several evidences for the dependence of the replication for recombinational factors, as delayed multiplication of the origin in *recO* and *recF* mutants (Rudolph *et al.*, 2008), requirement of RecBC in presence of high-expressed inverted *rrn* sequences (Septenville *et al.*, 2012) or increased sensitivity to thymidine less death (TLD) in *uvrD* mutants (Kuong & Kuzminov, 2010). Also, deficient replication mutants as *priA* and *dnaT* present high basal levels of SOS expression (Michel & Sandler, 2017). In *B. subtilis*, it has been shown that AddAB, RecO and RecA promotes survival of cells that experience severe head-on replication-transcription conflicts and that DnaD requires RecA to associate to the region affected (Million-Weaver *et al.*, 2015).

On the other hand, replication is needed during HR repair (Ayora *et al.*, 2011) and thus *priA* deficient mutants become more sensitive to UV-irradiation (Bruand *et al.*, 2001; Michel & Sandler, 2017).

I.4- RarA is highly conserved in evolution

RarA (Replication-Associated Recombination protein A), also named MgsA (Manteinance of Genome Stability A) was first described and renamed (from YcaJ) by David Sherratt's lab (Barre *et al.*, 2001) and found as a consequence of the similarity with RuvB and DnaX (26 and 24% in *E. coli*; 29 and 24% in *B. subtilis*). Its highly conserved sequence through evolution is remarkable (**Figure 1**B) (Barre *et al.*, 2001) with identities of ~38% between *B. subtilis* RarA compared to its homologues in eukaryotes Mgs1 in *S. cerevisae* or WHIP/WRNIP in *H. sapiens*, and also compared to the correspondent RuvB and DnaX analogues (Barre *et al.*, 2001). Thus, in the overview of all the residues changed among these for homologues (**Figure 1**A), there

are two predicted domains with highly resemblance, the ATPase and the tetramerization domain, compared to the helicase lid domain, and both N-terminal and C-terminal ends, where changes to completely different residues are more frequent, according to the predicted model for *E. coli* RarA proposed by Page *et al.* (Page *et al.*, 2011).

A

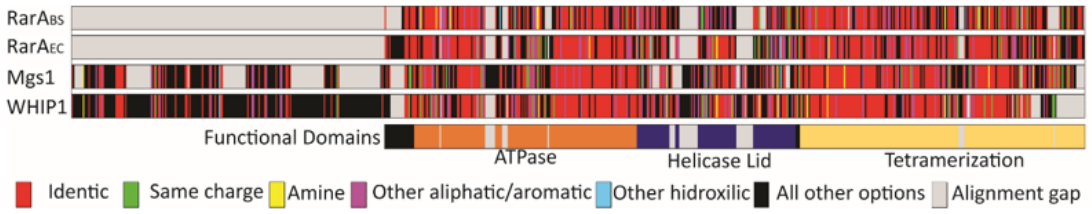

B

Species	Identity (%)			
	B. subtilis RarA	*E. coli* RarA	*S. cerevisae* Mgs1	*H. sapiens* WHIP1
B. subtilis RarA	100	35.7	38.9	38.2
E. coli RarA	35.7	100	40.3	40.6
S. cerevisae Mgs1	38.9	40.3	100	42.0
H. sapiens WHIP1	38.1	40.6	42.0	100
Aminoacids number	422	447	587	665

Figure 1. (A) BLASTA for the sequences obtained in NCBI database and the functional domains predicted by Page *et al.* (Page *et al.*, 2011) for *E. coli* RarA. Color-code represent the identities or the type of minor changes (polar with same charge, green; amine, yellow; or same kind of side chain, pink and blue). Figure is scaled to the size of proteins except of the gap needed for alignment. (B) Identity values for RarA homologues in Evolution. Although the protein increases its size in eukaryotes, the identity is conserved.

Although several studies agreed with the idea that RarA acts in both replication and recombination processes, the concrete function is still unknown. *E. coli* RarA, which is co-expressed with FstK, co-localizes/interacts with SeqA (Lau *et al.*, 2003), RecQ (Sherrat *et al.*, 2004), UvrD (Lestini & Michel, 2007) or RecA (Shibata *et al.*, 2005) and may act at blocked forks in certain replication mutants (Lestini & Michel, 2007; Shibata *et al.*, 2005). *In vitro*, *E. coli* RarA interacts with the SSB protein and shows helicase activity that preferentially unwinds 3'-ends from dsDNA ends or ssDNA gaps, suggesting that RarA acts at replication forks (Page *et al.*, 2011; Stanage *et al.*, 2017). Much less is known about *B. subtilis* RarA (also termed YrvN). The *rarA* gene, monocistronic, is constitutively expressed, but its expression is markedly enhanced by stressors such as diamide, ethanol, high salt or H_2O_2 (Nicolas *et al.*, 2012). RarA interacts with SsbA, which in turn interact with recombination (RecQ, RecS, RecJ,

RecG, RecO, RecD2) and replication (PriA, DnaG, DnaE) proteins (Costes *et al.*, 2010). In budding yeast, RarA's homologue Mgs1 is proposed to be part of an alternative pathway DNA damage tolerance and homologous recombination for resolving stalled replication forks, probably enhancing processivity and/or fidelity of the DNA polymerase δ, and partially overlapping functions of the helicases Sgs1 and Srs2 in genome stability (Barbour & Xiao, 2003), while in humans is known that WHIP physically interacts with WRN, a RecQ-like helicase (Kawabe *et al.*, 2001). One common point of RarA studies is the complex scenario required to produce a clear phenotype that explains all observations.

I.5- Role of helicases and of RecD2 in recombination

In many cellular processes, DNA needs to be unwound by DNA helicases. In *Bacillus subtilis*, there are at least ten helicases with putative helicase domains: AddA, HelD, PcrA, RecD2, RecG, RecQ, RecS DinG, PriA and RuvB (**Figure 2**) First four are part of the SF1 superfamily of helicases, while last six are part of the SF2 superfamily. Function of these helicases include: i) movement of the replication fork through obstacles (PcrA, DinG and HelD) (Atkinson & McGlynn, 2009; Epshtein, 2015; Gwynn *et al.*, 2013; Mirkin & Mirkin, 2007; Voloshin & Camerini-Otero, 2007; Wiedermannova *et al.*, 2014), ii) reversion of a stalled fork and its regression (RecG and RuvAB) (Atkinson & McGlynn, 2009; Ayora *et al.*, 2011; Michel *et al.*, 2001; Persky & Lovett, 2008), iii) recruitment of the primosome at the formed recombination intermediates (PriA) (Gabbai & Marians, 2010), iv) unwinding of duplex DNA and present to an exonuclease to generate 3'-ssDNA ends (RecQ, RecS and AddAB) (Alonso *et al.*, 1993; Alonso *et al.*, 2013; Dillingham & Kowalczykowski, 2008; Fernandez *et al.*, 1998), v) dissolution of HJ (RecQ and RecS, in concert with Topo III and SsbA proteins) (Alonso *et al.*, 2013; Wu & Hickson, 2006) and vi) RecA removal from nucleoprotein filaments (PcrA and HelD) (Carrasco *et al.*, 2001; Fagerburg *et al.*, 2012; Park *et al.*, 2010; Petit & Ehrlich, 2002).

Of all of the helicases of *B. subtilis*, only PcrA is essential. *B. subtilis* PcrA is able to compensate for the viability in *uvrD rep* double mutant of *E. coli* by compensate UvrD, but not Rep, activities (Petit & Ehrlich, 2002). All three helicases contribute to facilitate replication of transcribed DNA regions (Epshtein, 2015; Guy *et al.*, 2009; Merrikh *et al.*, 2015), while PcrA and UvrD, but not Rep, present anti-recombinase activity by displacing RecA from ssDNA (Fagerburg *et al.*, 2012; Park *et al.*, 2010;

Veaute *et al.*, 2005). Thus, the requirement of PcrA disappear in absence of RecA mediators RecO, RecR or RecF (Petit & Ehrlich, 2002).

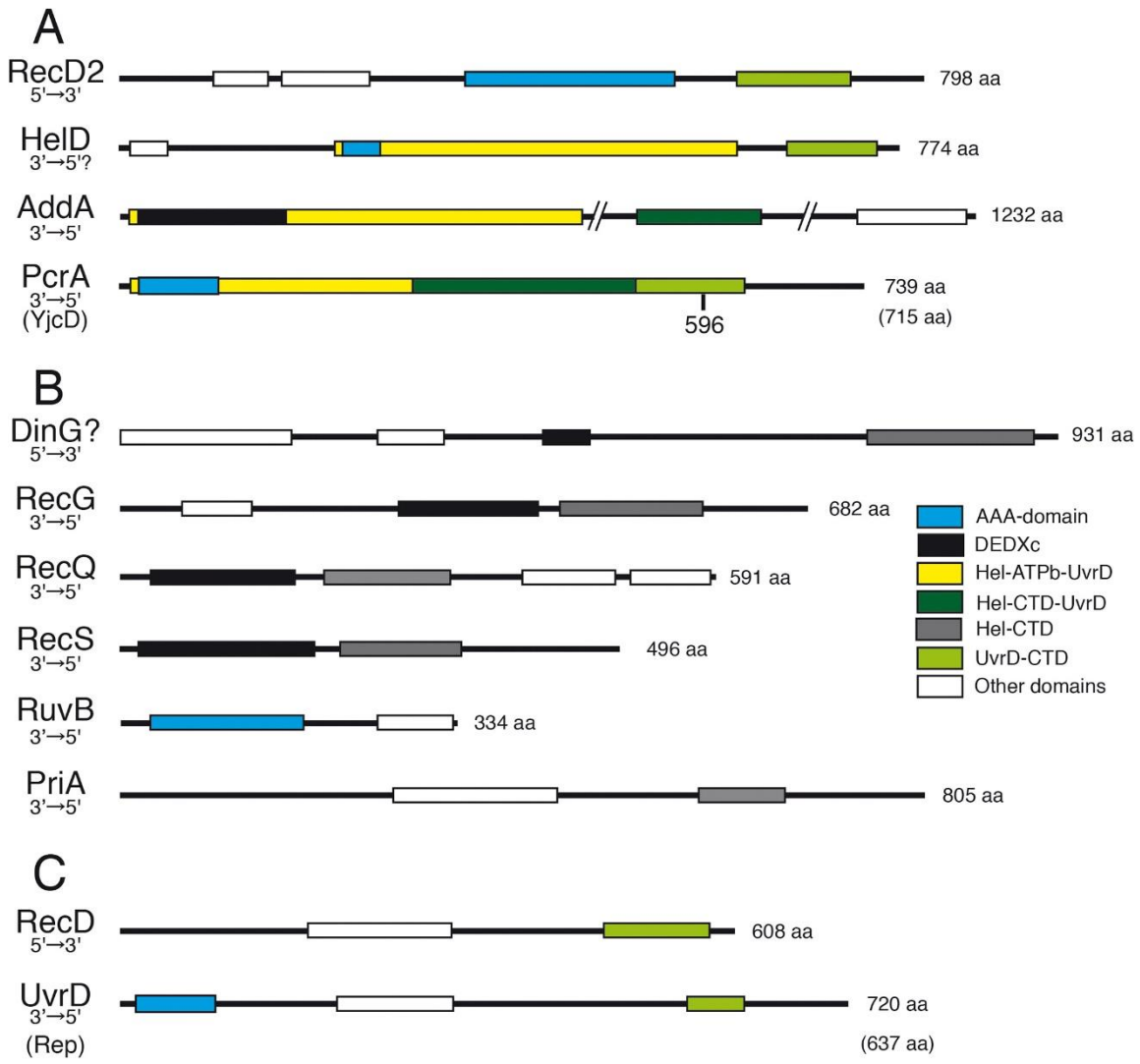

Figure 2. Functional domain alignment of recombinational repair DNA helicases. A. Domain alignment of *B. subtilis* SF1 RecD2, HelD, AddA, PcrA (or YjcD) DNA helicases. In HelD, the direction of unwinding is uncertain (?), as *E. coli* HelD shows 3′→ 5′, but D. radiodurans HelD shows 5′→ 3′ activity. B. Domain alignment of B. subtilis SF2 RecG, RecQ, RecS, DinG, RuvB and PriA DNA helicases or a putative (?) helicase. C. Domain alignment of E. coli helicases RecD and UvrD (or Rep), which share similarity with RecD2. Sequences were aligned based on data from http://www.ncbi.nlm.nih.gov./protein/. Conserved helicase domains and functions were assigned accordingly (Singleton *et al.*, 2007).

RecD2 shares structural similarity with different SF1A helicases (*B. subtilis* PcrA, *E. coli* Rep or UvrD and *S. cerevisae* Srs2) that moves in 3'-5' direction along the ssDNA, and with SF1B helicases (*E. coli* RecD and *S. cerevisae* Pif1) which have 5'-3' polarity. *In vitro* studies showed that *B. subtilis* and *D. radiodurans* RecD2 have a 5'-3' helicase activity (Saikrishnan *et al.*, 2009; Walsh *et al.*, 2014; Wang & Julin, 2004),

and studies in different organism suggest that it plays a role in maintenance of replication fork integrity during normal growth (Servinsky & Julin, 2007; Wang & Julin, 2004; Yang *et al.*, 2011), as arrested replication forks are more frequent in absence of RecD2 (Walsh *et al.*, 2014).

II. METHODS

II.1- Bacterial strains

The working model for all experiments is based in *Bacillus subtilis* BG214, a modified *B. subitilis* cured for the SPβ phage, non-inducible for PBSX and lacking the ICEbs1, that also presents autotrophy for tryptophan (*trpC2*) and methionine (*metB5*) (Yasbin *et al.*, 1980). Generation of the different recombination- or replication-defective mutants was performed by one of these following mechanism:

1. Transformation of natural competence cells with a linear plasmid containing the gene disrupted by an insertion of an antibiotic resistance cassette.
2. Transformation of natural competence cells with a linear plasmid containing the gene disrupted by an antibiotic gene flanked by two directly oriented β cognate sites (six sites) that are recognized by a β-site specific recombinase. These method, described by Sanchez *et al.* (Sanchez *et al.*, 2007), confers the advantage that allows the removal of the antibiotic resistance by adding a segregationally unstable plasmid (pT233-3) with a loss rate per cell generation 100-fold higher than expected for random segregation in the absence of selective pressure.
3. Gene conversion. Used only for *recF* gene, that contains the promoter for two essential genes (*gyrA* and *gyrB*). Mutant *recF15* is considered a null allele.
4. SPP1 transfection. SPP1 phage are used to infect the donor strain, and then to infect the recipient strain (Alonso *et al.*, 1986).
5. Phenol-chloroform DNA extraction from donor strain and transformation of natural competent recipient strain with chromosomal DNA. Mainly used to introduce the fluorescence-tagged proteins in the different backgrounds. Concrete method is described below.

Strains were tested by PCR, and viability assays or fluorescence were required to confirm the genotype. All strains used in this work are summarized in **Table 1**.

Table 1. Strains used on this work

Strain	Relevant genotype	Source
BG214	wt	Lab. strain
BG1095	Δ*addAB*	(Vlasic *et al.*, 2014)
BG1605	Δ*dinG*	This work
BG193	*dnaB37*	(Alonso *et al.*, 1988)
BG196	*dnaC30*	(Alonso *et al.*, 1988)
BG198	*dnaG20*	(Alonso *et al.*, 1988)
BG199	*dnaF33*	(Alonso *et al.*, 1988)
BG201	*dnaX51*	(Alonso *et al.*, 1988)
BG1679	*dnaE58*	This work
BG551	Δ*helD*	(Carrasco *et al.*, 2001)
BG1539	*pcrA596*	This work
BG1525	*pcrA-ssrA*	This work
BG907	Δ*polY1*	This work
BG905	Δ*polY2*	This work
BG1245	Δ*radA*	(Gándara & Alonso, 2015)
BG1067	Δ*rarA*	This work
BG190	Δ*recA*	(Ceglowski *et al.*, 1990)
BG1455	Δ*recD2*	This work
BG1557	*recD2-ssrA*	This work
BG129	*recF15*	(Alonso *et al.*, 1988)
BG1131	Δ*recG*	(Sanchez *et al.*, 2007)
BG775	Δ*recJ*	(Sanchez *et al.*, 2006)
BG631	Δ*recO*	(Fernandez *et al.*, 1999)
BG705	Δ*recQ*	(Sanchez *et al.*, 2006)
BG425	Δ*recS*	(Sanchez *et al.*, 2006)
BG855	Δ*recU*	(Fernandez *et al.*, 1998)
BG1065	Δ*recX*	(Cárdenas *et al.*, 2012)
BG703	Δ*ruvAB*	(Sanchez *et al.*, 2005)
BG1419	Δ*addAB* Δ*recD2*	This work
BG1607	Δ*dinG* Δ*recD2*	This work
BG1297	Δ*helD* Δ*recD*	This work
BG1579	Δ*recQ* Δ*recD2*	This work
BG1585	Δ*recS* Δ*recD2*	This work
BG1313	Δ*pcrA recF17*	This work
BG1583	*pcrA-ssRA* Δ*recD2*	This work
BG1061	Δ*recD2 pcrA596*	This work
BG1133	Δ*recD2 pcrA596* Δ*addAB*	This work
BG1569	*recD2-ssrA* Δ*ruvAB*	This work
BG1565	*recD2-ssrA* Δ*recG*	This work

Table 1 (continued). Strains used on this work

Strain	Relevant genotype	Source
BG1587	*recD2-ssrA* Δ*recU*	This work
BG1063	Δ*recJ* Δ*recD2*	This work
BG1423	Δ*recO* Δ*recD2*	This work
BG1051	*recF15* Δ*recD2*	This work
BG1261	Δ*recX* Δ*recD2*	This work
BG1579	Δ*recA* Δ*recD2*	This work
HR51	*recD2-mVenus*	This work
HR53	*pcrA596 recD2-mVenus*	This work
HR54	*pcrA-ssrA recD2-mVenus*	This work
HR55	*recF15 recD2-mVenus*	This work
HR56	Δ*recX recD2-mVenus*	This work
HR58	Δ*rarA recD2-mVenus*	This work
HR59	Δ*recG recD2-mVenus*	This work
BG1555	Δ*rarA* Δ*recA*	This work
BG1073	Δ*rarA* Δ*recN*	This work
BG1059	Δ*recJ* Δ*rarA*	This work
BG1563	Δ*rarA* Δ*recS*	This work
BG1575	Δ*rarA* Δ*recQ*	This work
BG1107	Δ*rarA* Δ*addAB*	This work
BG1433	Δ*rarA* Δ*recO*	This work
BG1055	*recF15* Δ*rarA*	This work
BG1371	Δ*rarA* Δ*recX*	This work
BG1421	Δ*rarA* Δ*recD2*	This work
BG1103	Δ*rarA* Δ*recG*	This work
BG1425	Δ*rarA* Δ*recU*	This work
BG1351	Δ*ruvAB* Δ*rarA*	This work
BG1403	Δ*polY1* Δ*rarA*	This work
BG1401	Δ*polY2* Δ*rarA*	This work
BG1373	Δ*rarA* Δ*radA*	This work
BG1687	*dnaB37* Δ*rarA*	This work
BG1681	*dnaC30* Δ*rarA*	This work
BG1661	*dnaG20* Δ*rarA*	This work
BG1685	*dnaF33* Δ*rarA*	This work
BG1659	*dnaX51* Δ*rarA*	This work
BG1683	*dnaE58* Δ*rarA*	This work
BG1331	*rarA-mVenus*	This work
PG3423	Δ*recJ rarA-mVenus*	This work
PG3318	Δ*recQ rarA-mVenus*	This work
PG3424	Δ*recS rarA-mVenus*	This work
PG3316	Δ*addAB rarA-mVenus*	This work

Table 1 (continued). Strains used on this work

Strain	Relevant genotype	Source
BG1445	Δ*recO rarA-mVenus*	This work
BG1345	*recF15 rarA-mVenus*	This work
BG1349	Δ*recX rarA-mVenus*	This work
BG1347	Δ*recD2 rarA-mVenus*	This work
PG3317	Δ*recG rarA-mVenus*	This work
BG1443	Δ*recU rarA-mVenus*	This work
PG3426	Δ*ruvAB rarA-mVenus*	This work
PG3427	Δ*polY1 rarA-mVenus*	This work
PG3428	Δ*polY2 rarA-mVenus*	This work
PG3426	Δ*radA rarA-mVenus*	This work
HR18	*dnaX-cfp*	This work
PG3174	*rarA-mVenus dnaX-cfp*	This work
BG1451	*dnaB37 rarA-mVenus*	This work
PG3430	*dnaB37 rarA-mVenus dnaX-CFP*	This work
BG1453	*dnaC30 rarA-mVenus*	This work
PG3431	*dnaC30 rarA-mVenus dnaX-CFP*	This work
HR24	*pcrA-ssrA rarA-mVenus*	This work

Table 1. Strain used in this work. All strain used are isogenic with BG214, considered wild type for all experiments, with the following genotype: *trpEC metA5 amyE1 ytsJ1 rsbV37 xre1 xkdA1att*$^{SP\beta}$ *att*I^{CEBs1}. The fluorescence constructions *rarA-mVenus*, *recD2-mVenus* and *dnaX-CFP* are located in the original locus of the gene and controlled by its natural promotor; strains containing a -ssrA tagged protein also contain P_{spac}*-SSB* in the *amy* locus to promote degradation upon IPTG induction.

II.2- DNA extraction

Plasmid minipreps Omega® was used to extract plasmid DNA from liquid cultures of *E. coli* DH5α cells.

Chromosomal DNA from *Bacillus subtilis* was obtained by phenol-chloroform extraction. Cells were lysated at 37ºC using lysozyme 1mg/ml in lysis buffer (NaCl 10mM, EDTA 50mM), incubated with N-lauryl-sarcocine 1.5% (w/v) in ice, mixed 1:1 with phenol and centrifuged. The aquose phase was extracted and diluted 1:1 in phenol/chloroform/isoamyl alcohol and centrifuged. Na-Acetate was added to the aquose phase prior to the slow addition of 100% ethanol to produce DNA precipitation. DNA was collect with a Pasteur and dried in ethanol 70% first and then in room temperature. Finally, DNA was diluted in TE buffer pH 8.0 (Tris 10 mM EDTA 1 mM) and stored at -20ºC.

II.3- Competence and transformation of *Bacillus* strains

Natural competence from *Bacillus* was induced by growing the cells to stationary phase in a SpC rich medium containing Tris-base, glucose 0.5%, $MgSO_4$ 0.018%, casaminoacids 0.025% and bacto-yeast extract and then dilute 1:5 in a SpII medium (tris-base, glucose 0.5%, $MgSO_4$ 0.084%, casaminoacids 0.01%, bacto-yeast and $CaCl_2$ 0.5 mM). The lack of nutrients and the presence of calcium induces the natural competence. Cells were centrifuged, resuspended in SpII medium with 5% glycerol, aliquoted and stored at -80%.

One aliquot of competent *B. subtilis* cells was thaw at room temperature, exposed to 3-6 µg of plasmid or 0.2-0.5 µl of chromosomal DNA for 45-60 min at 37ºC in gentle shaking and then plated in LB-agar plates containing the resistance of selection for 48 h at 30ºC. Colonies were checked by PCR, viability assays and/or epifluorescence microscopy to probe their phenotype.

II.4- Viability assays

Viability assays were performed for cultures in exponential phase of growth in LB cultures. Fresh streaked colonies were picked for an over-night (O/N) culture in LB at 30ºC. The O/N culture was diluted to OD_{600}=0.03 in fresh LB medium and grown to OD_{600}=0.4 at 37ºC with gentle shaking (200 rpm).

For chronic assays, 100 µl of the culture at OD_{600}=0.4 was serial diluted in 900 µl of fresh LB for 4 times, and for each dilution 10 µl were spotted in LB-agar plate and LB-H2O2, LB-MMC, LB-MMS or LB-4NQO at the concentration needed; or $S7_{50}$-agar, $S7_{50}$-MMS or $S7_{50}$-H_2O_2 in the special case of *pcrA596* mutants. Plates were grown O/N for 16-18 h at 37ºC protected from light. Images were taken in a ChemiDoc™ MP Imaging System (BIO-RAD) with the software Image Lab 6.0 (BIO-RAD). Thermosensitive assays were performed in the same way, only varying the temperature conditions: cells were grown at 30ºC and plates were incubated in 30, 38 or 42ºC O/N.

For acute assays, 1 ml aliquots of the culture at OD_{600}=0.4 were exposed to different concentrations of drug: 0, 0.5, 1, 2.5 or 5 mM H2O2 or 0, 1, 5, 10, 20 or 40 mM MMS for 15 minutes. 100 µl of the cells were serial diluted in 900 µl of fresh LB as many times as needed and 100 µl were platted and spread in LB-agar plates. After O/N incubation, colonies were counted. Only dilutions containing 30-300 colonies were

consider. UFC number was compared to UFC in absence of drug. When viability was compromised in absence of drug, the mean of at least three experiments were compared to the mean of WT cells.

MMS, H_2O_2, MMC, 4NQO and IPTG were obtained from Sigma Aldrich. Cells were induced by 250 or 500 µM IPTG when described.

II.3- Epifluorescence microscopy

B. subtilis cells dilutions were growth O/N at 25ºC in $S7_{50}$ minimal medium until reaching an OD_{600} 0.2-0.4. Cells were either induced with 1 mM H_2O_2 or 50 ng/ml MMC or not induced, and 2.5 µl of culture were spotted cover glasses and immobilized with coverslips coated with fresh agarose 1% (w/v) in $S7_{50}$ medium.

For chromosomal segregation, cells were grown in LB medium to OD_{560}=0.4 at 37ºC, or to OD_{560}=0.2 and then incubation 500 µM IPTG for 60 min in the case of the *recD2-ssrA*-derivated strains, fixed with 2% formaldehyde and stained with DAPI (1 µg/ml) and the visualization was done as described (Carrasco *et al.*, 2004).

Epifluorescence microscopy was performed using a Zeiss Axio Imager A1 microscope equipped with a 1.45 objective and a EVOLVE EMCDD camera (Photometrics). A 515 nm LED laser was used for YFP/mVenus detection, a 445 nm laser was used for CFP detection and UV lamp with DAPI filter was used DAPI stained cells images when needed. Picture acquisition was done using VisiView (2.1.2).

For the colocalization of RarA-mVenus with the replication fork, images were taken as described above and processed equally (background subtraction and Gaussian blur) using ImageJ (National Institutes of Health, Bethesda, MD) prior to the merging.

II.4- Single-molecule tracking (SMT)

Single-molecule tracking (SMT), also known as single-particle tracking, is a novel technique based on the excitation of fluorescence molecules by a slim field beam. The slim field generates a compact excitation field compared to conventional widefield imaging techniques as epifluorescence or TIRF, giving as a result an intensity of excitation higher by a factor of ~100, allowing single-molecule detection in an inexpensive manner requiring relatively simple optical components (Plank *et al.*, 2009).

There is an excitation of most of the molecules in an initial moment, followed by an exponential bleaching decay until it reaches a plateau (**Figure 3**A). This plateau corresponds to the recovery of one molecule that can be tracked for a short time until it bleaches again (**Figure 3**C, D).

Due to the higher intensity of excitation, there is higher risk to detect dust particles as molecules. To reduce the background, cover glasses were cleaned using Hellmanex II 2% (v/v) and sonicated for at least 15 minutes, washed with miliQ water and dried with sterile air spray duster before mounting the cells.

B. subtilis cells dilutions were growth O/N at 25ºC in $S7_{50}$ minimal medium until reaching an OD_{600} 0.2-0.4. Cells were either induced with 0.5 mM H_2O_2 or 50 ng/ml MMC or not induced, and 2.5 µl of culture were spotted in the cleaned cover glasses and immobilized with coverslips coated with fresh agarose 1% (w/v) in $S7_{50}$ medium.

Single-molecule tracking was performed using Nikon microscope equipped with a 1.45 objective and a EVOLVE EMCDD camera (Photometrics). A 515nm LED laser was used for YFP detection and UV lamp with CFP filter was used for CFP images when needed. Picture acquisition was done using VisiView (2.1.2). Time-lapse images of YFP were taken in a maximum of 1 minute, and the length of acquisition in a sample was limited to 20 minutes to avoid the heating of the sample. For every time-lapse, a 20 ms exposure time bright field image was taken to determine the shape of the cells. When required, CFP images in 200 ms exposure time were taken for additional tagged proteins using CFP. Time-lapse images were prepared with ImageJ (National Institutes of Health, Bethesda, MD) and tracks were obtained using U-track (Laboratory for Computational Cell Biology, Harvard Medical School). Tracks were exported with a shape of the cell generated with MicrobeTracker (Microbial Sciences Institute, Yale) to SMTracker (currently in development by Dr. Thomas Rösch and Dr. Luis Oviedo). All U-track, MicrobeTracker and SMTracker are software running in MATLAB (Mathworks). SMTracker automatically calculates: i) distribution of the tracks in the cells with overlapping with bright field or any other signal (CFP); ii) apparent diffusion coefficient (D) and population densities based on Gaussian fit to a step-size distribution (**Figure 3**B) with its statistical differences based in Z-test; iii) apparent diffusion coefficient (D), number of populations by Bayesian information criterium (BIC) and population densities based on square displacement model fit; iv) heat maps with the

preferential location of the tracks in normalized cells (sorted automatically by size into small, medium and long based on the data); v) distribution of confined and not-confined tracks in a normalized cell: confined is considered as three times the average step of the static population in the Gaussian fit in ii).

As the apparent diffusion coefficient D has some fluctuations in the different backgrounds and conditions, we defined a new parameter, the dynamic population difference (DPD), to describe the effect of the absence of one protein compared to wt or before and after of the induction with a drug in the same D conditions and provide a visual view of these effect allowing a fast comparison. Although in the concrete case of RarA is reasonable to expect that is the static, and not dynamic population, which is responsible of the function, as they probably represent the DNA-bound and free diffusion respectively, DPD is visually clearer than SPD (static population difference) and they are complementary. For RecD2, population weight defines the percentage of molecules given in SQD model of SMTracker, while PD consider 0 the weights on the correspondant control (wt for absence of drug comparisons or absence of drug for MMC or H_2O_2).

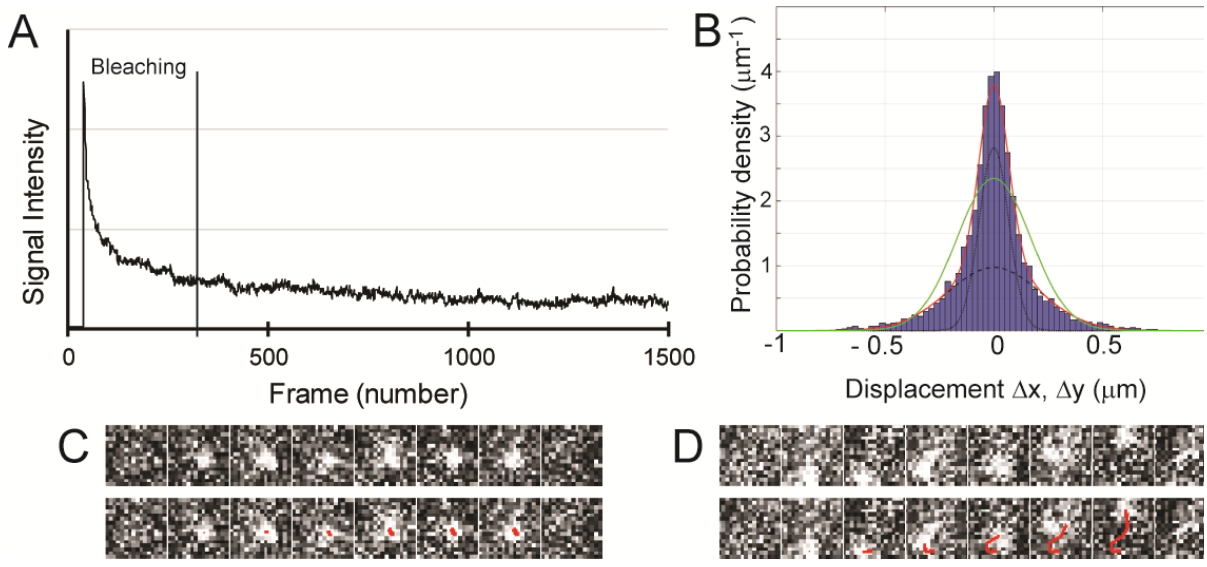

Figure 3. RarA-mVenus single-molecule microscopy (A) Signal intensity in a sample after slim field illumination with a 515 nm laser, showing a first bleaching decay and a single-molecule signal plateau; (B) Step size distribution given by SMTracker (blue) and Gaussian fits to one population (green) and two populations (red); (C-D) 1.5 μm^2 section of movies containing RarA-mVenus examples of static (C) and mobile (D) molecules, in raw movie (above) and after U-track processing and recognition (below).

II.5- Colocalization of replication fork with RarA-mVenus single molecules

Images were taken as described above. Then, CFP signal was improved by removing background in ImageJ (National Institutes of Health, Bethesda, MD) and overlapped with cell meshes obtained in microbeTracker. Molecules of RarA-mVenus were separately obtained in SMTracker with the reference of the cell meshes obtained in microbeTracker.

All images were loaded into Photoshop (Adobe®) and the following distances were measured: i) length and width of the cell, ii) diameter of the replication fork (expressed as the diameter of the smallest circle that contains all CFP signal), iii) diameter of the molecule (expressed as the diameter of the smallest circle containing all steps of the molecule) and iv) distance from the replication fork to the origin/end point of the molecule (distance from the centre of the circle ii) to the origin/end). Distances were normalized to a 3:1 (length: width) cell.

First, tracks were sorted by its size (iii) compared to DnaX-foci (ii) into three types: a) confined, when it was smaller or equal; b) random, when it was bigger; and c) dual, in the special cases that more than the half of the steps in an otherwise random track are confined. Then, track point-localization for each size was sorted in a similar way as it was expressed for epifluorescence localization in merge (contained in the DnaX-CFP foci), near (contained in the area between the DnaX-CFP foci and two times the average size of DnaX-CFP foci) and far (in all other cases). Finally, statistical significance was determined by chi-square (to confirm differences) and Marasculio test for probabilities (to determine the exact population that produce the differences).

II.6 Chromosomal segregation

O/N *B. subtilis* cultures were inoculated in LB medium. In the case of Δ*recD2*, Δ*recU*, Δ*ruvAB* or Δ*recG* cells were grown undisturbed in LB medium to OD_{560}=0.4 at 37ºC. Exponentially growing cells were fixed with 2% formaldehyde and stained with 1 µg/ml DAPI. In the *recD2-ssrA* double mutant cells were grown to OD_{560}=0.2 at 37ºC, divided in two, and incubated 60 min at 37ºC, one undisturbed and the other induced with 500 µM IPTG before fixing with 2% formaldehyde and staining with DAPI.

Cells were analysed by merging a bright field picture with DAPI fluorescence using ImageJ (National Institutes of Health, Bethesda, MD), following the method described in Carrasco *et al.*, 2004.

III. RESULTS

III.1- RarA- Romero *et al.*, 2017 (submitted)

Cell biological screen for protein interactions based on single molecule tracking reveals involvement of RarA with several proteins affecting RecA activity as well as with replication forks

Hector Romero[1,2,3], Thomas Rösch[1,2], Silvia Ayora[3], Juan C. Alonso[3*], Peter L. Graumann[1,2*]

[1]SYNMIKRO, LOEWE-Zentrum für Synthetische Mikrobiologie, Hans-Meerwein-Straße, Mehrzweckgebäude, 35043 Marburg, [2]Fachbereich Chemie, Hans-Meerwein-Straße 4, 35032 Marburg, Germany, [3]Department Microbial Biotechnology, Centro Nacional de Biotecnología, CNB-CSIC, 3 Darwin St., 28049 Cantoblanco, Madrid, Spain.

*corresponding authors. E-mail: peter.graumann@synmikro.uni-marburg.de; Tel. (+49) [0]6421 2822210; Fax (+49) [0]6421 2822262; and jcalonso@cnb.csic.es; Tel. (+34) 91585 4546; Fax (+34) 91585 4506

III.1.1- Contribution of H. Romero

For this manuscript I have been involved in design of experiment, together with PLG and JCA, I have performed all experiments except for **Figure 12** (done by SA) and writing the manuscript together with PLG and JCA. For the analysis of SMM, the program SMTracker has been developed by TR.

III.1.2- Abstract

Ubiquitous RarA is proposed to be involved in recombination-dependent replication. We present a novel cell biological approach to identify functional connections between proteins using single molecule tracking. We show that 50% of RarA molecules were static, mostly close to replication forks and likely DNA-bound, while the remaining fraction was highly dynamic throughout the cells. RarA alternated between static and dynamic states. Exposure to H_2O_2 increased the fraction of dynamic molecules, but not treatment with mitomycin C or methyl methanesulfonate. RarA movement was most strongly affected by the absence of RecJ, RecD2, RecS and RecU proteins. The ratio between static and dynamic RarA also changed in replication temperature-sensitive mutants, but in opposite manners, dependent upon inhibition of DnaB or of DnaC, revealing an intricate function related to DNA replication restart. RarA likely acts in the context of stalled replication forks, as well as in

conjunction with a network of proteins that affect the activity of the RecA recombinase. Our novel approach reveals intricate interactions of RarA, and is widely applicable for *in vivo* protein studies, to underpin genetic or biochemical connections, and is especially helpful for investigating proteins whose absence does not lead to any detectable phenotype.

III.1.3- Introduction

Maintenance of genome stability is one of the crucial functions in life, to preserve the appropriate genetic information. Genome integrity is very often challenged as a result of natural functions of the cell, or by exogenous agents, and multiple choices for DNA repair are available for the cells. Election of one or another repair pathway has to occur in consequence with the cell cycle and the damage generated. Because of this, a tight regulation and overlay between pathways has been developed during evolution. In *Bacillus subtilis*, several pathways for DNA repair of damaged or mispaired template bases have been characterized: nucleotide and base excision repair, mismatch repair, alkylation damage response, homologous recombination (HR), pathways for circumventing DNA damage, such as DNA damage tolerance or post-replication repair (template switching, translesion synthesis, etc.), and non-homologous end joining for direct reconnection of the two-ended double strand breaks (DSBs) (reviewed in Alonso *et al.*, 2013; Lenhart *et al.*, 2012). Some of these pathways are meant to repair DNA with high fidelity, e.g. HR, while others are thought as a mechanism to maintain survivability to the expense of fidelity on DNA sequence, such as non-homologous end joining and translesion synthesis. Altogether, the ability of the cell to select the correct pathway will determine its fate for every challenge it come. Despite of its importance, regulation and overlay of the different pathways is still poorly characterized due to its complexity. A major source of genomic stress in the absence of externally induced damage is the process of replication. To ensure high speed replication and genomic stability, bacteria have developed a factory composed of different proteins working together to create a stable complex with DNA known as replication fork, and associated repair proteins (Baker & Bell, 1998; Kelman & O'Donnell, 1995; Michel *et al.*, 2001).

During exponential growth HR, which is the main response to DSB, is also involved in repair of other lesions that produce a block of the replication fork. HR happens as a cascade of events (Alonso *et al.*, 2013). RecA is the central player of homologous recombination, and the different accessory factors that assist RecA can

be divided into four broad classes: those that act before homology search (end resection [AddAB or RecJ-RecQ(RecS)-SsbA] and mediators[RecO-RecR and SSbA]), those that act during homology search and DNA strand exchange (modulators RecF, RecX, RecD2, RecU]) and those that act after DNA strand exchange (processing of recombination intermediates [RadA, RecG, RuvAB, RecU, RecQ(RecS)-TopIII-SsbA]). {reviewed in Ayora *et al.*, 2011; Bell & Kowalczykowski, 2016; Cox, 2007}. At collapsed forks (one-ended DSBs) or at two-ended DSBs, RecN, which is amongst the first responders, is crucial for the assembly of a repair centre (Kidane *et al.*, 2004). The DNA ends are resected by the AddAB complex or by RecJ in concert with a RecQ-like helicase (RecQ or RecS) (Ayora *et al.*, 2011; Sanchez *et al.*, 2006). RecA-loading and filament formation are regulated by accessory factors including mediators (RecO, RecR) and modulators (RecF, RecX, RecD2 or RecU) {Cárdenas *et al.*, 2012; Kidane *et al.*, 2004; Kidane *et al.*, 2009; Lusetti *et al.*, 2006; Torres *et al.*, 2017}. After homology search, Holliday junction (HJ) structures are formed that are processed by RecG, RuvAB or RadA/Sms and resolved by RecU or dissolved by RecQ-TopoIII {reviewed in Ayora *et al.*, 2011; Bell & Kowalczykowski, 2016; Cox, 2007}.

RarA (Replication-Associated Recombination protein A), also named MgsA or YcaJ was first described and by David Sherratt's lab (Barre *et al.*, 2001), and found as a consequence of sequence identity with RuvB and DnaX (26 and 24%, in *E. coli*; and 29 and 24% in *B. subtilis*) (**Figure 1**) (Barre *et al.*, 2001). RarA is ubiquitous, *B. subtilis* RarA (YrvN) shares identity with *E. coli* RarA, and budding yeast Mgs1 and mammalian Werner helicase-interacting protein 1 (WRNIP1/WHIP) (**Figure 1**) (Barre *et al.*, 2001). There are two predicted domains with high resemblance, the ATPase and the tetramerization domain, compared to the helicase lid domain, and both N-terminal and C-terminal ends, where changes to completely different residues are more frequent, according to the predicted model for *E. coli* RarA (Page *et al.*, 2011).

Although several studies agreed with the idea that RarA acts in both replication and recombination processes, its function is still unknown. *E. coli* RarA, which is co-expressed with FtsK, co-localizes/interacts with SeqA (Lau *et al.*, 2003), RecQ (Sherrat *et al.*, 2004), UvrD (Lestini & Michel, 2007) or RecA (Shibata *et al.*, 2005) and may act at blocked forks in certain replication mutants (e.g., $DnaE^{ts}$) Lestini & Michel, 2007); Shibata *et al.*, 2005). *In vitro*, *E. coli* RarA interacts with the SSB protein, and shows

helicase activity that preferentially unwinds 3´-ends from dsDNA ends or ssDNA gaps, suggesting that RarA acts at replication forks (Page *et al.*, 2011; Stanage *et al.*, 2017). Much less is known about *B. subtilis* RarA (also termed YrvN). The *rarA* gene, which is monocistronic, is constitutively expressed, but its expression is markedly enhanced by stressors such as diamide, ethanol, high salt or H_2O_2 (Nicolas *et al.*, 2012). RarA interacts with SsbA, which in turn interacts with recombination (RecQ, RecS, RecJ, RecG, RecO, RecD2) and replication (PriA, DnaG, DnaE) proteins (Costes *et al.*, 2010). In budding yeast, Mgs1 is proposed to be part of an alternative pathway to DNA damage tolerance and homologous recombination for resolving stalled replication forks, probably enhancing processivity and/or fidelity of the DNA polymerase δ, and partially overlapping with functions of the helicases Sgs1 and Srs2 in genome stability (Barbour & Xiao, 2003). In humans, it is known that WRNIP1/WHIP physically interacts with WRN, a RecQ-like helicase (Kawabe *et al.*, 2001). One common point of RarA studies is the complex scenario required to produce a clear phenotype that explains all observations. In this study, we propose a novel approach to complement the basic genetic and biochemical approach to characterize novel proteins, in a comprehensive study of the interactions of RarA with the recombination and replication machinery.

III.1.4- Materials and methods

Bacterial strains

B. subtilis BG214 and its isogenic derivatives are listed in **Table S1**. Methyl methanesulfonate (MMS), H_2O_2 and mitomycin C (MMC) were obtained from Sigma Aldrich (Germany). Otherwise indicated the cells were grown and plated in LB medium and agar plates grown at 37 ºC. Acute and chronic viability assays were performed as previously described (Sanchez *et al.*, 2007).

Epifluorescence microscopy

B. subtilis cells dilutions were growth at 25ºC in $S7_{50}$ minimal medium to OD_{600} ~0.3. Cells were either induced with 1 mM H_2O_2 or 50 ng/ml MMC or not induced, and 2.5 µl of culture were spotted cover glasses and immobilized with coverslips coated with fresh agarose 1% (w/v) in $S7_{50}$ medium. Epifluorescence microscopy was performed using a Zeiss Axio Imager A1 microscope equipped with a 1.45 objective and a EVOLVE EMCDD camera (Photometrics). A 515 nm LED laser was used for YFP/mVenus detection, a 445 nm laser was used for CFP detection and UV lamp with

DAPI filter was used DAPI stained cells images when needed. Picture acquisition was done using VisiView (2.1.2).

For the colocalization of RarA-mVenus with the replication fork, images were taken as described above and processed equally (background subtraction and Gaussian blur) using ImageJ (National Institutes of Health, Bethesda, MD) prior to the merging.

Single molecule tracking (SMT): Due to the higher intensity of excitation, there is higher risk to detect dust particles as molecules. To reduce the background, cover glasses were cleaned using Hellmanex II 2% (v/v) and sonicated for at least 15 minutes, washed with miliQ water and dried with sterile air spray duster before mounting the cells.

B. subtilis cells dilutions were growth at 25 ºC in $S7_{50}$ minimal medium to OD_{600} ~0.3. Cells were either induced with 0.5 mM H_2O_2 or 50 ng/ml MMC or not induced, and 2.5 µl of culture were spotted in the cleaned cover glasses and immobilized with coverslips coated with fresh agarose 1% (w/v) in $S7_{50}$ medium.

Single-molecule tracking

Single-molecule tracking was performed using Nikon microscope equipped with a 1.45 objective and a EVOLVE EMCDD camera (Photometrics). A 515nm LED laser was used for YFP detection and UV lamp with CFP filter was used for CFP images when needed. Picture acquisition was done using VisiView (2.1.2). Time-lapse images of YFP were taken in a maximum of 1 min, and the length of acquisition in a sample was limited to 20 min to avoid the heating of the sample. For every time-lapse, a 20 ms exposure time bright field image was taken to determine the shape of the cells. When required, CFP images in 200 ms exposure time were taken for additional tagged proteins using CFP. Time-lapse images were prepared with ImageJ (National Institutes of Health, Bethesda, MD) and tracks were obtained using U-track (Laboratory for Computational Cell Biology, Harvard Medical School). Tracks were exported with a shape of the cell generate with MicrobeTracker (Microbial Sciences Institute, Yale) to SMTracker (currently in development by Dr. Thomas Rösch). All U-track, MicrobeTracker and SMTracker are software running in MATLAB (Mathworks). SMTracker automatically calculates: i) distribution of the tracks in the cells with overlapping with bright field or any other signal (CFP); ii) apparent diffusion coefficient

(D) and population densities based on Gaussian fit to a step-size distribution with its statistical differences based in Z-test; iii) heat maps with the preferential location of the tracks in normalized cells (sorted automatically by size into small, medium and long based on the data).

As the apparent diffusion coefficient D has some fluctuations in the different backgrounds and conditions, we defined a new parameter, the dynamic population difference (DPD), to describe the effect of the absence of one protein compared to wt or before and after of the induction with a drug in the same D conditions and provide a visual view of these effect allowing a fast comparison. Although in the concrete case of RarA is reasonable to expect that is the static, and not dynamic population, which is responsible of the function, as they probably represent the DNA-bound and free diffusion respectively, DPD is visually clearer than SPD (static population difference) and they are complementary.

III.1.5- Results

Functionality of the RarA-YFP construct

Traditionally, interactions of proteins are investigated by genetic (e.g. synthetic lethal, screens, two hybrid screens, etc.) and biochemical means (e.g. pull-down assays, protein cross-linking, etc.). We sought to investigate the cellular dynamics of RarA, using a RarA-mVenus (termed here RarA-YFP) construction, and test if its properties are altered in different genetic backgrounds. A test for the functionality of the protein was needed. Therefore, a strain expressing RarA-YFP from the original gene locus, as sole source of the protein in the cell (**Table S1**), was exposed to different doses of H_2O_2 for 15 min and plated in unperturbed conditions. The RarA-YFP functionality was analysed, showing no apparent phenotype for this drug, while null *rarA* mutant (Δ*rarA*) cells were sensitive to the drug (**Figure 4**A). To enforce this result, several replication or recombination mutants containing the RarA-YFP tagged protein were tested by chronic exposure to methyl methanesulfonate (MMS) (**Figure 4**B) or grown under non-permissive conditions (thermosensitivity assays) (**Figure 4**C). In all cases, the RarA-YFP construct had the same phenotype as the mutant strain not carrying the fusion for each condition and was clearly differenced from survival of the wild type.

Once the functionality of the protein was probed, we introduce the RarA-YFP fusion into 13 recombination-deficient mutants (Δ*recA*, Δ*recO*, *recF15*, Δ*addAB*, Δ*recJ*,

Δ*recQ*, Δ*recS*, Δ*recU*, Δ*recG*, Δ*ruvAB*, Δ*radA*, Δ*recX* and Δ*recD2*), two Y-polymerases mutants (Δ*polY1* and Δ*polY2*) related to DNA damage tolerance and into the only two replication termosensitive mutants (*dnaB*37 and *dnaC*30) that revealed a clear phenotype (see below).

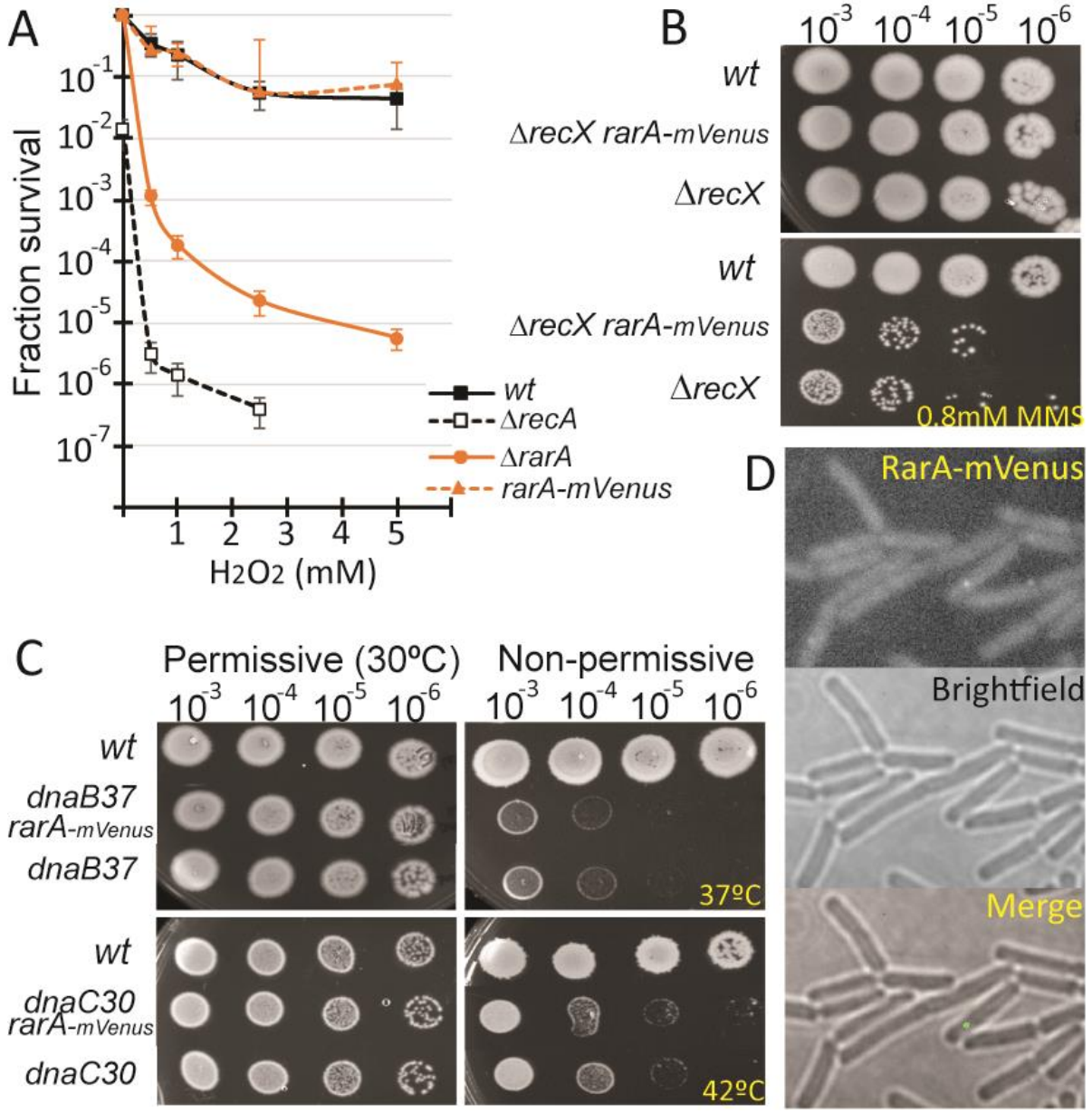

Figure 4. RarA-YFP characterization (A) Acute viability assay for the RarA-mVenus expressing strain. The presence of the m-Venus tag does not affect the viability of the strain, which is the same as wt; (B) chronic viability of ΔrecX/RarA-mVenus compared to wt and single ΔrecX mutant. The chronic exposure to MMS produces the death of both mutant strains in the same way while wt is still surviving; (C) Thermosensitivity assays for recombinational mutants dnaB37 and dnaC30 containing RarA-YFP. The fluorescence tag does not affect the response of any of the single mutants; (D) RarA-YFP foci in B. subtilis BG214 cells in exponential growth after 700 ms exposure to 515 nm laser. Only ~15% of the cells present foci.

RarA forms foci in the presence of DNA damage

Prior to the single-molecule microscopy, we screened wt cells by wide field epifluorescence microscopy to have an overview of the time response to the DNA drugs. In exponential growth conditions at 25ºC (OD_{600}= ~0.3), 15% of the cells contained RarA-YFP foci (**Figure 5**A). This percentage remained apparently constant at different time points (60 and 120 min), indicating that focus formation during unperturbed growth is maintained at about a constant rate. When cells were exposed to a DNA damaging agent, the population of cells containing RarA-YFP foci increased after some time. Cells were exposed to different drugs (MMS, MMC and H_2O_2) to compare the responses. After addition of MMS or of MMC, cells showed a similar type of response, starting at 30 min and reaching a plateau at 60 min with a maximum value that remained constant at least until 90 min (**Figure 5**A). The intensity of the response, considered as the increase of the percentage of cells containing RarA-YFP foci, was ~15% higher after MMC and ~6% after MMS addition (**Figure 5**A, grey shade). On the other hand, H_2O_2 addition produced an increase in the population of cells containing foci that occurred before (15 min) and had a higher maximum value (~45%) compared with MMS or MMC treatment. In epifluorescence, an accumulation of fluorescent molecules is needed for detection, so it is reasonable to say that in response to drugs that produce DNA damage, RarA is recruited to some position(s) within the cell in more cells than under exponential growth conditions. The presence of foci in 15% of cells under normal conditions suggest that RarA plays a physiologic function of RarA during the cell cycle, at least in a fraction of cells.

RarA-YFP focus formation is influenced by absence of RecA accessory proteins

The formation of RarA foci was tested in the absence of RecA mediators (RecO) or modulators (RecF, RecX, RecU and RecD2). As revealed in **Figure 5**A-C, we observed an increase (twice of that seen in wt cells) in the cells containing foci even during normal growth conditions. There were no considerable differences in the response to H_2O_2 and MMC, as both started at 15 min and reached a maximum between 45-60 min. This means that the response to MMC occurred faster than in wt cells (10% difference in 15, 30 and 45 min) but with the same increase in cells containing RarA-YFP foci. In contrast, when RecD2 was not present there was a delay in the H_2O_2 response (**Figure 5**C) and the increase in the plateau was less pronounced than in wt (~20% for H_2O_2 and 10% for MMC, ~10% and ~5% less than wt respectively). Also,

Δ*recX* cells (**Figure 5**C) show similar dynamics than wild type cells but the increase in the plateau is similar to that seen in Δ*recD2* cells.

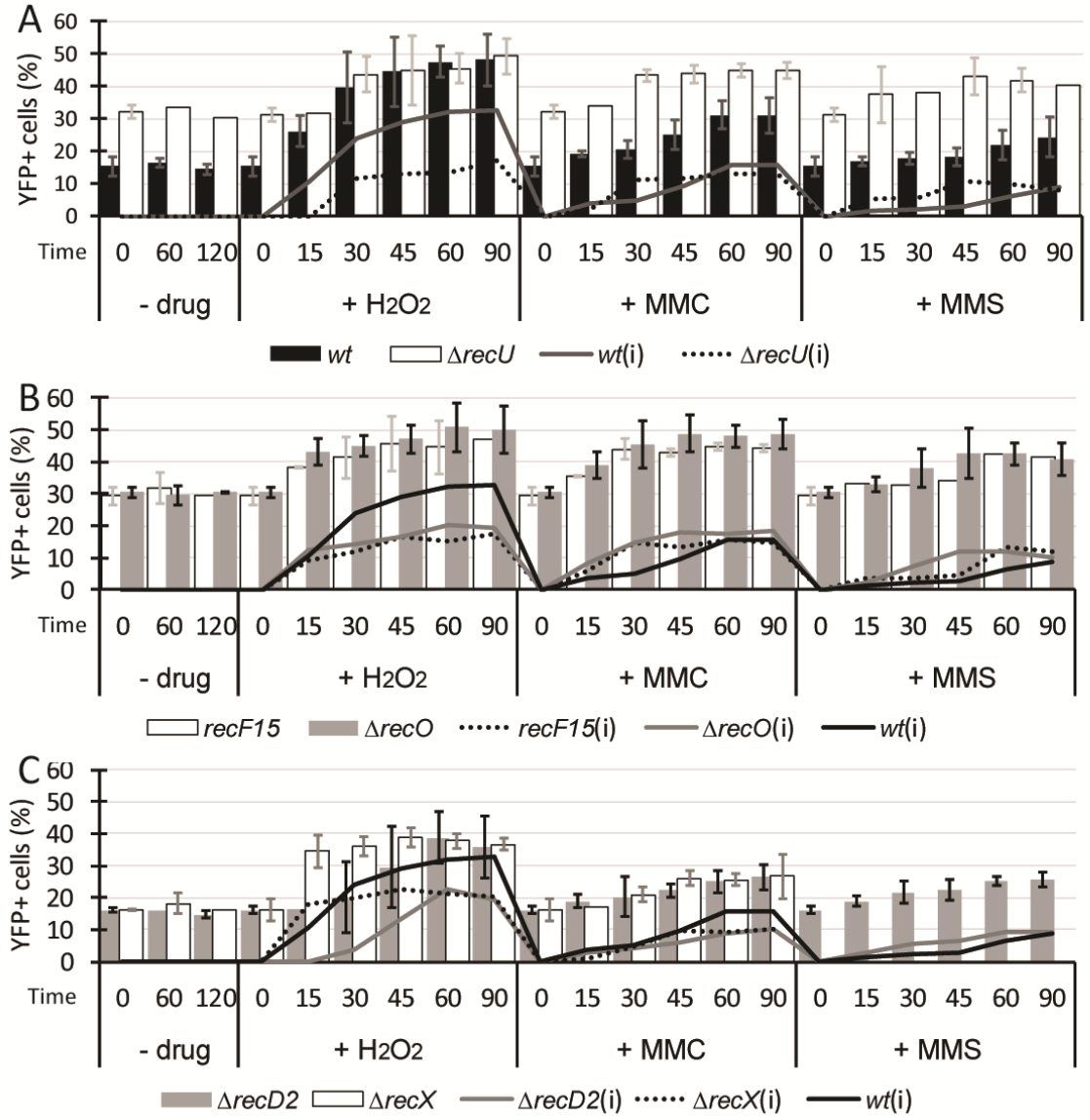

Figure 5. Epifluorescence for RarA-YFP recombinational backgrounds. (*A-C*) percentage of cells that contains foci in exponential growth and after induction with H_2O_2 (1 mM), MMC (50 ng/ml) or MMS (5 mM) in wt and Δ*recU* (*B*), Δ*recO* and *recF15* (*C*), Δ*recD2* and Δ*recX* (*D*) backgrounds. Lines correspond to the increase (i) of YFP^+ cells considering the exponential growth as time 0. Error bars represent the standard deviation of at least three independent experiments.

RarA-YFP dynamics are influenced by DNA damage

The finding that RarA-YFP foci are only found in a subset of cells could indicate that it assembles only in response to circumstances that occur is a fraction of cells. It is also possible that RarA-YFP foci assemble and disassemble within a short time frame, such that at any given time, they are present in a minority of cells, although all cells do

contain foci at different time points of the cell cycle. This was observed, e.g. for DNA gyrase and for topoisomerase I, which form foci within less than 1 min time scales (Tadesse and Graumann, 2006). We wished to obtain information on the dynamics of single RarA molecules, in order to assess how many are statically bound to the chromosome, and how many are moving through the cell. We employed single molecule fluorescence microscopy and automated single molecule tracking (SMT) (Schenk *et al.*, 2017), using three conditions: unperturbed exponential growth, treatment with H_2O_2 (0.5 mM) or with MMC (50 ng/ml). 60 min exposure to the drugs was considered as the best condition for the analysis of the mobility response, as the maximum plateau concerning focus formation was reached for every mutant in every condition in this time in the epifluorescence screening (see **Figure 5**).

When single RarA-YFP molecules where observed in single-molecule microscopy, we observed two major modes of movement: rapid random movement through the cell, and slow movement around a point. Both types of movement could be found for the same molecule, as the example given **Figure 6**A. **Figure 6**B represents the heat map of the molecule, and shows that initial long steps are followed by short steps, and ensuing longer steps. Thus, RarA molecules could be seen to alternate between random movement and confined motion around one point, i.e. a binding event.

SMT analysis of RarA-YFP revealed the presence of two populations of molecules considering their diffusion coefficient (D): a dynamic population, freely diffusing in the cytosol (D ~ 2.5 $\mu m^2 s^{-1}$) and a slow-moving subpopulation, probably interacting with DNA (D ~ 0.25 $\mu m^2 s^{-1}$). Free diffusion of YFP (a YFP derivative) in *B. subtilis* occurs at about 3 $\mu m^2 s^{-1}$ (our unpublished data), while a large protein such as SMC (270 kDa as a dimer) moves through the DNA with 0.45 $\mu m^2 s^{-1}$ (Luise *et al.*, 2013). With 2.5 $\mu m^2 s^{-1}$, mobile RarA-YFP is thus likely a freely diffusing monomer, and slow 0.25 $\mu m^2 s^{-1}$ molecules a DNA-bound fraction of RarA. Different patterns of movement (i.e. where are fast and slow molecules within the cell) will be described below. Diffusion coefficients were similar in the different backgrounds studied, as expected for the same protein (**Table S2**, **Figure S1**A), but we found considerable changes in population sizes depending on the background and the kind of DNA damage that was induced. To compare different backgrounds and conditions we defined a parameter, Dynamic Population Difference (DPD) that compares the weight

on the dynamic population for one condition, and its effect on the same D value. In other words, DPD reflects the changes in the number of dynamic molecules, which are inverse for the static population.

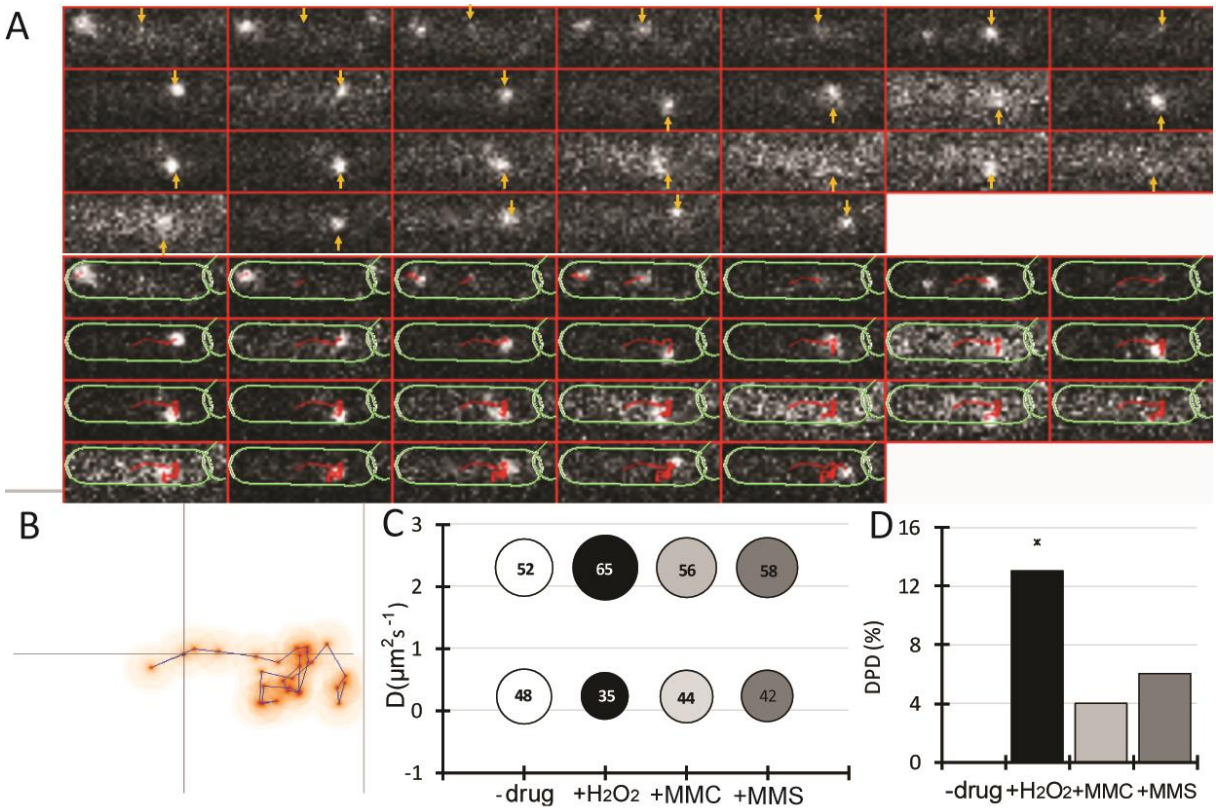

Figure 6. RarA dynamic behaviour. (*A*) Single-RarA-YFP molecule moving in the cell (top) and the automatic detection of U-track (down). Exposure time was 10 ms. (*B*) Representation of the molecule showed in *A* in a heat map. Red colour indicates intensity of the signal. (*C*) Diffusion coefficient and weight of populations for RarA-YPF in wt background in exponential growth and 60 minutes after the addition of 0.5 mM H_2O_2, 50 ng/ml MMC or 5 mM MMS. Surface of the circles indicates % of molecules. (*D*) Comparison of dynamic population in the different graphs. Significant differences were only seen upon H_2O_2 treatment.

In wt cells, 48% of RarA molecules were static (i.e. interacting with DNA) during unperturbed exponential growth. Note that the true number is somewhat lower, because even freely diffusing molecules can stop for very short time periods. The presence of DNA damage in all stress conditions (H_2O_2, MMS and MMC) produced an increase in the dynamic population (**Figure 6**C), but differences were statistically significant only for H_2O_2 treatment (**Figure 6**D). As the absence of RarA leads to a stronger phenotype after H_2O_2 treatment than for MMS or MMC (see below), it is reasonable to suggest that this increase of the dynamic population is influenced due to the function of RarA.

RarA-YFP dynamics were clearly modified in the absence of several HR proteins. In the Δ*recD2,* Δ*recJ,* Δ*recS* and Δ*ruvAB* mutant backgrounds the dynamic population was reduced, whereas it increased in the Δ*recU* cells growing unperturbed (**Figure 7**A). Please note that the changes shown in **Figure 7** not only incorporate the differences between wt and mutant strains considering percentage of static/dynamic fractions (**Table S2.**), but also incorporate changes in the diffusion rates of the dynamic fraction. In other words, RarA-YFP molecules in many cases not only quantitatively become more dynamic, but the diffusion rates also differ, which can arise from differences in the transitions between static and dynamic movement.

The response of RarA-YFP dynamics to H_2O_2 damage in wt cells included a significant increase in the dynamic population (**Figure 6**D). Interestingly, RarA showed no response to H_2O_2 treatment in the Δ*recO*, Δ*recD*2, and Δ*recX* compared to the wt strain (**Figure 7**B), ln Δ*recS*, Δ*ruvAB* and Δ*polY1* mutant cells the dynamic population was significantly increased, whereas it was significantly decreased in the *recF*15, Δ*addAB*, Δ*recJ*, Δ*recQ*, Δ*recU*, Δ*recG*, Δ*radA* and Δ*polY2* mutant cells (**Figure 7**B).

Upon MMC treatment, wt cells did not show a significant change in the dynamics of RarA (**Figure 6**D). Lack of RecD2, RecS or of PolY1 significantly increased the dynamic population of RarA, while absence of AddAB and RecU significantly decreased the dynamic population (**Figure 7**C). Our data revealed that RarA movement is altered in the absence of end-resection proteins (AddAB, RecJ, RecS and RecQ) and Holliday junction-processing enzymes (RecU, RuvAB, RecG and RadA/Sms), while the Y-polymerases modified the response to either H_2O_2 (PolY2) or MMC (PolY1). The RarA movement in cells lacking RecA mediators and modulators is dependent of the DNA damaging agents tested. As will be further shown below, these findings corroborate with genetic interactions, showing that our tracking analysis produced important and interesting connections between RarA and proteins involved in HR.

In addition to the changes in dynamics, the preferential location of RarA molecules was studied by generation of heat maps in cells normalized to a size of 3 x 1 μm. For that purpose, cells were sorted into three cell fractions: small, medium and big. This approach produced homogeneity in the cell prior to the normalization (**Figure S1**B), and thus allowed us a more accurate comparison between conditions and different mutants in the subcellular distribution of the molecules.

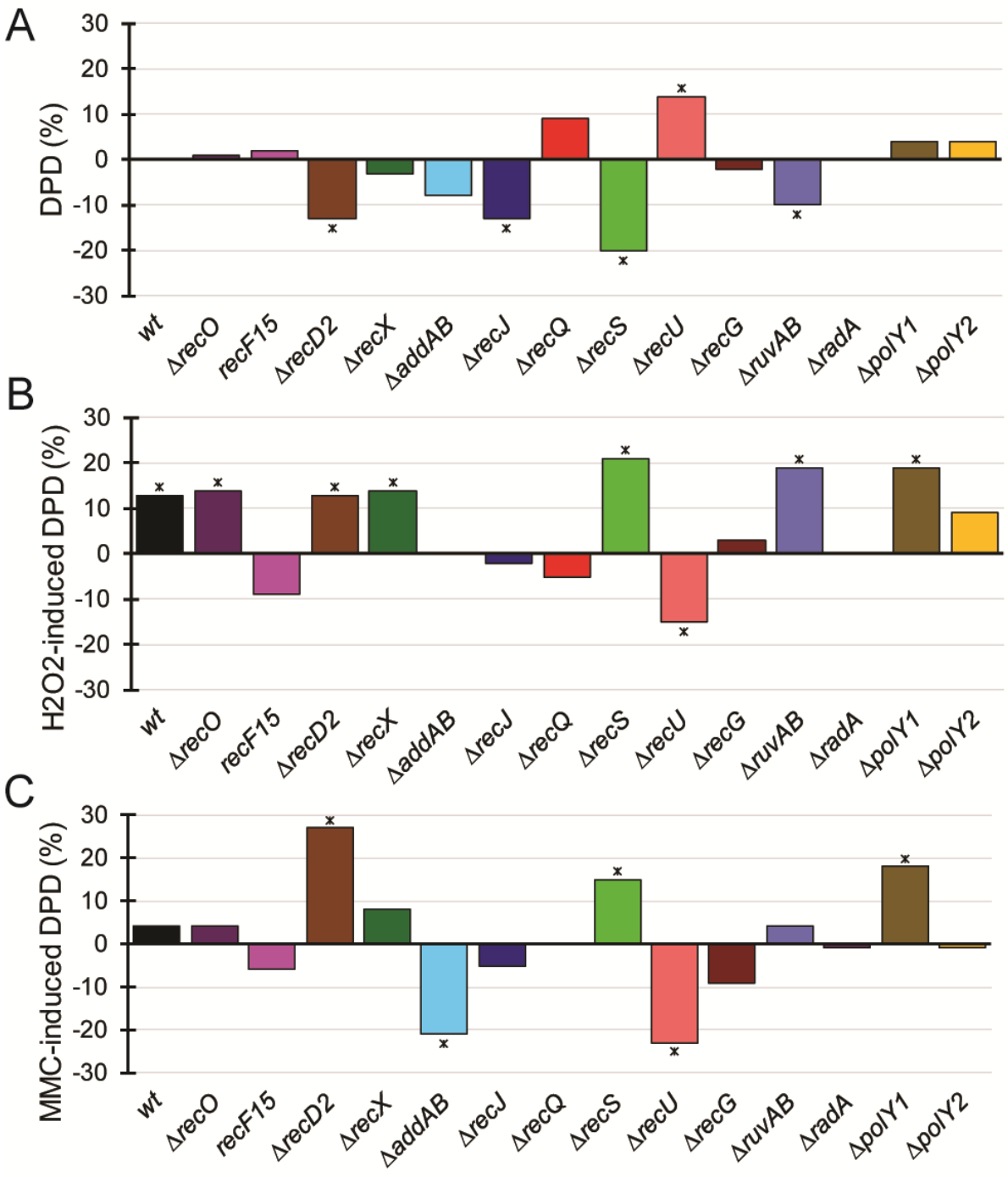

Figure 7. Single molecule tracking analysis for RarA-YFP in recombinational and Y-polymerases backgrounds. (*A*) RarA-YFP dynamic population difference in the backgrounds studied compared to wt in -drug condition. RarA-YFPs DPD after addition of H_2O_2 (0.5 mM, *B*) or MMC (50 ng/ml, *C*) for 60 min compared to -drug conditions in each background. * represent statistical significance in Z-test (included in SMTracker, see methods).

For exponential growth conditions in wt cells (**Figure S2**C), RarA-molecules were found throughout the cytosol with a slight preference for the 3/4 position of the cell. After H_2O_2 addition, this distribution was somewhat changed with a preference to the

middle of the cell. In contrast, MMC did not change RarA distribution. Although there was no clear correlation of distributions and dynamics, after H_2O_2-induced DNA damage, RarA-YFP was more spread out through the cells with slight preference to the centre. This behaviour correlated with a significant increase of the dynamic population for wt, Δ*recO*, Δ*recD2* (**Figure S1**C), Δ*recS* (**Figure S2**A) and Δ*ruvAB* (**Figure S2**) backgrounds, but also occurred on *recF15* (**Figure S1**C) and Δ*recJ* (**Figure S2**A), where there were no significant changes in population sizes. Moreover, Δ*recU* cells showed an opposite behaviour (**Figure S2**B), concentrating RarA in the 3/4 regions of the cells after H_2O_2 treatment, and this is correlated with a significant decrease in the dynamic population. MMC-induced DNA damage also changed the distribution of RarA-YFP, as seen by spreading of the molecules throughout the cell, but there was no detectable preference for the centre, in the backgrounds in which RarA dynamics were significantly increased: Δ*recD2* (**Figure S1**C), Δ*recS* (**Figure S1**A), and ΔpolY1 (**Figure S2**B) cells.

RarA location and dynamics are related to the replication machinery

We wondered if changes in RarA dynamics might be related to effects occurring at the DNA replication forks. Therefore, we investigated RarA-YFP in the *dnaB*37 or *dnaC*30 context that revealed a clear phenotype in the Δ*rarA* context (see below). As these genes are essential, thus a thermosensitive mutant strategy was followed. All fluorescence analyses were performed using 25ºC as permissive temperature and 42ºC as non-permissive temperature.

In the first epifluorescence screening, in permissive conditions, RarA focus formation was similar in both mutant backgrounds compared with the wt strain, before and 60 min after the addition of MMC (50 ng/ml) (**Figure 8**A). Interestingly, after thermal inactivation of DnaB or DnaC, RarA focus formation increased to levels that were similar to the induction of MMC, while wt cells were not affected by the higher temperature (**Figure 8**A).

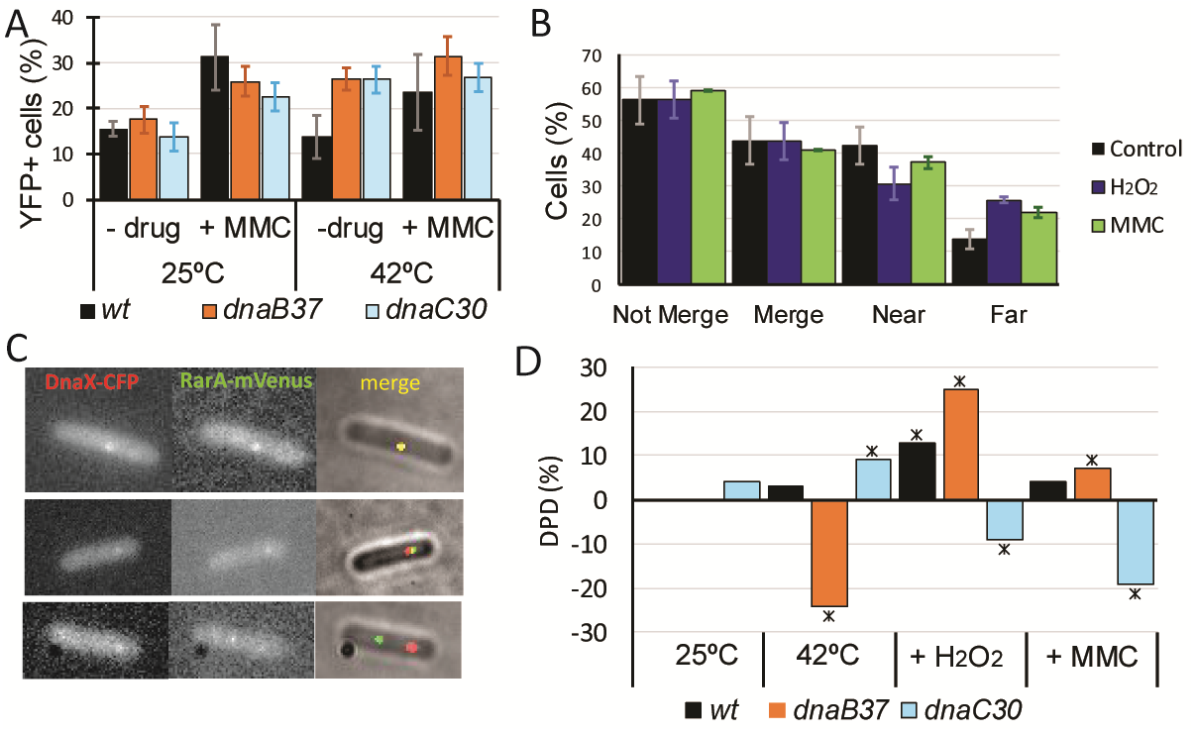

Figure 8. RarA interactions with the replication machinery. (*A*) Percentage of cells that contains RarA-YFP foci in thermosensitive replication mutants compared to wt cells in epifluorescence microscopy, in exponential growth at 25ºC (OD_{600}= ~0.3) and after addition of MMC (50 ng /ml) or swift to non-permissive conditions (42ºC). Error bars shows standard deviation of at least three independent experiments; (*B*) Weight of different colocalization patterns after addition of H_2O2 (1 mM) or MMC (50 ng/ml) for 60 min compared to exponential growth. (*C*) Examples of the colocalization of DnaX-CFP and RarA-YFP (up) and non-colocalizing patterns defined as near (medium) and far (down). (*D*) RarA-YFP single-molecule DPD in thermosensitive mutants. Swift to non-permissive temperature (42ºC) leads to drastic changes in dynamics in absence of external DNA damage and alters the normal response of RarA after addition of H_2O_2 or MMC.

To study if the RarA-YFP foci observed upon inactivation of DnaB or DnaC are related to the replication factory, a new strain was constructed by adding a DnaX-CFP construct to the RarA-YFP background. DnaX-CFP is a good marker for the replication machinery, as it is part of the clamp loader complex. Under exponential growth conditions, ~40% of the RarA-YFP foci co-localised with DnaX-CFP foci, and this number did not change when cells were exposed to H_2O_2 or MMC (**Figure 8**B). The observation of the non-colocalising RarA-YFP and DnaX-CFP foci showed two clear different possibilities: ~40% of the RarA molecules were close to the replication machinery (**Figure 8**C, medium panel; **Figure 8**B) while only ~10% were far from the DnaX-CFP foci (**Figure 8**C, down panel; **Figure 8**B). Interestingly, these values changed drastically in the presence of DNA damage, increasing in 12% and 8%, for the far RarA molecules 60 min after the addition of H_2O_2 or MMC, respectively (**Figure 8**B). During

normal growth conditions, almost 80% of the foci were located next to the replication machinery, and this can explain the heat maps for the exponential growth detected in SMT experiments (**Figure S1**C, **Figure S2**), as the cells analysed were in a size for which it is reasonable to expect two replication forks (Berkmen & Grossman, 2006). To further characterize the co-localization, SMT was done. This is possible as the replication machinery movement is in a different time-scale than the tracking: it takes several minutes for changing the position of the fork (Migocki *et al.*, 2004), so a single DnaX-CFP image is valid for the first minute of exposure time to the laser for SMT. DnaX-CFP is not interfering with RarA-YFP movement as the D values and population weights are similar to those of wt cells lacking DnaX-CFP (**Table S2.**) and there is no differences when DPD is considered (data not shown). Although RarA-YFP tracks are located all over the cell, there is a concentration around the replication machinery in a cloud-like manner (**Figure 9**A-C), and in these "clouds", molecule tracks appear to be confined (in a manner we cannot yet explain), whereas for tracks that are not related to these clouds, also long steps of movement could be observed. To verify these observations, we measured the distance between the signal for the visible replication fork(s) and the origin and end point of each track, providing us with the estimation of localization of the tracks compared to replication forks, with the minimum diameter of a circle that contains every point of the tracks of a single molecule, which yields information about the movement of each molecule. Further, tracks were sorted by the size of the circle compared to the average size of DnaX-CFP foci (i.e. 250 nm in diameter) into three types: a) confined, when it was smaller or equal; b) random, when it was bigger; and c) dual, in the special case that more than half of the steps in an otherwise random track were confined. Track point-localization for each size was sorted in a similar way as it was expressed for epifluorescence in merge (contained in the DnaX-CFP foci), near (contained in the area between the DnaX-CFP foci and two times the average size of DnaX-CFP foci) and far (in all other cases).

In the absence of drugs (**Figure 9**A), tracks were preferentially confined (~55%) and in these confined tracks, half of the track origin and ends were located merging with the replication machinery (**Figure 9**D). After H_2O_2 exposure (**Figure 9**B), confined RarA-YFP tracks were located preferentially far from replication machinery instead of merging. Finally, MMC induction (**Figure 9**C) markedly increased the percentage of random tracks.

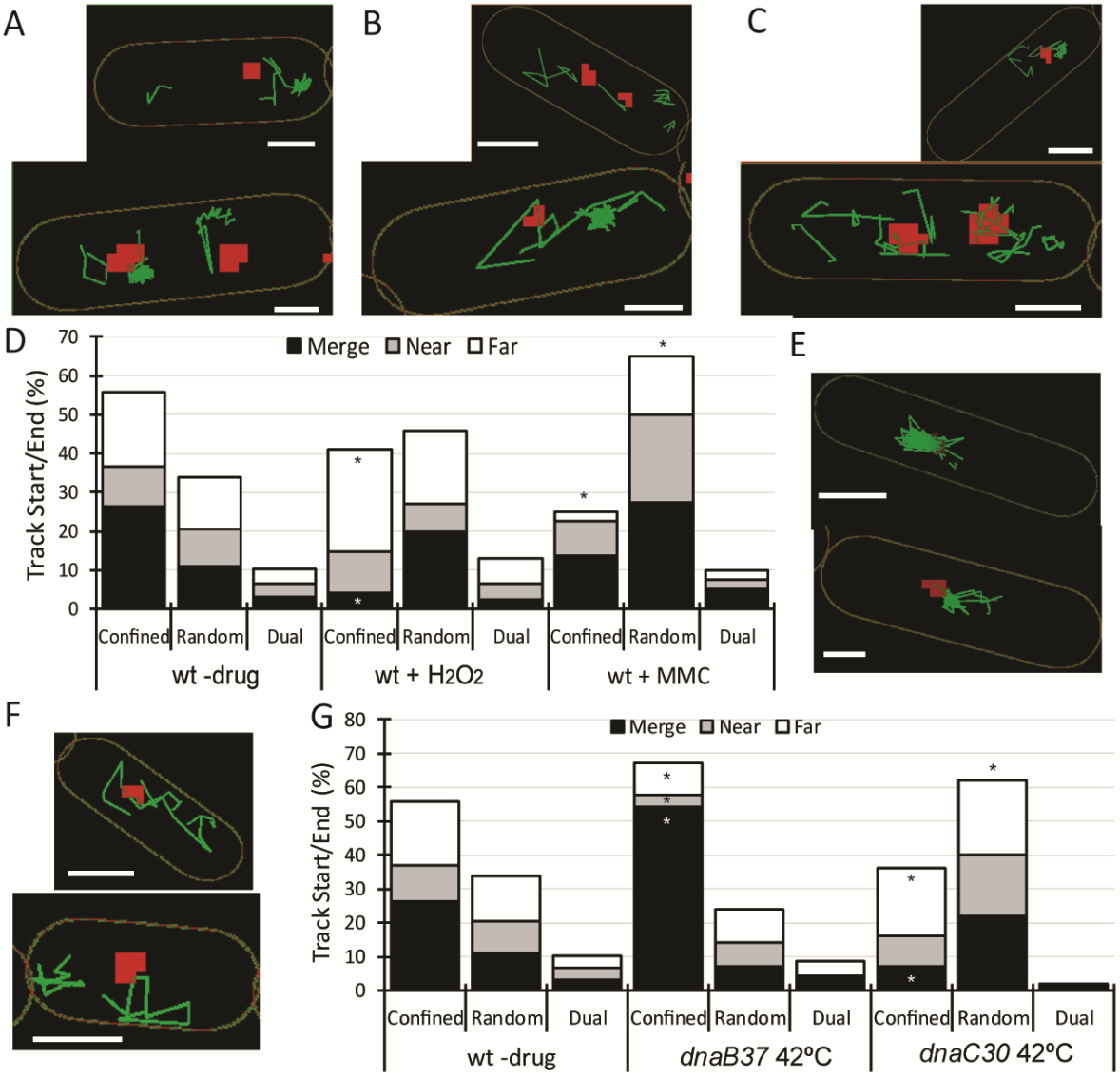

Figure 9. RarA interactions with the initiation complex in the presence of DnaB37 at non-permissive temperature. (A-C and E-F) Examples of cells with the distribution of RarA-YFP tracks (green) in relation to the replication fork, marked as DnaX-CFP (red), in absence of DNA damage (A), in presence of H_2O_2 (0.5 mM, B) or MMC (50 ng/ml, C) for 60 min at non-permissive temperature (42ºC) in the *dnaC30* (E) and *dnaB37* (F) mutants. Scale bars correspond to 1 µm. (D, G) Distribution of the weights of colocalization of the origin and end points of the RarA-YFP tracks sorted by its movement with DnaX-CFP in exponential growth, H_2O_2 (0.5 mM) and MMC (50 ng/ml) (D) in *dnaB37* and *dnaC30* mutant at non-permissive temperatures (G). * means significant differences in Marasculio test.

Non-functional DnaB37 led to a drastic decrease in the dynamic population of RarA (**Figure 8**D, **Table S3**). On the other hand, thermal inactivation of DnaC led to an increase in the dynamic population of RarA. The RarA tracks in *dnaB*37 cells (**Figure 9**E) were mostly confined (~70%), and specially merged with the replication machinery (54%) (**Figure 9**G), while tracks in *dnaC30* cells (**Figure 9**F), mostly presented random

movement (~60%), and confined tracks were located preferentially in “far” positions relative to replication forks (**Figure 9**G). Taken together, these data suggest that DnaC contributes directly to RarA binding to DNA (as judged by static localization) while a potential DnaB interaction could be related to the removal of RarA from forks.

When either H_2O_2 or MMC were added under semi-permissive temperatures, the dynamic RarA population was significantly increased in *dnaB*37 cells, while in the *dnaC*30 strain, it became significantly more static (**Figure 8**D).

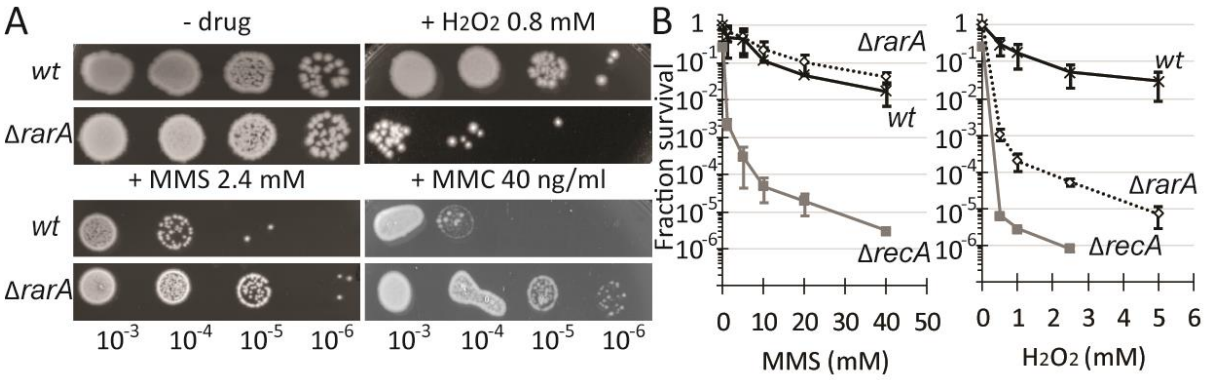

Figure 10. Characterization of Δ*rarA* mutant strain. (*A*) Compared viability of wt and Δ*rarA* growing in plates containing MMC (40 ng/ml), H_2O_2 (0.4 mM) and MMS (2.4 mM). (*B*) Compared viability of wt, Δ*rarA* and Δ*recA* after 15 min exposure to increasing MMS (1, 5, 10, 20 or 40 mM) and H2O2 (0.5, 1, 2.5 or 5 mM) concentrations, expressed as CFU counted compared to CFU in absence of drug.

Phenotypic correlations for drug exposure

We wondered if changes in RarA movement would correlate with “genetic interactions” in double mutant backgrounds. We therefore analysed phenotypes of a Δ*rarA* deletion in recombination-deficient strains testing for drug sensitivity. Upon chronical exposure to MMS or MMC, the Δ*rarA* mutation partially suppressed the sensitivity of the wt strain, while mutant cells were more sensitive than wt cells when grown on H_2O_2 containing LB plates (**Figure 10**A). When cells were acutely (15 min) exposed to drugs, and then allow to grow under unperturbed conditions on LB plates, Δ*rarA* cells showed a similar resistance to MMS compared to the wt strain or even slightly more resistant (**Figure 10**B). In contrast, Δ*rarA* cells were very sensitive to H_2O_2 (**Figure 10**B). Since Δ*recA* cells were extremely sensitive, much more than Δ*rarA* cells (**Figure 10**B), we assume that lack of RarA did not abolish recombinational DNA.

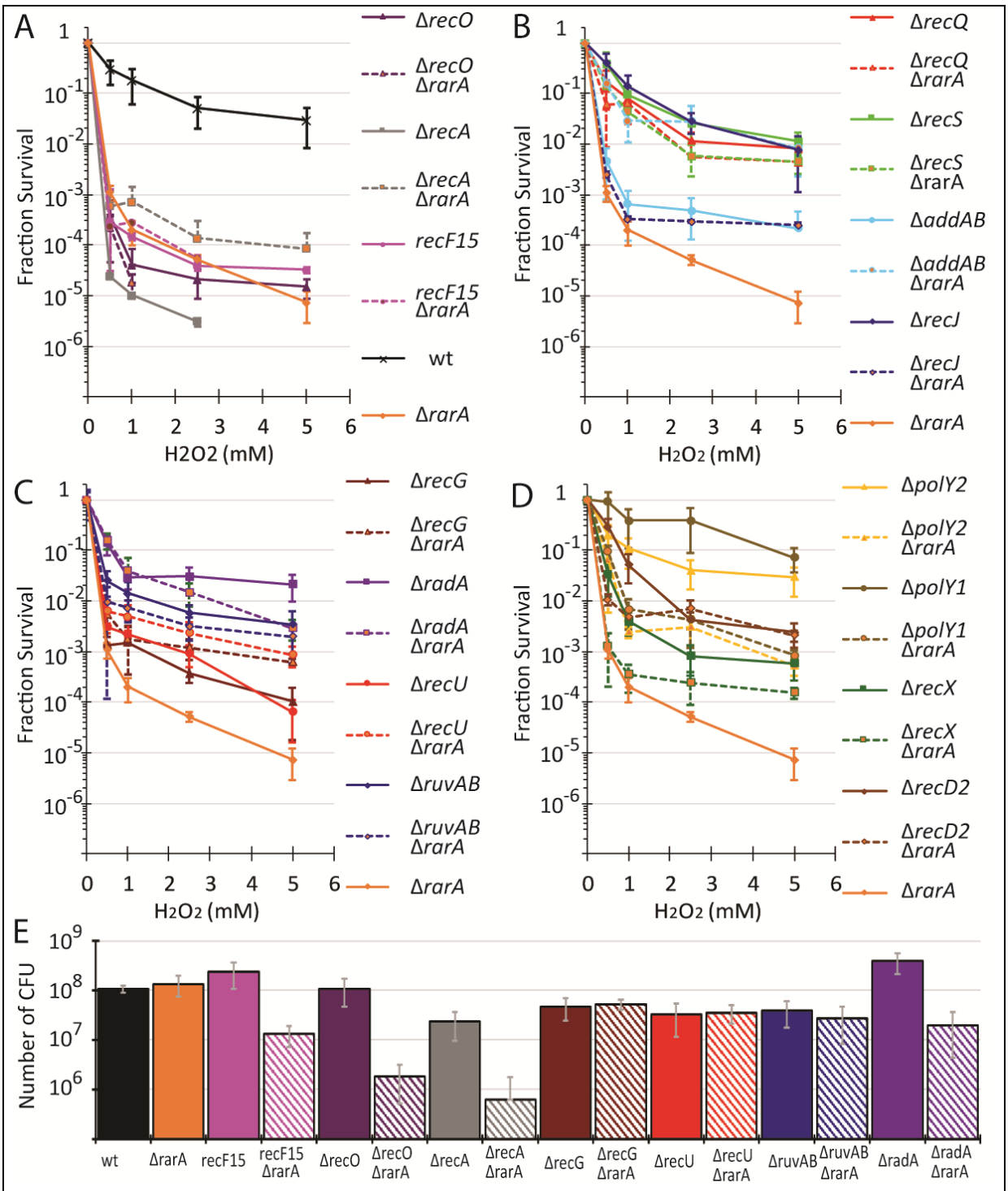

Figure 11 Genetic interactions of Δ*rarA*. (A-D) Acute viability of Δ*rarA* double mutants. Cells were grown to reach exponential phase (OD_{560}=0.4) and exposed to different concentrations of H_2O_2 for 15 min prior to serial dilutions. Cells were counted as CFU after a O/N culture in LB from correspondent dilutions and expressed compared to -drug CFU. (E) Number of CFU in exponential growth when viability is compromised and parental strains.

When cells were grown in unperturbed conditions, absence of RecO, RecF or RecA severely compromised cell viability in the Δ*rarA* context (**Figure 11**D). The absence of RecO, RecF, RecX, RecU or RecD2 rendered the cells from very to

extremely sensitivity to H_2O_2 or MMS treatment (**Figure 11**, **Figure S3**). A lack of RarA did not increase the sensitivity of Δ*recO, recF15,* Δ*recU or* Δ*recD*2 cells to H_2O_2 or MMS treatment (**Figure 11**, **Figure S3**). When we generated a Δ*recR* Δ*rarA* double mutant strain, it revealed a severe growth defect and a similar survival curve than Δ*recO* Δ*rarA* cells (data not shown). The absence of RarA did not increase the sensitivity of *ΔrecA* cells to H_2O_2 or MMS treatment (**Figure 11**A, **Figure S3**A). Lack of RarA, however, only moderately increased the sensitivity in the Δ*recX* or Δ*radA* context (**Figure 11**C, D, **Figure S3**C, D). Altogether, these data suggest that RarA works in concert with RecA, and with proteins related to RecA loading and/or regulation of filament dynamics.

Lack of DSB recognition (RecN) or functions involved in long-range end-resection (AddAB, RecJ, RecS or RecQ) partially suppressed the acute sensitivity to increasing H_2O_2 and MMS concentrations in the Δ*rarA* context (**Figure 11**B, **Figure S3**B), suggesting that RarA does not work in concert with these processes.

The absence of branch migration translocases (RuvAB, RecG) partially suppressed the acute sensitivity to increasing H_2O_2 or MMS concentrations in the Δ*rarA* context (**Figure 11**C, **Figure S3**C), suggesting that RarA also does not work in concert with functions involved branch migration, also in agreement with the SMT data.

Furthermore, we determined the influence of a lack of RarA in the absence of translesion synthesis type-Y polymerases (PolY1 or PolY2). Both Δ*polY1* Δ*rarA* and Δ*polY2* Δ*rarA* double mutants partially suppressed the acute sensitivity to increasing H_2O_2 (**Figure 11**D) or to MMS treatment (**Figure S3**C). Thus, RarA does not appear to work in concert with functions involved in translesion synthesis.

Finally, we tested the influence of lack of RarA under semi-permissive temperature of thermosensitive mutants impaired on the essential DNA polymerases (PolC and DnaE), the clamp loader (DnaX), DNA primase (DnaG), or one subunit of the preprimosome (DnaB) involved in helicase loading or in the replicative hexameric helicase (DnaC). The Δ*rarA* cells were not affected by temperature shifts. Only the dnaB37 or dnaC30 mutants grown at semi-permissive temperature showed a stronger phenotype in the Δ*rarA* context when compared to their correspondent single mutant parent (**Figure 12**).

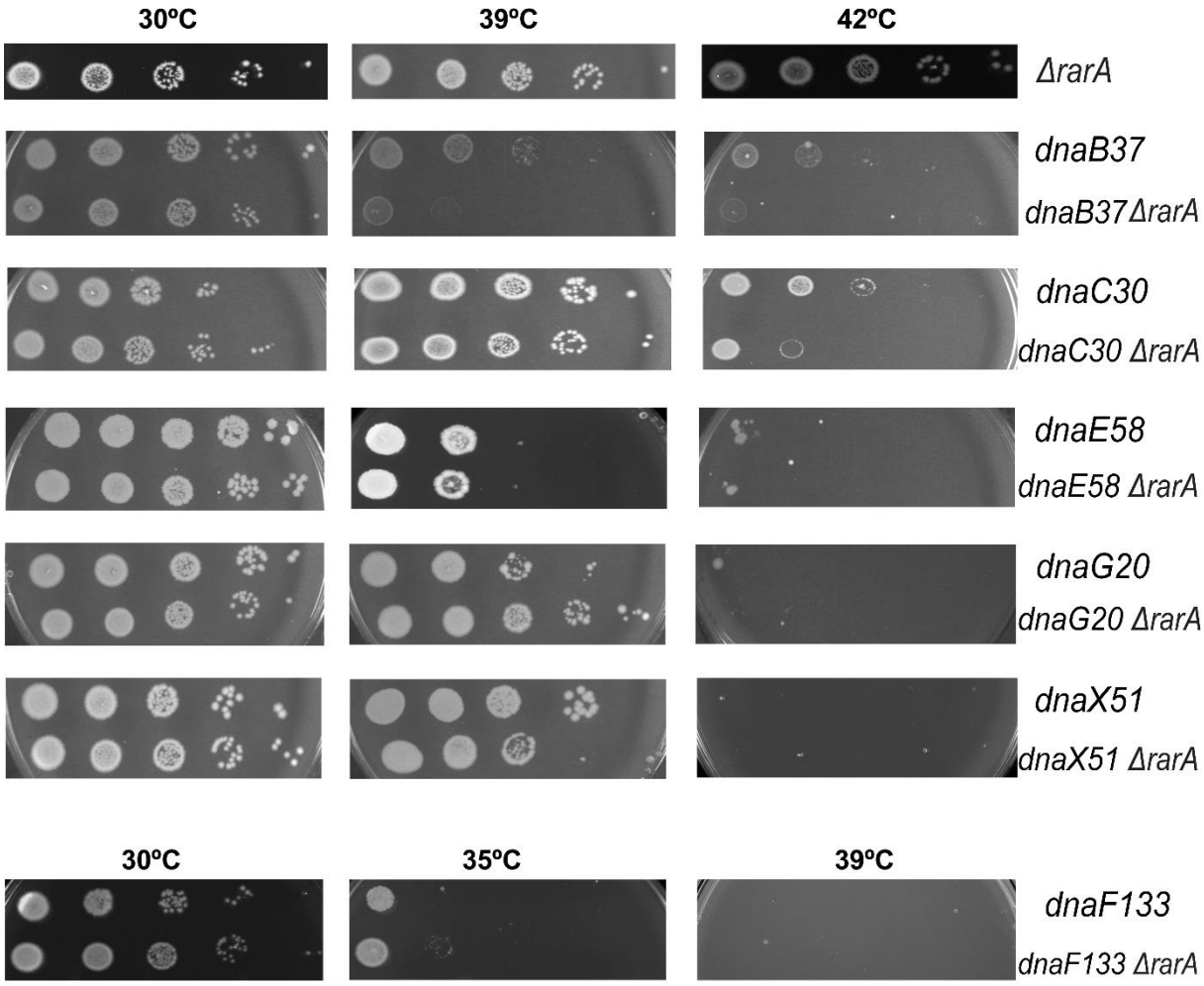

Figure 12. The Δ*rarA* mutation increases the thermosensitivity of *dnaB37* and *dnaC30* mutant strains. Cells were grown to reach exponential phase ($OD5_{60}$= 0.25) at 30ºC, diluted, spotted in LB plates and grown overnight at the indicated.

III.1.6- Discussion

Our work shows that the ubiquitous RarA protein, an ATPase of unknown function, plays an important role in the maintenance of DNA integrity, in close connection to proteins involved in replication fork re-start (DnaB and DnaC), and those that positively (RecO, RecF) or negatively (RecU, RecX, RecD2) regulate RecA activities. We also show that single molecule tracking provides a novel concept for a screen for protein interactions, or more generally for protein connectivity.

In *E. coli*, RarA has been traditionally associated with the replication machinery, even used as a marker for replication fork (Sherrat *et al.*, 2004). Here, we have probed by epifluorescence and single-molecule microscopy that, for *B. subtilis*, this is not always the case, as ~20% of the foci found were not related to the replication fork(s)

(**Figure 8**B, **Figure 9**D). Thus, after H_2O_2 damage, movement of RarA become increased, but also there was a higher number of molecules confined far from the replication forks (**Figure 9**B) and the number of foci far from the replication fork was also increased (**Figure 8**B), suggesting that RarA can be recruited to stalled forks and broken DNA ends (Atkinson & McGlynn, 2009; Gabbai & Marians, 2010; Kuzminov & Stahl, 1999; Michel *et al.*, 2001; Yeeles & Dillingham, 2010).

Under exponential growth conditions, the location of RarA in the replication machinery can be mainly explained considering the interactions with SsbA (Costes *et al.*, 2010) and with pre-primosomal components (e.g. DnaB, PriA) rather than with the DnaC replicative DNA helicase (data not shown). DnaC, which translocates on the lagging-strand template in a 5´→3´direction, is the hexameric replicative helicase that is part of the primosome and initiates the assembly of the replisome (Sanders *et al.*, 2010; Velten *et al.*, 2003). In contrast, DnaB is a pre-primosome component involved in DnaA- or PriA-dependent initiation of DNA replication by contributing to loading of DnaC (Bruand *et al.*, 2001; Polard *et al.*, 2002; Smits *et al.*, 2010; Smits *et al.*, 2011; Soultanas, 2002; Zhang *et al.*, 2005). When *dnaC30* thermosensitive mutants were exposed to non-permissive temperatures, RarA movement became significantly more dynamic, while the opposite effect occurred in *dnaB37* cells (**Figure 8**D). Localisation of the tracks shows that RarA molecules confined to the replication forks are more abundant with a non-functional DnaB (**Figure 9**E, F). Altogether, these data suggest that DnaC contributes to the confinement of RarA, whereas DnaB contributes to the removal of RarA from to the replication forks. Alternatively, RarA, working prior DnaB, contributes to control preprimosome assembly, and then leaves the pre-initiation complex together with all primosome components (PriA, DnaD and DnaI). This location must be related to a role of RarA during replication, as its absence in both backgrounds lead to a loss of viability in semi-permissive conditions (**Figure 12**), although it is unclear if these effects are caused due to a direct interaction of RarA with a component of the preprimosomal complex, or due to in an indirect interaction involving SsbA (Costes *et al.*, 2010). The importance of RarA, in combination with other recombination factors, to correct and repair DNA damage during replication is confirmed by the genetic interaction of RarA with RecA mediators (RecO, RecR) and modulators (RecF, RecD2, RecU) (**Figure 11**, **Figure S3**). In addition, our novel SMT approach revealed a silent regulation of the dynamics of RarA in the absence of other recombination factors, such

as RecJ, RecS, AddAB, RuvAB or RecG (**Figure 7**A), if we consider that in all these backgrounds, deleting *rarA* partially suppressed the sensitivity to DNA damaging agents. Further studies are needed to determine what is the concrete effect of these changes on RarA behaviour in the cell. All genes and proteins mentioned above have been characterized in the context of replication fork regression and replication fork restart in previous studies (Courcelle & Hanawalt, 1999; Seigneur *et al.*, 2000; Walsh *et al.*, 2014), including RarA for both prokaryotes (Barre *et al.*, 2001; Lau *et al.*, 2003) and eukaryotes (Barbour & Xiao, 2003).

Observation by epifluorescence, and especially with SMT, revealed differences in RarA mobilization in the presence of DNA damage (**Figure 5**, **Figure 6**), depending if the function is crucial for survival, e.g. after addition of H_2O_2, or not, i.e. when cells are exposed to MMS or MMC (**Figure 10**). H_2O_2-induced DNA damage lead to an increase in the dynamic population of RarA (**Figure** 7C, D), but also in the recruitment of RarA (**Figure 6**B) to areas located out of the influence of the replication forks (**Figure 8**B, **Figure 9**B-D). This mobilization is influenced by many recombination factors, like RecQ, RecJ, RecF, RecU and RecG (**Figure 7**B), which have a different impact on the capacity for cell survival (**Figure 11** and **Figure S3**). Is possible that the inhibition of the mobilization of RarA in the absence of long-range end resection (as defined by *ΔaddAB*, *ΔrecQ* and *ΔrecJ*) is due to the ssDNA platform needed for the recruitment of SsbA proteins, and consequently for RarA recruitment as a part of the SsbA-interactome (Costes *et al.*, 2010). Using cell biological approaches, we have identified functional differences between both RecQ-like DNA helicases (RecQ and RecS) for the first time. *B. subtilis* RecS (56.5 kDa) shares 36% identity with RecQ (67.3 kDa) (Fernandez *et al.*, 1998). The RarA movements are significantly more static in the *ΔrecS* context, while they become more dynamic upon DNA damage (**Figure 7**). In contrast, the opposite effect occurred in the absence of RecQ, the RarA movements are significantly less static in the absence of damage, while they become less dynamic upon H_2O_2 (**Figure 7**). In humans, it is known that WRNIP1/WHIP physically interacts with WRN, a RecQ-like helicase (Kawabe *et al.*, 2001). We predict that RarA interacts with both RecS and RecQ via SsbA (Costes *et al.*, 2010).

Once RarA is recruited, its main function seems to be related with RecA and its regulators, as we found major genetic and dynamic interactions with RecO, RecF, RecR and RecX. Microscopy observations revealed an opposite behaviour of RarA in

the Δ*recO* or *recF15* context compared to a Δ*recX* strain, as foci formation observed in the latter was decreased while in the other two it was enhanced compared to wt cells, and additionally, it occurred earlier (**Figure 5**C, D). Moreover, SMT pointed out that RecF is an essential factor for RarA mobilization in response to H_2O_2 (**Figure 7**B).

SMT analysis also revealed an interaction with PolY1, indicating that RarA could play a role in MMC-mediated mutagenesis by translesion synthesis, for which PolY1 is needed (Duigou *et al.*, 2004), and thus this function could be conserved in evolution, as yeast Mgs1 is known to physically interact with DNA polymerase δ and proposed to regulate its processivity and fidelity (Barbour & Xiao, 2003).

Taken together, our data suggest a dual role for RarA, in replication-related repair and in non-replication-related DNA repair, which is consistent with the data obtained in *E. coli* (Lau *et al.*, 2003; Stanage *et al.*, 2017), and thus support the idea of DNA repair centres formed outside of the replication forks in *B. subtilis* (Kidane *et al.*, 2004) rather than the absolute need of the presence of a replication fork for homologous recombination (Lenhart *et al.*, 2014). The role of RarA in replication is related to interactions with pre-primosome component directly, or indirectly, via SsbA. RarA is also important for replication fork progression, in an alternative pathway to RecF, RecO and RecA. It is likely that RarA could be the main factor for regulating preprimosomal activity, for providing a substrate for suitable helicase activity (Stanage *et al.*, 2017) or in a more complex pathway implicating RecG, RuvAB and/or RecU for replication restart (Baharoglu *et al.*, 2006). According with our study using SMT, RarA's role in replication might be regulated by a lack of end resection (RecS, RecJ and AddAB) and absence of RecD2 or RuvAB, which strongly affect RarA mobility in exponentially growing cells.

In the presence of a DNA-damaging agent, there is a specificity in the RarA response. During H_2O_2-induced damage, RarA plays an important role in cell survival, and this effect is correlated with an increase in dynamics and with a recruitment of RarA far from the replication fork, probably in a DNA repair centre. Once RarA is within such a repair centre, it could regulate RecA activity directly, or indirectly through positive mediators (e.g., RecO) or modulators (e.g, RecF), or by counteracting negative modulators, such as RecX or RecD2. On the other hand, after MMC-induced DNA damage, RarA was mobilized in the absence of potential negative modulators

such RecD2, and also in cells lacking RecS. The physiological role of RecS, which is absent in proteobacteria is poorly understood. Altogether, these findings point to a regulatory role of RarA in replication fork restart at several different levels.

III.1.7- Acknowledgements

We thank M. López-Sanz and C. Marchisone for technical assistance. H.R. thanks Fundación Mutua Madrileña (Spain) as a PhD fellow of the IX Edición de Becas de Posgrado.

Competing interests:

The authors declare that no competing interests exist.

Funding

This work was supported by LOEWE funding to SYNMIKRO (state of Hessen) and by the Philipps Universität Marburg to P.L.G, and by the Ministerio de Economía, Industria y Competitividad (MINECO/FEDER) BFU2015-67065-P to J.C.A and S.A.

III.1.8- References

See section VI.

III.1.9- Supplementary information

Supplementary tables

Table S1A. *Bacillus subtilis* strains used.

Strains	Relevant genotype	Source	Strains	Relevant genotype	Source
BG214	(*rec*$^{+}$)[a]	Lab. strain	BG1067	+ Δ*rarA*	This work
BG190	+ Δ*recA*	(1)	BG1555	+ Δ*recA*, Δ*rarA*	This work
BG439	+ Δ*recO*	(2)	BG1433	+ Δ*recO*, Δ*rarA*	This work
BG129	+ *recF15*	(3)	BG1055	+ *recF15*, Δ*rarA*	This work
BG1455	+ Δ*recD2*	(4)	BG1421	+ Δ*recD2*, Δ*rarA*	This work
BG1065	+ Δ*recX*	(5)	BG1371	+ Δ*recX*, Δ*rarA*	This work
BG1337	+ Δ*addAB*	(6)	BG1107	+ Δ*addAB*, Δ*rarA*	This work
BG675	+ Δ*recJ*	(7)	BG1059	+ Δ*recJ*, Δ*rarA*	This work
BG705	+ Δ*recQ*	(7)	BG1575	+ Δ*recQ*, Δ*rarA*	This work
BG425	+ Δ*recS*	(7)	BG1563	+ Δ*recS*, Δ*rarA*	This work
BG855	+ Δ*recU*	(8)	BG1083	+ Δ*recU*, Δ*rarA*	This work
BG1131	+ Δ*recG*	(9)	BG1103	+ Δ*recG*, Δ*rarA*	This work
BG703	+ Δ*ruvAB*	(10)	BG1351	+ Δ*ruvAB*, Δ*rarA*	This work
BG1245	+ Δ*radA*	(11)	BG1373	+ Δ*radA*, Δ*rarA*	This work
BG905	+ Δ*polY1*	This work	BG1401	+ Δ*polY1*, Δ*rarA*	This work
BG907	+ Δ*polY2*	This work	BG1403	+ Δ*polY1*, Δ*rarA*	This work
BG193	+ *dnaB*37	(12)	BG1687	+ *dnaB*37, Δ*rarA*	This work
BG196	+ *dnaC*30	(12)	BG1681	+ *dnaC*30, Δ*rarA*	This work
BG198	+ *dnaG*20	(12)	BG1661	+ *dnaG*20, Δ*rarA*	This work
BG199	+ *dnaF*33	(12)	BG1685	+ *dnaF*33, Δ*rarA*	This work
BG201	+ *dnaX*51	(12)	BG1659	+ *dnaX*51, Δ*rarA*	This work
BG1679	+ *dnaE*58	This work	BG1683	+ *dnaE*58, Δ*rarA*	This work

[a]*trpCE metA*5 *amyE1 ytsJ*1 *rsbV*37 *xre*1 *xkd*A1 *att*$^{SP\beta}$ *att*^{ICEBs1}

Table S1B. *B. subtilis rarA-yfp* and its mutant variants.

Strains[a]	Relevant genotype	Source
BG1331	+ *rarA-yfp*	This work
BG1445	+ *rarA-yfp*, Δ*recO*	This work
BG1345	+ *rarA-yfp*, *recF15*	This work
BG1347	+ *rarA-yfp*, Δ*recD2*	This work
BG1349	+ *rarA-yfp*, Δ*recX*	This work
PG3316	+ *rarA-yfp*, Δ*addAB*	This work
PG3423	+ *rarA-yfp*, Δ*recJ*	This work
PG3318	+ *rarA-yfp*, Δ*recQ*	This work
PG3424	+ *rarA-yfp*, Δ*recS*	This work
BG1443	+ *rarA-yfp*, Δ*recU*	This work
PG3317	+ *rarA-yfp*, Δ*recG*	This work
PG3426	+ *rarA-yfp*, Δ*ruvAB*	This work
PG3429	+ *rarA-yfp*, Δ*radA*	This work
PG3427	+ *rarA-yfp*, Δ*polY1*	This work
PG3428	+ *rarA-yfp*, Δ*polY2*	This work
PG3174	+ *rarA-yfp*, *dnaX-cfp*	This work
BG1451	+ *rarA-yfp*, *dnaB*37	This work
BG1453	+ *rarA-yfp*, *dnaC30*	This work

[a]*trpCE metA*5 *amyE1 ytsJ*1 *rsbV*37 *xre*1 *xkd*A1 *att*$^{SP\beta}$ *att*^{ICEBs1}

Table S2.

Background	D ($\mu m^2 s^{-1}$)		- drug		+ H_2O_2		+ MMC	
	static	dyn[a]	static	dyn	static	dyn	static	dyn
WT	0.23	2.3	48	52	35	65	44	56
Δ*recO*	0.39	2.3	61	39	47	53	57	43
recF15	0.2	2.1	42	58	51	49	48	52
Δ*recD2*	0.26	2.2	63	37	50	50	36	64
Δ*recX*	0.26	2.4	54	46	40	60	46	54
Δ*addAB*	0.24	2.2	55	45	55	45	76	24
Δ*recJ*	0.21	2.3	59	41	61	39	64	36
Δ*recQ*	0.19	2.2	43	57	48	52	43	57
Δ*recS*	0.28	2.6	71	29	50	50	56	44
Δ*recU*	0.37	2.1	42	58	57	43	65	35
Δ*recG*	0.21	2	46	54	43	57	55	45
Δ*ruvAB*	0.26	2.7	63	37	44	56	59	41
Δ*radA/sms*	0.28	2.9	57	43	57	43	58	42
Δ*polY1*	0.3	2.5	52	48	33	67	34	66
Δ*polY2*	0.28	2.1	47	53	38	62	48	52
DnaX-CFP	0.28	2.2	53	47	41	59	49	51

[a]dyn; dynamic.

Table S2. Diffusion coefficients (in $\mu m^2 s^{-1}$) and static/dynamic population weights (in %) calculated by step-size distributions and Gaussian fits for RarA-YFP in the different backgrounds studied in exponential growth, and after 60 min induction with 0.5 mM H_2O_2 or 50 ng/ml MMC. Cells were grown at 25ºC and images were taken at room temperature. At least 200 tracks/condition were considered for the analysis.

Table S3

Background	D ($\mu m^2 s^{-1}$)		25 ºC -drug		42 ºC -drug		42 ºC H_2O_2		42 ºC MMC	
	Static	dyn[a]	Static	dyn	Static	dyn	Static	dyn	Static	Dyn
wt	0.23	2.3	48	52	45	55				
*dnaB*37	0.2	1.8	41	59	65	35	40	60	58	42
*dnaC*30	0.19	2	38	62	29	71	38	62	48	52

[a]dyn; dynamic.

Table S3. Diffusion coefficient (in $\mu m^2 s^{-1}$) and population weights (in %) calculated by step-size distribution and Gaussian fit for RarA-YFP in the replication deficient thermosensitive mutants studied in exponential growth for 60 min at permissive temperature (25 ºC) and non-permissive (42ºC) temperature in the presence or absence of H_2O_2 (0.5 mM) or MMC (50 ng/ml). At least 200 tracks/condition were considered for the analysis.

References

1. Ceglowski, P., Luder, G. and Alonso, J.C. (1990) Genetic analysis of recE activities in Bacillus subtilis. *Mol Gen Genet*, **222**, 441-445.
2. Fernandez, S., Kobayashi, Y., Ogasawara, N. and Alonso, J.C. (1999) Analysis of the Bacillus subtilis recO gene: RecO forms part of the RecFLOR function. *Mol Gen Genet*, **261**, 567-573.
3. Alonso, J.C., Tailor, R.H. and Luder, G. (1988) Characterization of recombination-deficient mutants of Bacillus subtilis. *Journal of bacteriology*, **170**, 3001-3007.
4. Torres, R., Romero, H., Rodriguez-Cerrato, V. and Alonso, J.C. (2017) Interplay between Bacillus subtilis RecD2 and the RecG or RuvAB helicase in recombinational repair. *DNA repair*, **55**, 40-46.
5. Cardenas, P.P., Carrasco, B., Defeu Soufo, C., Cesar, C.E., Herr, K., Kaufenstein, M., Graumann, P.L. and Alonso, J.C. (2012) RecX facilitates homologous recombination by modulating RecA activities. *PLoS Genet*, **8**, e1003126.
6. Vlasic, I., Mertens, R., Seco, E.M., Carrasco, B., Ayora, S., Reitz, G., Commichau, F.M., Alonso, J.C. and Moeller, R. (2014) Bacillus subtilis RecA and its accessory factors, RecF, RecO, RecR and RecX, are required for spore resistance to DNA double-strand break. *Nucleic acids research*, **42**, 2295-2307.
7. Sanchez, H., Kidane, D., Cozar, M.C., Graumann, P.L. and Alonso, J.C. (2006) Recruitment of Bacillus subtilis RecN to DNA double-strand breaks in the absence of DNA end processing. *Journal of bacteriology*, **188**, 353-360.
8. Fernández, S., Sorokin, A. and Alonso, J.C. (1998) Genetic recombination in Bacillus subtilis 168: effects of recU and recS mutations on DNA repair and homologous recombination. *Journal of bacteriology*, **180**, 3405-3409.
9. Sanchez, H., Carrasco, B., Cozar, M.C. and Alonso, J.C. (2007) Bacillus subtilis RecG branch migration translocase is required for DNA repair and chromosomal segregation. *Mol Microbiol*, **65**, 920-935.
10. Sanchez, H., Kidane, D., Reed, P., Curtis, F.A., Cozar, M.C., Graumann, P.L., Sharples, G.J. and Alonso, J.C. (2005) The RuvAB branch migration translocase and RecU Holliday junction resolvase are required for double-stranded DNA break repair in Bacillus subtilis. *Genetics*, **171**, 873-883.

11. Gándara, C. and Alonso, J.C. (2015) DisA and c-di-AMP act at the intersection between DNA-damage response and stress homeostasis in exponentially growing Bacillus subtilis cells. *DNA repair*, **27**, 1-8.
12. Alonso, J.C., Stiege, C.A., Tailor, R.H. and Viret, J.F. (1988) Functional analysis of the dna (Ts) mutants of Bacillus subtilis: plasmid pUB110 replication as a model system. *Mol Gen Genet*, **214**, 482-489.

Supplementary Figures

Figure S1

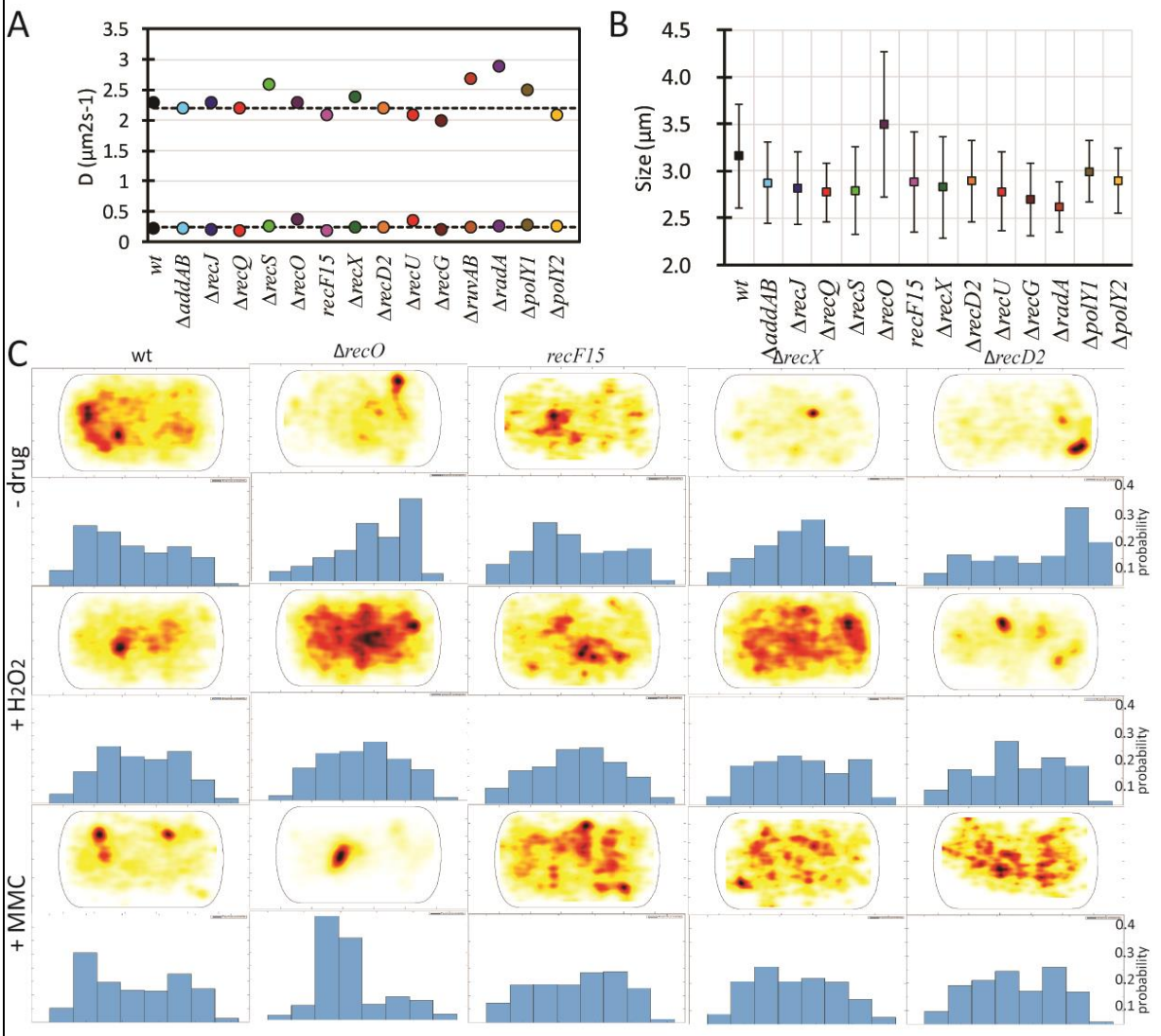

Figure S1. (A) Diffusion coefficients for static and dynamic populations calculated by Gaussian fit based in the step-size distribution. Values of each background were analysed separately, while dotted lines correspond to the analysis of all together; (B) Cell size considered prior to the normalization for the heat maps for the different backgrounds; (C) Heat maps and track distribution probability in X-axis for medium cells in wt, Δ*recO*, *recF15*, Δ*recX* and Δ*recD2* in absence of DNA damage, or after induction with H_2O_2 (0.5 mM) or MMC (50ng/ml).

Figure S2

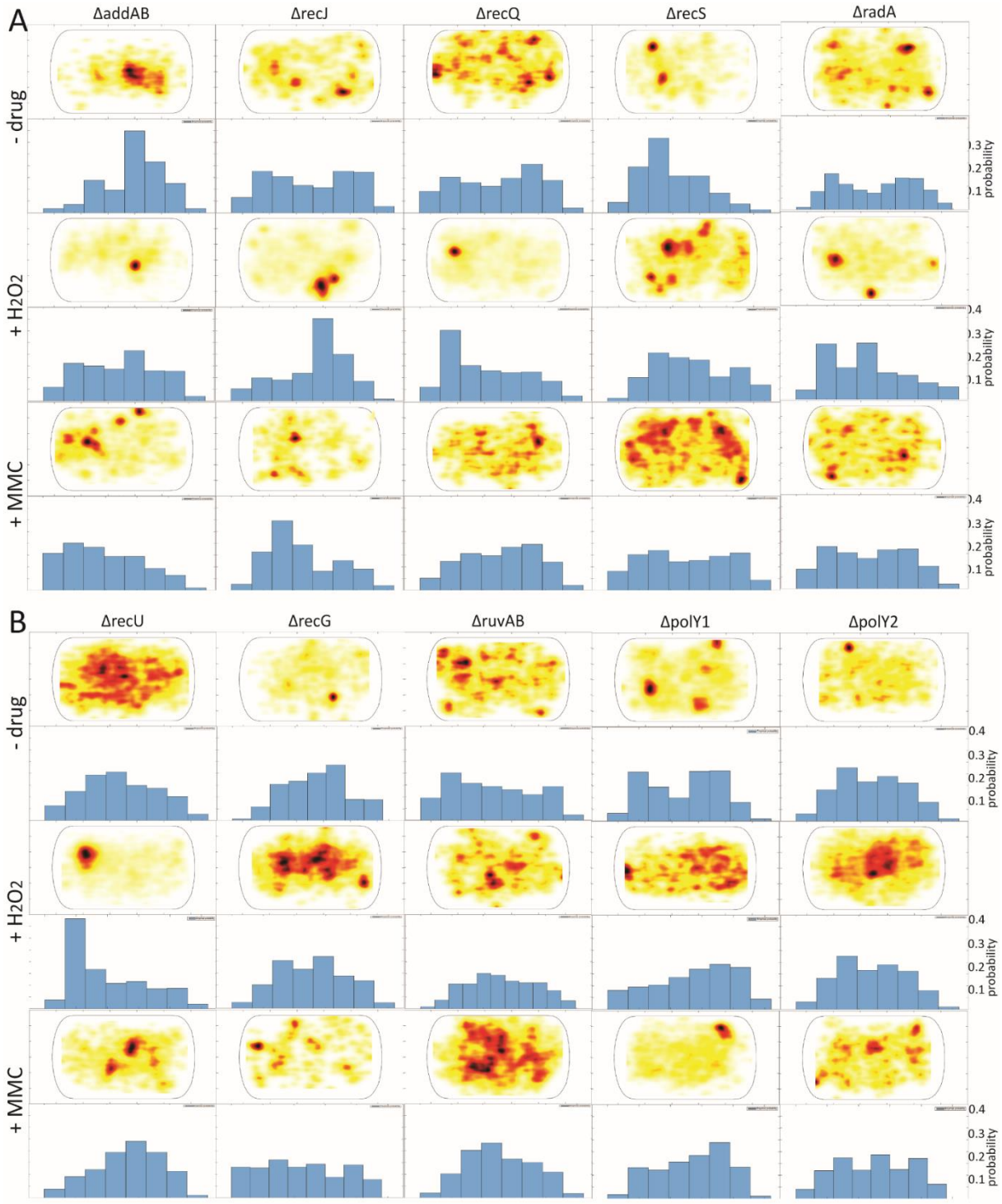

Figure S2. (A-B) Heat maps and track distribution probability in X-axis for medium cells in different backgrounds in absence of DNA damage, or after induction with 0.5 mM H_2O_2 or 50ng/ml MMC.

Figure S3

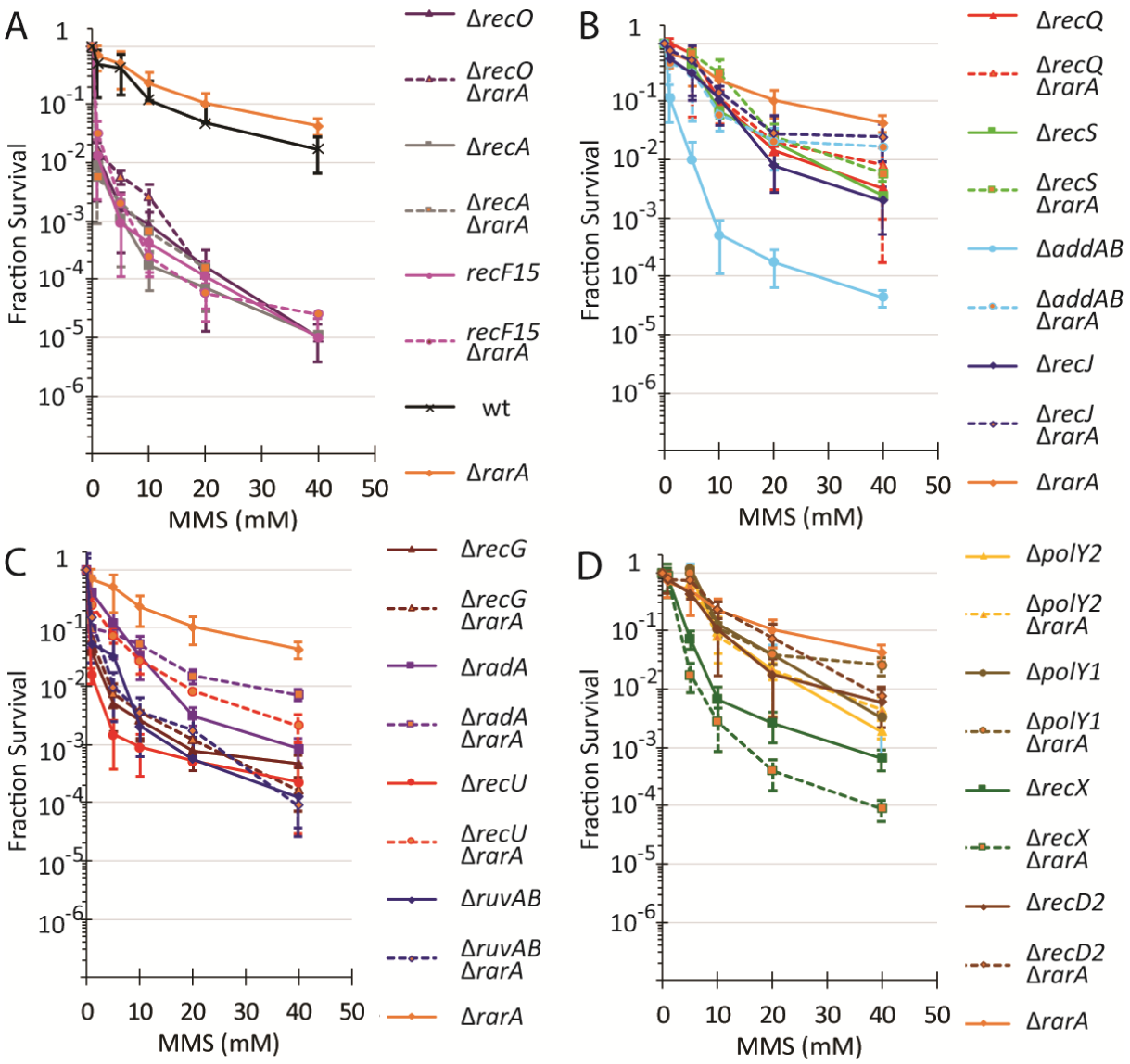

Figure S3. Acute viability of Δ*rarA* double mutant strains. Cells were grown to reach exponential phase (OD_{560}= 0.4) and exposed to increasing MMS concentrations for 15 min prior to serial dilutions. Cells were counted as CFU after a O/N incubation in LB and expressed compared to CFU in absence of drug.

III.2- RecD2-Torres *et al.*, 2017 (DNA repair, 55: 40-46)

DNA Repair 55 (2017) 40–46

Contents lists available at ScienceDirect

DNA Repair

journal homepage: www.elsevier.com/locate/dnarepair

Interplay between *Bacillus subtilis* RecD2 and the RecG or RuvAB helicase in recombinational repair

Rubén Torres, Hector Romero, Violeta Rodríguez-Cerrato, Juan C. Alonso*

Department of Microbial Biotechnology, Centro Nacional de Biotecnología (CNB-CSIC), 3 Darwin Str., 28049, Cantoblanco, Madrid, Spain

III.2.1- Contribution of H. Romero

For this manuscript I have been involved in design and performance of experiments for **Figure 13** and **Figure 14** together with RT and JCA, in the characterization of the *pcrA596* and *pcrA596 ΔaddAB ΔrecD2* mutants together with RT and VRC, construction of **Figure 2** and correction of the manuscript together with RT and JCA.

Please note that the manuscript has been modified in its format, in special figures 13 and 14, but not in the content, for this thesis.

III.2.2- Abstract

Bacillus subtilis AddAB, RecS, RecQ, PcrA, HelD, DinG, RecG, RuvAB, PriA and RecD2 are genuine recombinational repair enzymes, but the biological role of RecD2 is poorly defined. A *ΔrecD2* mutation sensitizes cells to DNA-damaging agents that stall or collapse replication forks. We found that this *ΔrecD2* mutation impaired growth, and that a mutation in the *pcrA* gene (*pcrA596*) relieved this phenotype. The *ΔrecD2* mutation was not epistatic to *ΔaddAB*, *ΔrecQ*, *ΔrecS*, *ΔhelD*, *pcrA596* and *ΔdinG*, but epistatic to *recA*. Specific RecD2 degradation caused unviability in the absence of RecG or RuvAB, but not on cells lacking RecU. These findings show that there is notable interplay between RecD2 and RecG or RuvAB at arrested replication forks, rather than involvement in processing Holliday junctions during canonical double strand break repair. We propose that there is a trade-off for efficient genome duplication, and that recombinational DNA helicases directly or indirectly provide the cell with the means to tolerate chromosome segregation failures.

III.2.2- Introduction

DNA metabolic processes such as replication, recombinational repair, homologous recombination (HR), and resuscitation of blocked replication forks require DNA helicases for a variety of functions (Wu & Hickson, 2006). DNA helicases are molecular motors that convert the chemical energy of nucleoside triphosphate (NTP) hydrolysis (typically of ATP) into mechanical force to translocate along single-stranded (ss) or doublestranded (ds) DNA. These helicases translocate in a directionally specific manner (3′→5′ or 5′→3′) along the strand they interact with and thus remodel the DNA structure (Singleton *et al.*, 2007). These enzymes, identified by a series of conserved sequence motifs, can be classified into six superfamilies (SF1-SF6), with the recombinational repair DNA helicases mainly included in SF1 and SF2 (Fairman-Williams *et al.*, 2010; Gilhooly *et al.*, 2013; Beyer *et al.*, 2013; Singleton *et al.*, 2007). *Bacillus subtilis* has at least 11 proteins with helicase domains, five SF1 (AddA [the counterpart of *Escherichia coli* RecB], HelD, PcrA, YjcD and RecD2 [also termed YrrC]), and six SF2 (RecG, RecQ [YocI], RecS [YpbC], DinG, PriA and RuvB) (**Figure 2**A, B) (Singleton *et al.*, 2007; Wu & Hickson, 2006). The YjcD classification has been questioned, because a null *B. subtilis yjcD* (or *B. anthracis yycJ*) mutant strain shows no obvious phenotype when exposed to DNA-damaging agents (Petit *et al.*, 1998; Petit & Ehrlich, 2002; Yang *et al.*, 2011), which would reduce the list of recombinational repair DNA helicases to ten. The remaining enzymes facilitate i) movement of the replication fork through obstacles (unusual DNA structures, bound proteins, transcribing polymerases, RNA transcripts), including PcrA, DinG, and HelD (Atkinson & McGlynn, 2009; Epshtein, 2015; Gwynn *et al.*, 2013; Merrikh *et al.*, 2012; Mirkin & Mirkin, 2007; Voloshin & Camerini-Otero, 2007; Wiedermannova *et al.*, 2014), ii) reversion of a stalled fork and its regression, as do RecG and RuvAB and RuvAB-mediated branch migration of Holliday junctions (HJs) during canonical double strand break (DSB) repair (Atkinson & McGlynn, 2009; Ayora *et al.*, 2011; Michel *et al.*, 2001; Persky & Lovett, 2008), iii) recruitment of the primosome at the formed recombination intermediates, like PriA (Gabbai & Marians, 2010), iv) unwinding of duplex DNA that, in concert with exonuclease(s), generates the 3′-tailed duplex substrate to be used by RecA, including AddAB, RecQ or RecS (Alonso *et al.*, 1993; Alonso *et al.*, 2013; Fernandez *et al.*, 1998; Dillingham & Kowalczykowski, 2008), v) dissolution of HJ, as do RecQ or RecS in concert with Topo III and SsbA proteins (Alonso *et al.*, 2013; Wu & Hickson, 2006), and vi) RecA removal from nucleoprotein filaments, such as PcrA

and HelD (Carrasco *et al.*, 2001; Fagerburg *et al.*, 2012; Park *et al.*, 2010; Petit & Ehrlich, 2002). RecD2, of *Deinococcus radiodurans*, *B. subtilis* and *B. anthracis* origin, is assumed to contribute to maintenance of replication fork integrity during normal growth (Servinsky & Julin, 2007; Walsh *et al.*, 2014; Wang & Julin, 2004; Yang *et al.*, 2011), but its mechanism of action is poorly defined.

In bacteria, there are two types of RecD-like enzymes, the long RecD2 (SF1A; **Figure 2**A) and the short RecD (SF1B) in complex with RecB and RecC (**Figure 2**C); the former is usually absent in bacteria that have the RecBCD complex (counterpart of B. subtilis AddAB) (Gilhooly *et al.*, 2013; Singleton *et al.*, 2007). *In vitro*, *B. subtilis* and *D. radiodurans* RecD2 act as 5′→ 3′ DNA helicases (Saikrishnan *et al.*, 2009; Walsh *et al.*, 2014; Wang & Julin, 2004). RecD2 shows a significant degree of structural similarity with SF1A helicases (such as *B. subtilis* PcrA, E. coli Rep or UvrD, and *Saccharomyces cerevisiae* Srs2), which move along single-stranded (ss) DNA in 3′→ 5′ direction, and with SF1B helicases (such as *E. coli* RecD and *S. cerevisiae* Pif1), which move along dsDNA with 5′→ 3′ polarity (Gilhooly *et al.*, 2013; Singleton *et al.*, 2007). DNA helicases of the UvrD-like and Pif1-like families are conserved from bacteria to man (Bochman *et al.*, 2011; Fairman-Williams *et al.*, 2010; Wu & Hickson, 2006).

Mutations in the *E. coli* recD gene lead to resistance to DNA-damaging agents such as UV light (Amundsen *et al.*, 1986), with no obvious phenotype when exposed to other DNA-damaging agents (Dillingham & Kowalczykowski, 2008). *B. subtilis*, which lacks *recD*, has a two-subunit enzyme (AddAB); loss of the AddA or AddB subunit sensitizes cells to DNA-damaging agents that collapse replication forks to a similar extent [reviewed in Alonso *et al.*, 2013; Ayora *et al.*, 2011].

PcrA is essential for *B. subtilis* growth (Petit *et al.*, 1998). Expression of the *B. subtilis pcrA* gene in *E. coli* restores viability of the *uvrD rep* double mutant, with PcrA partially compensating for the lack of UvrD, but not of Rep (Petit & Ehrlich, 2002). PcrA, UvrD and Rep facilitate replication of transcribed DNA regions (Epshtein *et al.*, 2014; Guy *et al.*, 2009; Merrikh *et al.*, 2015), whereas PcrA and UvrD have anti-recombinase activity related to their ability to displace RecA from ssDNA (Fagerburg *et al.*, 2012; Park *et al.*, 2010; Veaute *et al.*, 2005). Cells lacking PcrA (or *E. coli* lacking UvrD and Rep) are only viable in the absence of the RecA mediators (RecO, RecR, RecF) (Petit

& Ehrlich, 2002). The biological role of RecD2 in recombinational repair is little understood.

In vivo cytological studies provide indirect support for the roles of RecD2, RecS, RecQ, RecG and PriA DNA helicases in replication fork integrity (Costes *et al.*, 2010; Lecointe *et al.*, 2007). These enzymes interact with the essential "hub" SsbA protein (counterpart of E. coli SSB), which in turn co-localizes with B. subtilis replisome components DnaE and DnaG (Costes *et al.*, 2010; Lecointe *et al.*, 2007). Measurement of replication fork progression showed that arrested forks are more frequent in the absence of RecD2 than in its presence (Walsh *et al.*, 2014). B. anthracis RecD2 also acts as a mismatch repair helicase (Yang *et al.*, 2011).

Table 2
Bacillus subtilis strains used.

Strains	Relevant genotype	Source
BG214 (*rec*$^+$)	*trpCE metA5 amyE1 ytsJ1 rsbV37 xre1 xkdA1 att$^{SP\beta}$ att^{1CEBs1}*	Laboratory strain
BG703	+ *Δ*ruvAB	(Sanchez *et al.*, 2005)
BG1131	+ *Δ*recG	(Sanchez *et al.*, 2007)
BG855	+ *Δ*recU	(Sanchez *et al.*, 2005)
BG425	+ *Δ*recS	(Sanchez *et al.*, 2006)
BG705	+ *Δ*recQ	(Sanchez *et al.*, 2006)
BG551	+ *ΔhelD*	(Carrasco *et al.*, 2001)
BG1337	+ *ΔaddAB*	(Vlasic *et al.*, 2014)
BG1455	+ *ΔrecD2*	This work
BG1061	+ *ΔrecD2 pcrA596*	This work
BG1133	+ *ΔaddAB ΔrecD2 pcrA596*	This work
BG1585	+ *ΔrecS ΔrecD2*	This work
BG1297	+ *ΔhelD ΔrecD2*	This work
BG1605	+ *ΔdinG*	This work
BG1607	+ *ΔdinG ΔrecD2*	This work
BG1313	+ *ΔpcrA recF17*	This work
BG1525	+ pcrA-ssrA	This work
BG1583	+ pcrA-ssrA *Δ*recD2	This work
BG1557	+ recD2-ssrA	This work
BG1569	+ recD2-ssrA *Δ*ruvAB	This work
BG1565	+ recD2-ssrA *Δ*recG	This work
BG1587	+ recD2-ssrA *ΔrecU*	This work

To determine whether the DNA helicases provide redundant pathways for recombinational repair, and to study the role of *B. subtilis* RecD2, we transferred a null recD2 (*ΔrecD2*) mutation into multiple cell lines, each of which lacks one recombinational repair helicase except PriA. PriA (**Figure 2**B), a specificity factor for origin-independent assembly of a new replisome at the stalled fork (Gabbai & Marians, 2010), has an essential function in *B. subtilis* [see Peters *et al.*, 2016]. The absence of PriA greatly impairs cell growth (< 5% of total *ΔpriA* cells form viable colonies), and in the *ΔpriA* mutant, gain-of-function suppressors in the essential DnaB primosome component accumulate at very high frequency (Bruand *et al.*, 2005). Since this suppressor is also essential, we reduced the list to nine recombinational repair DNA helicases to be analyzed.

We characterized the genetic linkage of RecD2 with the other nine recombinational repair DNA helicases. Lack of RecD2 sensitized cells to DNA-damaging agents that stall (methyl methanesulfonate [MMS]) or collapse replication forks (hydrogen peroxide [H2O2]) via HR (Fu *et al.*, 2012; Sedgwick, 2004). RecD2 was epistatic with RecA, but it was non-epistatic with AddAB, RecS, RecQ, PcrA, HelD, DinG, RecG or RuvAB enzymes. Following RecD2 degradation, we observed synthetic lethality in the *recG* or *ruvAB* context, but not in the *recU* (counterpart of *E. coli ruvC*) background. *ruvAB*, *recG* and *recU* encode branch migration translocases and a HJ specific endonuclease that work with RuvAB to resolve HJ intermediates (Alonso *et al.*, 2013; Ayora *et al.*, 2011). Thus, strains lacking the RecD2 helicase appear to require a branch migration translocase for viability. We showed that cells lacking RecD2 and RuvAB or RecG promote accumulation of unsegregated nucleoids in cells proficient in a specific type of branch migration, mediated by RuvAB (when RecD2 and RecG are absent) or RecG (when RecD2 and RuvAB are lacking).

III.2.3- Results

Absence of RecD2 accumulates a mutation suppression in the* pcrA *gene.

B. subtilis or *D. radiodurans ΔrecD2* mutation sensitizes cells to MMS, UV radiation-mimetic 4-nitroquinoline-1-oxide (4NQO), H_2O_2, mitomycin C (MMC) and even to ionizing radiation that induced two-ended double strand breaks (**Figure 13**A) (Servinsky & Julin, 2007; Walsh *et al.*, 2014). RecD2 is considered a genuine recombinational repair DNA helicase, although when and how it functions are poorly characterized. To characterize the role of *B. subtilis* RecD2 in concert with other

recombinational repair DNA helicases we constructed mutant strains lacking RecD2 and another DNA helicase (see Methods and **Table 2**).

Cells lacking RecD2 showed a poor-growth phenotype, an impairment that was significantly increased in the *ΔaddAB* background. The appearance of large colony variants at low (in *ΔrecD2*) and high frequency (in *ΔrecD2 ΔaddAB*) nonetheless facilitated identification of suppressors. To identify mutation(s) in the background, we performed nucleotide sequence analyses of five independent suppressors isolated from *ΔrecD2* or *ΔrecD2 ΔaddAB* strains, followed by whole-genome comparison in parallel with the isogenic *rec*+ and the original *ΔrecD2* strains (Cárdenas *et al.*, 2012). In the *ΔrecD2* large colony variants, we confirmed *recD2* replacement by the presence of the single six site sequence and identified a single point mutation in the *pcrA* gene, in which the 596 GCG was replaced by a GTG codon. After PcrA translation, the highly conserved Ala596 was changed to Val596 (A596V). The pleotropic mutation, which maps between domain 5 and 6 of the highly conserved UvrD-like C-terminal domain (**Figure 2**A) (Dillingham, 2011), gave rise to the *ΔrecD2 pcrA596* strain. We found similar mutations in the *ΔrecD2 ΔaddAB* context, which led to the *ΔrecD2 ΔaddAB pcrA596* strain.

The* pcrA596 *mutation increases the sensitivity of* ΔrecD2 *cells to DNA damaging agents.

PcrA is a multi-functional DNA helicase that functionally interacts with UvrB (crucial for nucleotide excision repair), RNA polymerase and with the RecA recombinase (Merrikh *et al.*, 2015; Park *et al.*, 2010). It was proposed that PcrA and *E. coli* UvrD act at forks stalled by replication-transcription collisions, and that these conflicts might be resolved via HR (Epshtein, 2015; Merrikh *et al.*, 2012). Similarly, *D. radiodurans* RecD2 act at forks blocked by replication-transcription collisions (Epshtein, 2015; Gupta *et al.*, 2013). To gain insight into the mechanism of *pcrA596* suppression of the poor growth phenotype of *ΔrecD2* cells and to analyze whether the *pcrA596* strain is impaired in recombinational repair, the *ΔrecD2*, *pcrA596* and *ΔrecD2 pcrA596* strains were exposed to different DNA-damaging agents (such as MMS, H_2O_2, 4NQO or MMC). It is generally accepted that MMS- and H_2O_2-induced lesions are specifically removed by base excision repair (Fu *et al.*, 2012; Sedgwick, 2004), and

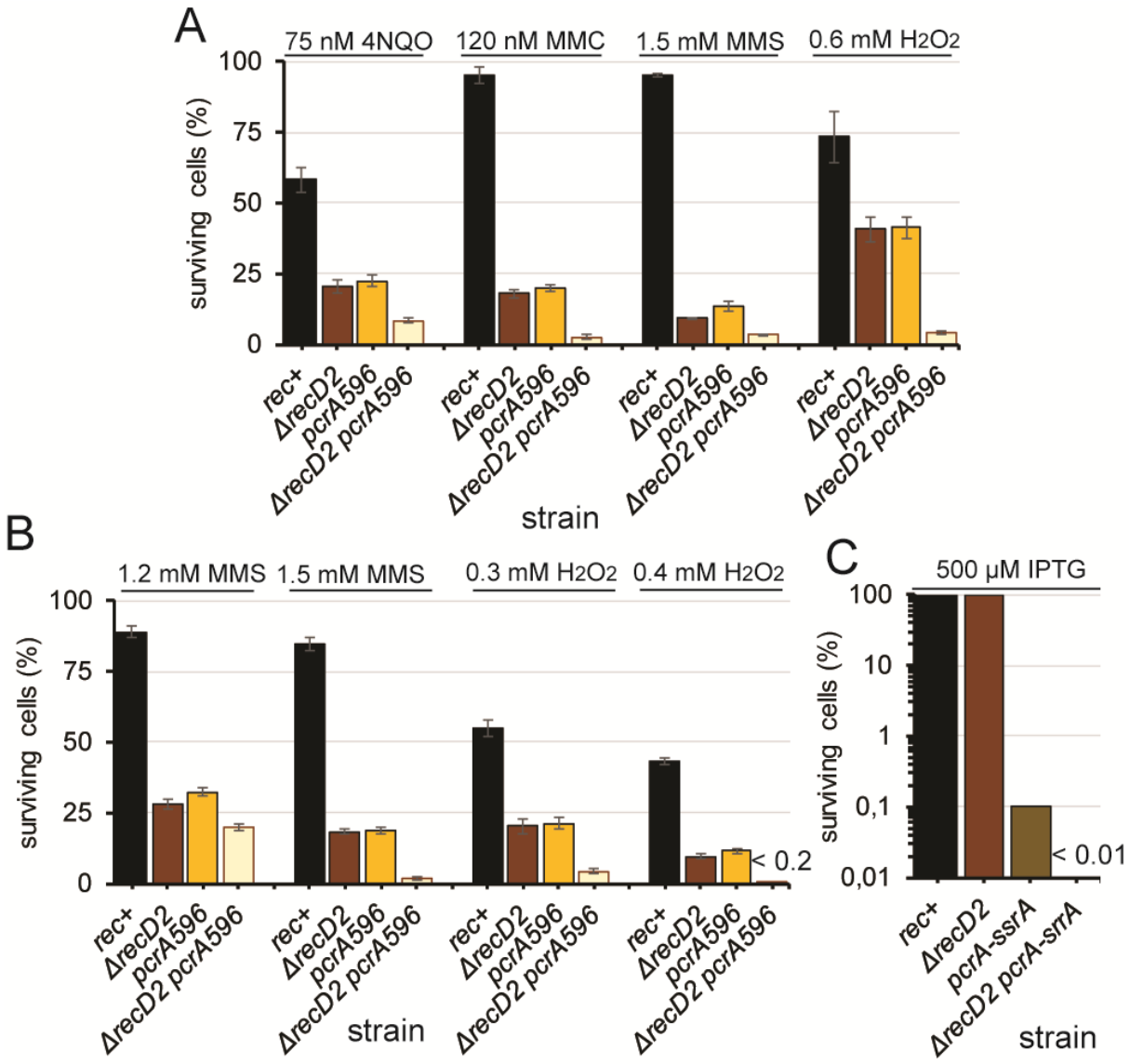

Figure 13. The *pcrA596* mutation increases the sensitivity of *ΔrecD2* cells to DNA damages. (A) Log phase *rec*$^{+}$, *ΔrecD2*, *pcrA596* or *ΔrecD2 pcrA596* cells were diluted and plated in LB agar plates containing indicated concentration of MMS, H2O2, 4NQO or MMC. (B) Log phase *rec*$^{+}$, *ΔrecD2*, *pcrA596* or *ΔrecD2 pcrA596* cells were diluted and plated in MMS7 agar plates containing indicated concentration of MMS or H_2O_2. Plates were incubated (37 °C, 16–18 h) and surviving colonies were counted. (C) Synthetic lethality assays showing that PcrA degradation affects *ΔrecD2* cell viability. Log phase cultures of indicated strains were diluted and plated on LB agar containing 500 µM IPTG. Experiments were performed at least four times. Data are shown as mean fractional survival ± SEM.

4NQO- and MMC-induced lesions are repaired by nucleotide excision repair (Almeida & Sobol, 2007; Reardon & Sancar, 2005). If unrepaired, the MMS- and 4NQO-induced lesions mainly block elongation of most DNA polymerases, and thereby stall replication fork progression; whereas H_2O_2- and MMC-induced lesions collapse replication forks

and lead to DSBs (Almeida & Sobol, 2007; Fu *et al.*, 2012; Reardon & Sancar, 2005; Sedgwick, 2004). Homologous recombination plays a central role in the restart of stalled replication forks and in the repair of DSBs (Atkinson & McGlynn, 2009; Ayora *et al.*, 2011; Gabbai & Marians, 2010; Michel *et al.*, 2001; Persky & Lovett, 2008). We constructed a *pcrA596* strain (**Table 2**).

The sensitivity of cells to chronic exposure to MMS, H_2O_2, 4NQO or MMC was determined by growing cells to an OD_{560} = 0.4 at 37° C in LB rich medium (**Figure 13**A). Appropriate dilutions of exponentially growing wild type (*rec*$^+$), *ΔrecD2*, *pcrA596* and *ΔrecD2 pcrA596* isogenic cells were plated in LB agar plates containing different concentrations of the chemicals, and the rate of survival was observed. For simplicity, the drug concentrations that moderately affects the survival of the *rec*$^+$ strain was shown (**Figure 13**A). The *ΔrecD2* or *pcrA596* mutation rendered cells sensitive to the four tested DNA-damaging agents, and the *pcrA596* mutation increased the sensitivity of *ΔrecD2* cells (**Figure 13**A). Since the *pcrA596* mutation rescues the growth defect of *recD2*, but it renders the cells more susceptible to DNA damage, we assume that RecD2 contributes to circumvent a replicative stress, and that the *pcrA596* mutation confers a maladaptation rather than an adaptive fitness in the *ΔrecD2* context. We can envision that by reducing the replication rate (growth in minimal medium) the *pcrA596* mutation might be disadvantageous.

To study whether the cell proliferation rate (or the number of intact homologous templates) affects the sensitivity of cells to chronic exposure to MMS or H_2O_2, we analyze the effect of these drugs, whose lesions are repaired by nucleotide excision repair, in minimal medium S7 (MMS7). In MMS7 the duplication time is ~60 min or twice lowlier than in LB rich medium (see Materials and methods). Cells were grown to an OD_{560} =0.4 at 37 °C in MMS7 (**Figure 13**B). Then, appropriate dilutions were plated on MMS7 agar plates containing different concentration of the chemicals, and the rate of survival of *rec*$^+$, *ΔrecD2*, *pcrA596* and *ΔrecD2 pcrA596* isogenic cells was observed after overnight incubation at 37 °C (**Figure 13**B). Exposure to 1.5 mM MMS varied by 1.7–2-fold the survival of *ΔrecD2*, *pcrA596* or *ΔrecD2 pcrA596* cells grown in MMS7 agar plates when compared to *rec*+ cells grown in LB agar plate (**Figure 13**B vs A). In contrast, cells grown in MMS7 agar plates were significantly more sensitive to H_2O_2 than those grown in LB agar plates (**Figure 13**A, B). When grown in LB agar plates containing 0.6 mM H_2O_2, the viability of *ΔrecD2* or *pcrA596* cells was reduced

~1.7-fold, and of *ΔrecD2 pcrA596* cells was diminished ~18-fold when compared to (**Figure 13**A). However, exposure to 0.6 mM H_2O_2 reduced over 100-fold the viability of *rec*+ cell grown in MMS7 agar plates (data not shown), thus the drug concentration of was decreased. In the presence of 0.3 mM H_2O_2, the viability of *ΔrecD2* or *pcrA596* cells was decreased ~2.7-fold and the viability of the *ΔrecD2 pcrA596* strain reduced ~14- fold when compared to *rec*+ cells grown in MMS7 agar plate (**Figure 13**B). It is likely that: i) independently of the cell proliferation speed (in minimal vs in rich medium) *recD2* is involved in recombinational DNA repair; ii) the essential PcrA is required for recombinational repair via HR (**Figure 13**A) as well as for nucleotide excision repair (Epshtein, 2015); and iii) *recD2* is not epistatic to *pcrA* in response to DNA damage.

To confirm whether lack of RecD2 further reduced the synthetic lethality of the absence of PcrA, the *ΔrecD2* mutation was transferred into the *pcrA-ssrA sspB* degron strain ($PcrA_T$) (**Table 2**) (Merrikh *et al.*, 2015). Addition of IPTG (500 µM) to the culture induced expression of the SspB adaptor, which bound to the SsrA peptide tag, and delivered the tagged PcrA-SsrA protein ($PcrA_T$) to the ClpXP protease for degradation [see Griffith & Grossman, 2008; Keiler *et al.*, 1996; Merrikh *et al.*, 2015]. The *pcrA-ssrA* cell viability was reduced by ~1000-fold when plated onto 500 µM IPTG-containing plates (**Figure 13**C) (Merrikh *et al.*, 2015). The absence of RecD2 significantly decreased cell viability (~104-fold) after IPTG addition in the *pcrA-ssrA* context (**Figure 13**C), which confirmed that *recD2* is not epistatic with *pcrA*, and showed that the lack of RecD2 did not suppress the lethality of a *pcrA* mutation.

RecD2 is non-epistatic with AddAB, RecQ, RecS, HelD and DinG.

As in previous studies, we showed that the single or double mutant *B. subtilis* strains impaired in the *ΔaddAB*, *ΔrecQ*, *ΔrecS*, *ΔhelD*, *ΔrecG* or *ΔruvAB* recombinational DNA helicases were sensitive to MMS or H_2O_2 treatment (**Figure 14**A, B) (Carrasco *et al.*, 2001; Sanchez *et al.*, 2005; Sanchez *et al.*, 2006; Sanchez *et al.*, 2007). We constructed a *ΔdinG* strain and showed that lack of DinG rendered cells marginally sensitive to MMS and sensitive to H_2O_2 (**Figure 14**A–B).

We constructed *B. subtilis* cells lacking RecD2 and one of the recombinational repair DNA helicases or the RecA recombinase (as control) (**Table 2**). The double or triple mutant strains were either more sensitive to MMS or H_2O_2 than the most sensitive single-mutant parent or a helicase mutation partially suppressed the recD2 defect

following MMS exposure (**Figure 14**A–B). It is likely that the *ΔrecD2* mutation is non-epistatic with *ΔaddAB*, *ΔrecQ*, *ΔrecS*, *ΔhelD* and *ΔdinG*.

The *ΔrecQ*, *ΔrecS*, *ΔhelD*, or *ΔdinG* mutation partially suppressed the *recD2* defect following MMS exposure. A RecQ-like helicase (RecQ or RecS; the latter is absent in *E. coli*) acts at early and late stages of recombinational repair (Alonso *et al.*, 2013; Ayora *et al.*, 2011). At early stages, RecJ in concert with RecQ or RecS, catalyzes end resection, whereas at late stages, Topo III in concert with RecQ or RecS, could dissolve HJ to render non-crossover (NCO) products (Ayora *et al.*, 2011; Wu & Hickson, 2006). A *topB* mutation showed no phenotype after DNA damage (not shown), and we thus constructed a *ΔrecD2 ΔrecJ* double mutant that, as above, was more resistant to MMS than the single-mutant *ΔrecD2* strain (not shown). It is unclear why absence of the RecJ-RecQ(RecS) end resection pathway, or of HelD or DinG partially suppressed the RecD2 defect after MMS exposure, and it would be of interest to determine.

The *ΔrecD2 ΔrecA* strain was as sensitive to MMS or H_2O_2 as was the *ΔrecA* strain (**Figure 14**A, B). The *ΔrecD2* mutation in the *pcrA596 ΔaddAB* or the *dinG* strain nonetheless showed a synergistic effect that rendered cells more sensitive than the *recA* strain (**Figure 14**A, B).

Absence of RecD2 is synthetically lethal with* ruvAB *or* recG *mutation.

In standard chromosomal transformation and/or bacteriophage SPP1-mediated transduction conditions [see Sanchez *et al.*, 2007], we were unable to transfer the *ΔrecG* or *ΔruvAB* mutation in the *ΔrecD2* or *ΔrecD2 pcrA596* contexts. RuvAB and RecG catalyze branch migration of stalled forks (reversed fork or HJ-like structure), and RuvAB, in concert with RecU, drives cleavage of the double HJ generated during canonical DSB repair (Ayora *et al.*, 2004; Cañas *et al.*, 2014; Suzuki *et al.*, 2014). To test whether double HJ accumulation was responsible for our failure, we transferred the *ΔrecU* mutation on the *ΔrecD2* background, and the *ΔrecD2 ΔrecU* strain was successfully constructed (**Table 2**).

To determine why we were unable to construct a *ΔrecG ΔrecD2* or *ΔruvAB ΔrecD2* strain, and to define the step at which RecD2 acts, we generated a conditional mutant by developing a RecD2 degron strain, as described (Griffith & Grossman, 2008; Keiler *et al.*, 1996). When compared to the *recD2*+ strain, the C-terminal residues of

the *recD2-ssrA*-encoded peptide tag in the recD2-ssrA strain did not affect cell proliferation (**Figure 14**C). Upon addition of IPTG (500 µM), the SspB adaptor delivered the tagged RecD2-SsrA protein ($RecD2_T$) to the ClpXP protease for degradation [see Griffith & Grossman, 2008; Keiler *et al.*, 1996]. As anticipated, $RecD2_T$ depletion did not affect cell viability, but revealed its poor growth (**Figure 14**C and not shown). We constructed *ΔruvAB recD2-ssrA* and *ΔrecG recD2-ssrA* strains (**Table 2**). After addition of 500 µM IPTG, we found that *ΔruvAB recD2-ssrA* or *ΔrecG recD2-ssrA* cell viability decreased by ~500- and ~300-fold, respectively (**Figure 14**C). In contrast, $RecD2_T$ depletion did not markedly decrease the plating efficiency of *ΔrecU recD2-ssrA* cells (**Figure 14**C), consistent with the viability of the *ΔrecD2 ΔrecU* strain.

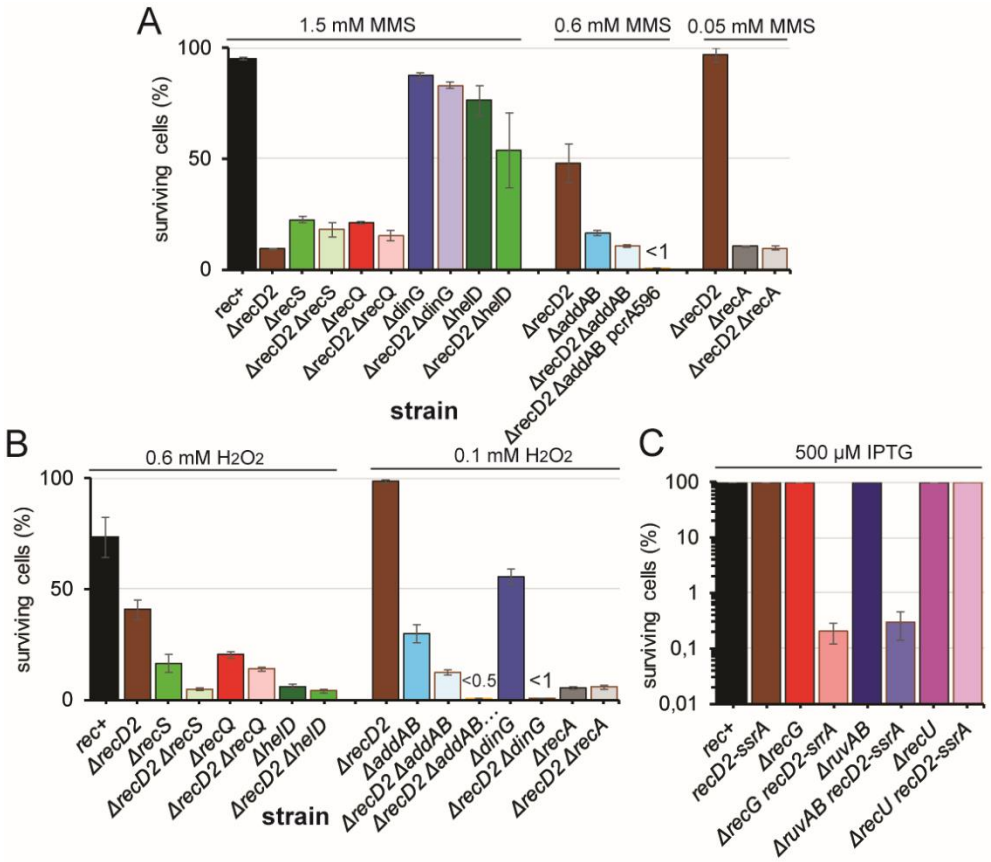

Figure 14. The *ΔrecD2* mutation in not epistatic to *addAB*, *recQ*, *recS*, *helD*, *dinG*, *recG* or *ruvAB*. (A) The log phase *ΔrecD2 addAB*, *ΔrecD2 recQ*, *ΔrecD2 recS*, *ΔrecD2 helD* or *ΔrecD2 dinG* cells were diluted and plated on LB agar containing the indicated concentration of MMS (A) or H_2O_2 (B). Plates were incubated (37 °C, 16–18 h) and surviving colonies were counted. Synthetic lethality assays showing that RecD2 degradation affects *ΔrecG* or *ΔruvAB* cell viability. (C) Survival was tested of log phase cultures of single (*recD2-ssrA*) and mutant strains (*recD2-ssrA ΔrecG* or *recD2-ssrA ΔruvAB*). The *recD2-ssrA ΔrecU* strain was used as control. Log phase cultures of indicated strains were diluted and plated on LB agar containing 500 µM IPTG. Experiments were performed at least four times. Data are shown as mean fractional survival ± SEM

Loss of RecD2 promotes accumulation of unsegregated chromosomes

The absence of RecG, RuvAB or RecU increases over 150-fold the amount of non-partitioned chromosomes (Sanchez *et al.*, 2007), thus chromosome segregation of the *ΔrecD2* strain was analyzed. To test whether the lack of RecD2 leads to a net accumulation of anucleates and cells with unresolved chromosomes, we visualized DAPI-stained *ΔrecD2* cells by fluorescence microscopy. During vegetative growth, anucleated cells (< 0.1% of total cells) and cells with unsegregated chromosomes (< 0.1%) were rare in *rec*$^{+}$ strain (**Figure 15**). In this case, ~35% of total cells had two nucleoids, and ~65% of total cells contained only one nucleoid with about twice the fluorescence signal, which suggested that they were replicating cells with yet-unsegregated nucleoids (**Figure 15**). Absence of DAPI staining increased ~20-fold in exponentially growing *ΔrecD2* cells (~2% of total cells). A small but significant fraction (~0.6%) of total cells was elongated, with one symmetrically located bright nucleoid (unsegregated nucleoids) (**Figure 15**). Since the signal was much brighter than that of two condensed nucleoids as observed during replicative stress (Kidane *et al.*, 2004), and cell length was much greater than that of normally dividing cells, we assumed that the symmetrically located nucleoids are due to accumulation of “dead-end repair intermediates” rather than replicating cells with yet-unsegregated chromosomes.

RecD2 depletion leads to accumulation of unsegregated chromosomes in* ΔruvAB *or* ΔrecG *cells

We analyzed DAPI-stained *recD2-ssrA ΔrecU, recD2-ssrA ΔruvAB* and *recD2-ssrA ΔrecG* cells by fluorescence microscopy to determine net accumulation of anucleates and cells with unsegregated chromosomes. The absence of RecG, RuvAB or RecU increased the proportion of anucleated cells by 50- to 90-fold, and of cells with unresolved chromosomes by 150- to 200-fold (**Figure 15Figure 15**). Cells that also showed minor defects such as DNA stretched across the septum of the dividing cell (guillotine effect) and those with low DNA content were not quantitated. These is consistent with previous results (Carrasco *et al.*, 2004; Sanchez *et al.*, 2005; Sanchez *et al.*, 2007).

Mutant strain	% of normal cells (no. of cells counted)	% of anucleate cells	% of unsegregated nucleoids
rec^{+a}	99.7 (3000)	< 0.1	< 0.1
Δ*recD2*^{a}	96.8 (2560)	2.2	0.6
Δ*recG*^{a}	73.4 (1854)	7.4	18.6
Δ*ruvAB*^{a}	76.6 (1748)	5.2	17.5
Δ*recU*^{a}	79.2 (1854)	4.4	14.7
recD2-ssrA Δ*recG*^{a}	74.2 (1442)	7.6	17.5
recD2-ssrA Δ*ruvAB*^{a}	75.0 (2323)	6.9	17.6
recD2-ssrA Δ*recU*^{a}	78.9 (1675)	4.9	15.0
recD2-ssrA Δ*recG*^{b}	49.6 (2274)	8.1	41.8
recD2-ssrA Δ*ruvAB*^{b}	53.7 (1422)	7.8	38.0
recD2-ssrA Δ*recU*^{b}	79.7 (1675)	5.2	14.6

Figure 15. Chromosome segregation defect of *ΔrecG* or *ΔruvAB* after RecD2 degradation. Cells were grown in LB medium to OD_{560}= 0.2; after 60 min, cells were harvested, prepared for DAPI DNA-fluorescence microscopy, and the percentage of anucleate and unsegregated nucleoids determined (condition *a*). In parallel, at OD_{560} =0.2, IPTG (500 μM) was added and after 60 min, cells were harvested, DAPI-stained, and the percentage of anucleate and unsegregated nucleoids determined (condition *b*). Representative fluorescent images are shown of two dividing DAPI-treated cells (DNA stain, light blue). The mean of at least 3 independent experiments is shown. (For interpretation of the references to colour in this Fig. legend, the reader is referred to the web version of this article.)

The absence of DAPI-stained material and the chromosome segregation defect in *recD2-ssrA ΔrecG*, *recD2-ssrA ΔruvAB* and *recD2-ssrA ΔrecU* cells in permissive conditions (no IPTG) resembled the more defective single (or double) mutant strains (**Figure 15**). In parallel, we examined the lack of DAPI-stained material and of chromosome segregation in these cells after 60 min IPTG treatment (restrictive conditions). A massive increase in the proportion of unresolved chromosomes after RecD2 degradation was found in the *ΔrecG* and *ΔruvAB* contexts (**Figure 15**), whereas anucleated cells (lack of DAPI staining) changed only marginally. Accumulation of unsegregated chromosomes did not increase after IPTG addition in *recD2-ssrA ΔrecU* cells (**Figure 15**). It is therefore likely that i) the symmetrically located, unsegregated

nucleoids were due to net accumulation of "dead-end repair intermediates" rather than to replicating cells with yet-unsegregated chromosomes or to dimeric chromosomes (crossover products) in the *recD2-ssrA* context, and that ii) the synthetic lethality of *recD2-ssrA* in the *ΔruvAB* or *ΔrecG* contexts after IPTG addition correlated with unsegregated nucleoid accumulation.

III.2.4- Discussion

Potential role of RecD2 in homologous recombination

The biological function of RecD2 in *B. subtilis* cells has yet to be established. Several lines of genetic evidence indicate the RecD2 involvement in circumventing replicative stress and in the re-establishment of an arrested replication fork after DNA damage. Following exposure to MMS or H_2O_2, RecD2 was not epistatic with DNA helicases needed for end resection (AddAB, RecQ, RecS), for HJ dissolution (RecQ, RecS), for RecA removal from DNA recombination intermediates (PcrA, HelD), for resolving replication conflicts (HelD, DinG, PcrA), for resolving DNA structures such as G-quadruplex DNA, or for unwinding D- and R-loops (RecQ, RecS, DinG) (**Figure 13** and **Figure 14**A, B).

A *ΔrecD2* mutation could not be transferred to the *ΔrecG* or *ΔruvAB* backgrounds, but *ΔrecD2 ΔrecU*, *ΔrecD2 ΔrecQ* and *ΔrecD2 ΔrecS* were viable. Depletion of RecD2 was synthetically lethal in the *ruvAB* or *recG* contexts (**Figure 14**C). It is likely that a defect in HJ translocation revealed a synthetic lethality rather than impairment of HJ resolution or dissolution. One might hypothesize that the RecD2 and RuvAB or RecG DNA helicases act at the interface between DNA replication and homologous recombination and participate in arrested fork recovery, rather than in the resolution or dissolution of single or double HJ by the RecU HJ resolvase or TopoIII in concert with RecQ or RecS helicases, respectively. Absence of RecD2 is synthetically lethal in *ruvAB* or *recG*, but not in the *recU* context

DNA damage within one of the template strands prevents DNA synthesis, and this stress stalls the replication fork. The branch migration translocases RuvAB and RecG act at stalled replication forks, or at the late stage during canonical DSB repair (Atkinson & McGlynn, 2009; Ayora *et al.*, 2011; Gabbai & Marians, 2010; Michel *et al.*, 2001; Persky & Lovett, 2008). In *E. coli* and *B. subtilis* cells, RecG-mediated reversion of a replication fork results in annealing of nascent strands, which can subsequently

base pair to form a HJ-like structure; after the original lesion is removed or bypassed, RuvAB-mediated regression of the reversed fork or helping RecU to cleave HJs contributes to cell survival (Atkinson & McGlynn, 2009); Gabbai & Marians, 2010; Michel *et al.*, 2001). The requirements to overcome arrested forks in *E. coli* and *B. subtilis* cells nonetheless differ. In *E. coli*, *ruvABC recG* cells are viable, but the lack of UvrD and of RuvAB or RuvC (the counterpart of *B. subtilis* RecU) (Magner *et al.*, 2007), or the lack of Rep and thermal inactivation of RecB and RecC (Seigneur *et al.*, 1998) are synthetically lethal. These mutations promote death via accumulation of toxic recombination intermediates. The absence of RecQ, RecJ or RecF rescues *ΔruvAB ΔurvD* or *ΔruvC ΔuvrD* viability (Magner *et al.*, 2007). Lack of RuvAB similarly rescues *Δrep recBtsCts* viability in non-permissive conditions, but RuvC inactivation renders cells inviable, as DSB cannot be generated at reversed forks (Seigneur *et al.*, 1998). In contrast, a *B. subtilis* mutation in the *pcrA* gene (*pcrA596*) was needed to restore normal cell growth in the *ΔrecD2* context, and *pcrA596 ΔrecD2 ΔaddAB* strain was viable. Degradation of RecD2 was synthetically lethal on the *ΔrecG* or *ΔruvAB* background, but a *ΔrecU* mutation was viable in *ΔrecD2*. A *ΔruvAB* mutation is also synthetically lethal in the *ΔrecG* or *ΔrecU* context (Sanchez *et al.*, 2005; Sanchez *et al.*, 2007), but a *ΔrecU* mutation is viable in *ΔrecG* (Sanchez *et al.*, 2005; (Sanchez *et al.*, 2007).

We hypothesize that RecG (in the absence of RecD2 and RuvAB), RuvAB (lacking both RecD2 and RecG) or RecD2 (without RuvAB and RecG) stabilize certain recombination intermediates, leading to pathological intermediates at any arrested fork, and thus leading to cell death. For example, they might eliminate substrates that PriA could otherwise exploit to re-replicate the chromosome. Alternatively, RecD2 could facilitate net accumulation of intermediates with which PriA could trigger a cascade of events that interferes with chromosome segregation. This is consistent with the observation that the physical association of RecD2, RecG and PriA with SsbA (Costes *et al.*, 2010; Lecointe *et al.*, 2007) bound to ssDNA regions can facilitate replisome re-assembly provided that RecD2, RecG and RuvAB are present.

III.2.5- Materials and methods

Bacterial strains and plasmids

BG214 and its isogenic derivatives are listed in **Table 2**. The gene to be characterized was deleted by gene replacement with the *six-cat-six* cassette (SCS)

flanked by homology up and downstream. The SCS cassette is composed of two directly oriented β-recombinase cognate sites (*six* sites) and the *cat* gene, which confers chloramphenicol resistance (Cm^R). Natural competent cells were transformed with the SCS cassette flanked by homologous regions to the gene to be deleted with selection for Cm^R. Integration of the SCS cassette, through double crossover recombination, replaced the gene under characterization. This was followed by β site-specific recombinase-mediated excision between the two directly oriented *six* sites, leading to deletion of the *cat* gene and one *six* site. The final outcome of this strategy is that the gene to be characterized is deleted, being replaced by a single *six* site [(Sanchez *et al.*, 2005; Sanchez *et al.*, 2007).

The *recD2* gene fused to an *ssrA* degradation tag (*recD2-ssrA*) was used to replace wild type *recD2*. The *sspB* gene, under the control of an IPTG-inducible promoter, was integrated ectopically at the *amy* locus. IPTG addition induced expression of SspB, which then bound the SsrA peptide tag and delivered the tagged RecD2 ($RecD2_T$) to the ClpXP protease for degradation (RecD2 degron strain) (Griffith & Grossman, 2008; Keiler *et al.*, 1996; Merrikh *et al.*, 2015). RecD2 or PcrA degron cultures were grown to OD_{560} = 0.4. Cells were divided and aliquots plated in LB agar plates alone or with IPTG (500 μM).

Survival studies

MMS, H_2O_2, 4NQO, MMC and IPTG were from Sigma Aldrich. Cell sensitivity to chronic MMS or H_2O_2 exposure was determined by growing cultures to OD_{560} = 0.4 and plating 10 μl of serial 10-fold dilutions (10^{-3} to 10^{-6}) on LB or MMS7 agar plates supplemented with the required amino acid (methionine and tryptophan, at 50 μg/ml each) and the indicated concentrations of the DNA-damaging agent, as described (Sanchez *et al.*, 2007). Cells grew in LB and MMS7 with a doubling time of 28–35 min and 55–65 min, respectively. Plates were incubated overnight (16–18 h, 37 °C). At least four independent experiments were performed; fractional survival data are shown as mean ± SEM. Cell sensitivity to IPTG was determined as above.

Fluorescence microscopy of* B. subtilis *cells and data analysis

To obtain exponentially growing cells, overnight cultures were inoculated in LB medium. The *ΔrecD2*, *ΔrecU*, *ΔruvAB* or *ΔrecG* cells were grown undisturbed in LB medium to OD_{560} = 0.4 (37 °C). Midlog-phase cells were fixed with 2% formaldehyde

and stained with DAPI (4′,6′-diamino-2-phenylindole; 1 µg/ml). The *recD2-ssrA ΔruvAB*, *recD2-ssrA ΔrecG* or *recD2-ssrA ΔrecU* cells were grown undisturbed in LB medium to OD_{560} = 0.2 (37 °C). IPTG (500 µM) was added to half the culture, and both cultures were incubated (60 min) before fixing with 2% formaldehyde and DAPI staining. Samples were visualized by fluorescence microscopy as described (Carrasco *et al.*, 2004).

III.2.6- Conflict of interest

The authors declare that the research was conducted in the absence of any commercial or financial relationships that could be construed as a potential conflict of interest.

III.2.7- Author contributions

R.T., H.R., V.R.-C. and J.C.A. designed the experiments; R.T., H.R. and V.R.-C. performed the experiments, J.C.A. coordinated the research; R.T., H.R., V.R.-C. and J.C.A. interpreted the data; R.T., H.R., V.R.-C. and J.C.A. drafted the manuscript; and J.C.A. wrote the manuscript.

III.2.8- Funding

This work was supported by the Spanish Ministerio de Economía y Competitividad (MINECO/FEDER) grant BFU2015-67065-P to J.C.A.

III.2.9- Acknowledgments

We are grateful to Houra Merrikh and Christopher Merrikh for the *pcrA-ssrA* degron strain, DNA from the *sspB* adaptor gene and information to target tagged proteins for proteolysis, C. Marchisone for technical assistance and C. Mark for editorial help. RT is a PhD fellow of the International Fellowship Programme of La Caixa Foundation (La Caixa-CNB).

III.2.10- References

See section VI.

III.3- RecD2-Unpublished Results

III.3.1- RecD2 interacts with RecA accessory factors

In our previous study, we showed some evidences that suggest that RecD2 can be involved in homologous recombination (Torres *et al.*, 2017). In order to further characterize this possibility, we introduced Δ*recD2* in different recombination deficient mutants.

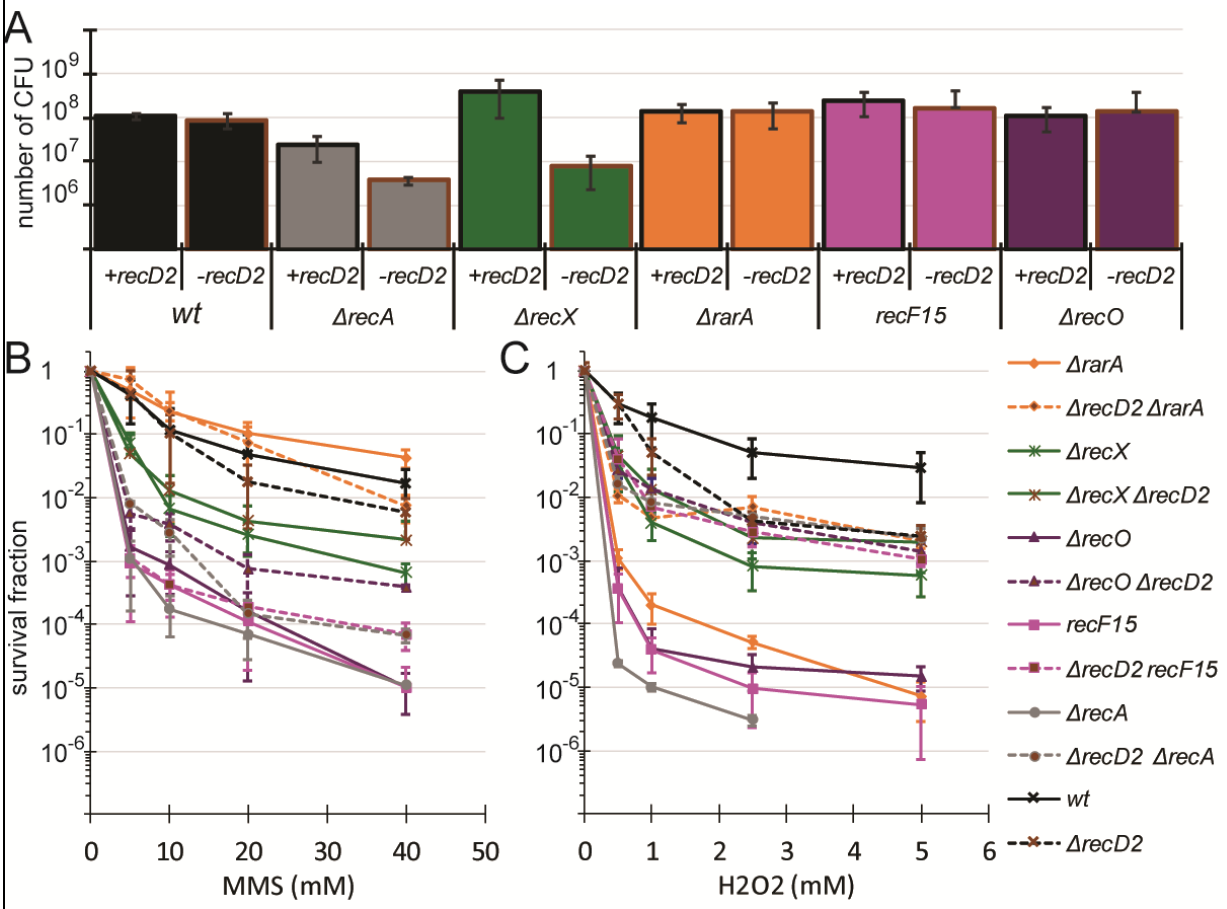

Figure 16. Effect of Δ*recD2* on the viability of recombination-defective mutants in the absence of drug-induced DNA damage (A), or after 15 min exposure to MMS (B) or H_2O_2 (C). Error bars shows standard deviation of at least three independent experiments.

Deletion of *recD2* in either Δ*recA* or Δ*recX* backgrounds leaded to a loss of viability in absence of DNA damage, but not in Δ*recO*, *recF15* or Δ*rarA* (**Figure 16**A). When cells were exposed to MMS (**Figure 16**B), Δ*recD2* did not change viability of Δ*rarA* or Δ*recX* cells, and had a modest impact in the recovery of viability in *recF15* and Δ*recA* cells, whereas there was a partial suppression of Δ*recO*. In the other hand, when cells were exposed to H_2O_2 (**Figure 16**C), deletion of *recD2* in combination with Δ*recA*, Δ*recO*, *recF15* or Δ*rarA* leaded to a huge recovery of viability whereas Δ*recX*

this effect was modest. All double mutants, in higher doses of H_2O_2, behaved as Δ*recD2* alone.

III.3.2- RecD2-mVenus construction

In order to further characterize the role of RecD2, we constructed a fluorescent-tagged RecD2-mVenus. After checking with PCR, we probed its functionality in MMS chronic viability assays. Cells containing RecD2-mVenus had the same resistance as wt cells, and clearly differed of the Δ*recD2* phenotype (**Figure S4**A). Then, we introduced RecD2-mVenus construction in backgrounds in which deletion of *recD2* was leading to an impairment in viability or resistance to DNA damage agents.

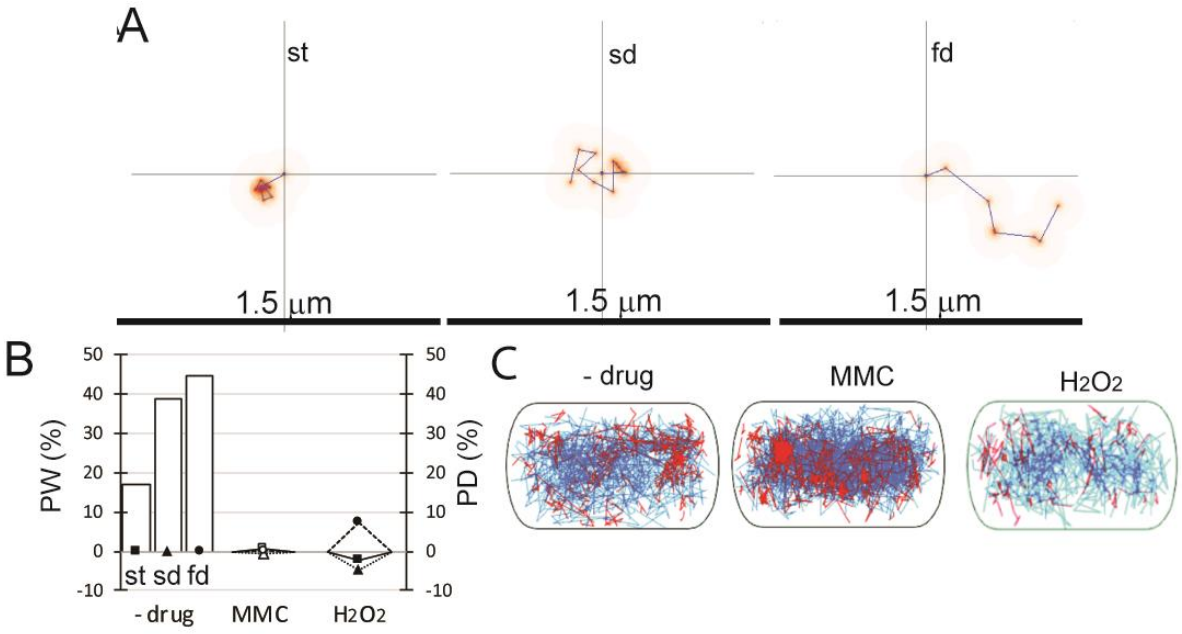

■ st: static; ▲sd: slow-dynamic; ●fd: fast-dynamic; PW: population weight; PD: population difference

Figure 17. RecD2 m-Venus characterization. (A) Examples of the three types of molecules founded for RecD2: static (st, left), slow-dynamic (sd, centre) and fast-dynamic (fd, right). (B) Population weights (PW) for RecD2 in wt cells in absence of drug and changes in these population (PD), considering 0 the PW in absence of damage, after the incubation for 60 min in either 50 ng/ml MMC or 0.5 mM H_2O_2. Black (■▲●) and white (□○Δ) markers represent significance or not of the population difference (PD) respectively compared to its control in a Z-test (see Methods). (C) Distribution of the confined (red) and not confined (blue) tracks in wt cells in absence of DNA damage (left) or after 60 min incubation with 50 ng/ml MMC (centre) or 0.5 mM H_2O_2 (right).

Around 30% of wt cells containing RecD2-mVenus showed fluorescence in exponential growth in epifluorescence microscopy. Of these 30%, most of them were presenting a diffuse pattern among the cytosol and only a few were presenting foci. We screened possible effects of either drug induction or recombination-deficient backgrounds, revealing a modest increase in spots after addition of either MMC or

MMS and no variation in the background studied, but we noticed huge differences in the replicates (data not shown). Thus, when we exposed the cells to first epifluorescence, and then slimfield laser, almost every cell was presenting fluorescence and they were several spots per cell (**Figure S4**B, C), indicating that epifluorescence was not enough resolving for localising RecD2-mVenus.

III.3.3- RecD2-mVenus dynamics are affected by other recombination factors

Due to the interactions with RecA and its accessory factors, we considered that 60 min induction with a DNA drug would be a good time to evaluate RecD2 dynamics, as RecF (Alonso *et al.*, 2013; Kidane *et al.*, 2004), and RarA (**Figure 5**) have been previously shown to be recruited in the DNA repair centre between 45 and 60 minutes.

An initial observation in single-molecule microscopy (SMM) of RecD2-mVenus revealed three distinct ways of movement (**Figure 17**A). This observation was confirmed by the Bayesian information criterium (BIC) for square displacement, that considered three populations as the best fitting model (included in SMTracker, see Methods): one population is completely static, with an apparent D=0.032±0.023 $\mu m^2 s^{-1}$, and two mobile fractions, a slower with a D=0.254±0.170 $\mu m^2 s^{-1}$, which is a value similar as the obtained for other DNA-binding proteins such as SMC (0.45 $\mu m^2 s^{-1}$) (Luise *et al.*, 2013), DisA (0.28 $\mu m^2 s^{-1}$) (Gándara *et al.*, 2017) or RarA (0.25 $\mu m^2 s^{-1}$) (**Table S2.**), and a fast population with a D=1.547 ±0.395 $\mu m^2 s^{-1}$ that could correspond to the cytosol pool fraction. These D were similar in the different background studied, as is expected for the same protein (data not shown), but not the weight for each population, indicating possible effects on RecD2 dynamics by the absence of these recombination factors.

In wild type cells, 17% of the molecules were static, 39% moved with low D (slow-dynamic) and 44% moved fast (**Figure 17**B). However, these weights were affected by inducing DNA damage and/or in defective recombination backgrounds, thus providing information about possible interactions.

In absence of DNA damage (**Figure 18**A), deletion of RecG leaded to a significant increase of the slow-dynamic population. As deletion of *recD2* is not possible in cells that already have *ΔrecG* due to the accumulation of unsegregated chromosomes (**Figure 15**), it is reasonable to say that slow-dynamic population is the responsible of the RecD2 role in chromosome segregation. Interestingly, in the

suppressor mutant *pcrA596*, RecD2-mVenus was presenting an increase in this population by reducing cytosol pool, but it did not happen in the complete deletion of PcrA, in which only the static population was decreased but none of the dynamic populations showed significance variance from wt cells (**Figure 19**A). Deletion of any RecA accessory factor (Δ*recA*, Δ*recX*, *recF15* or Δ*rarA*) produced an increase of the static population by reducing the cytosol fraction and, in the cases of Δ*recA* and Δ*rarA* mutants, the slow-dynamic population (**Figure 20**A).

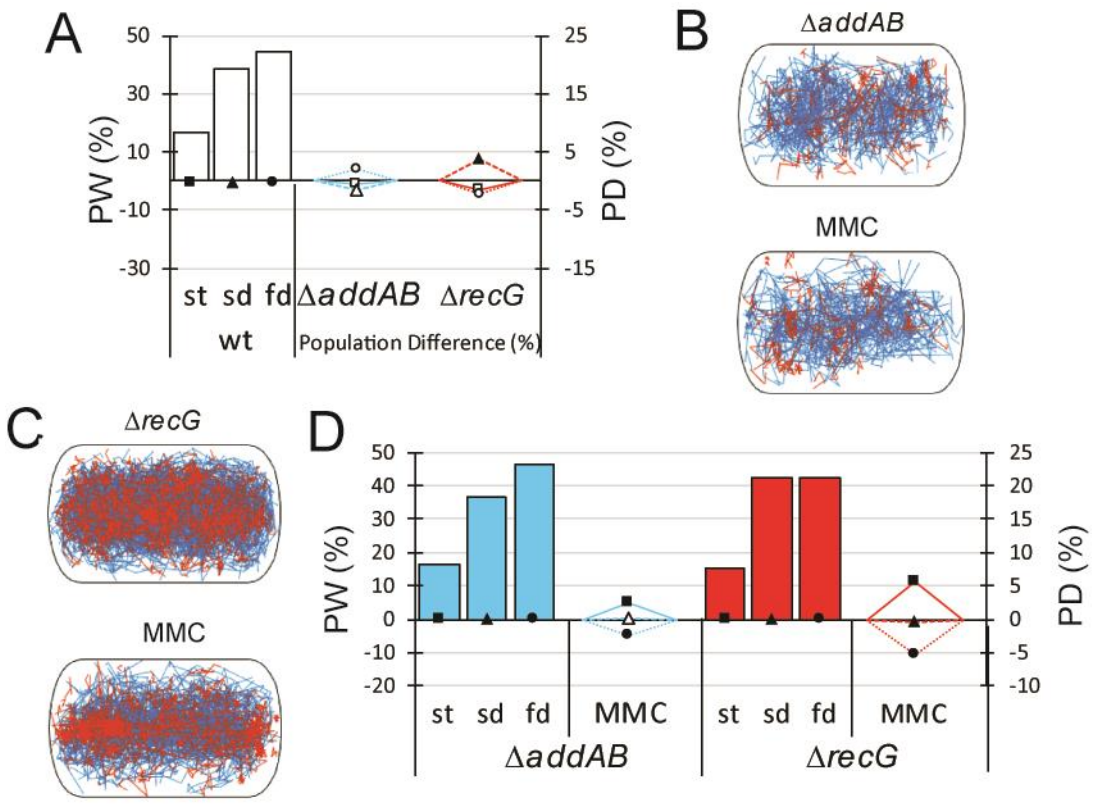

■ st: static; ▲sd: slow-dynamic; ●fd: fast-dynamic; PW: population weight; PD: population difference

Figure 18. RecD2-mVenus dynamics in absence of AddAB and RecG. (A, D) Changes in the population distribution in Δ*addAB* (blue) or Δ*recG* (red) cells, considering 0 population weights (PW) in wt background in absence of damage (A) or after the induction of DNA damage with 50 ng/ml MMC for 60 min (D), considering 0 the population weigths (PW) of the correspondent background in absence of damage. Black (■▲●) and white (□○Δ) markers represent significance or not of the population difference (PD) respectively compared to its control in a Z-test (see Methods). (B, C) Distribution of the confined (red) and not confined (blue) tracks in Δ*addAB* (B) and Δ*recG* (C) cells in absence of DNA damage (up) or after 60 min incubation with 50 ng/ml MMC (down).

Induction with H_2O_2 produced significant changes in all three populations of RecD2-mVenus, increasing the cytosol pool and reducing the expected DNA-bindings populations, slow-dynamic and static (**Figure 17**B). In contrast, in *pcrA596* cells, only

the static population was formed, while deletion of either *recA* or *rarA* leaded to an increase in the DNA-binding populations by decreasing the cytosol pool.

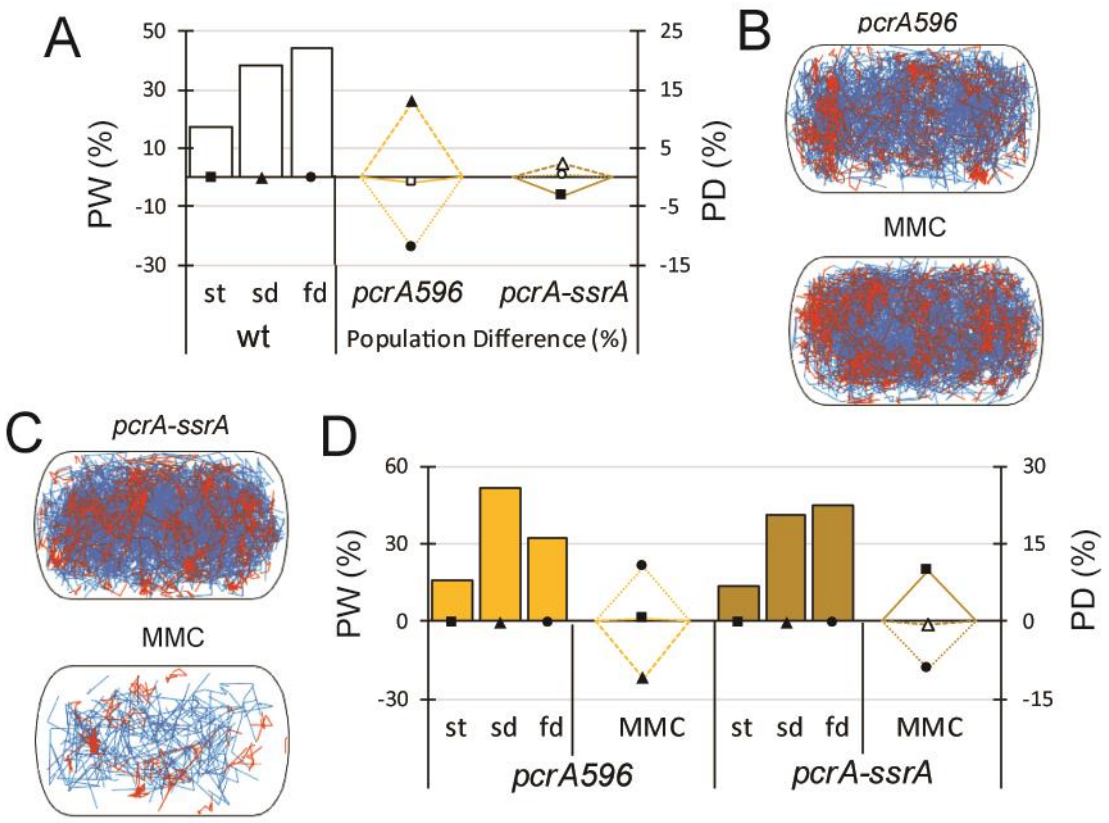

■ st: static; ▲sd: slow-dynamic; ●fd: fast-dynamic; PW: population weight; PD: population difference

Figure 19. RecD2-mVenus dynamics are affected by PcrA. (A, D) Changes in the population distribution in *pcrA596* (yellow) or *pcrA-ssrA* (gold) cells, considering 0 the population weights (PW) in wt background in exponential growth (A) or after the induction of DNA damage with 50 ng/ml MMC for 60 min (D), considering 0 the population weights (PW) of exponential growth. Black (■▲●) and white (□○Δ) markers represent significance or not of the population difference (PD) respectively compared to its control in a Z-test (see Methods). (B, C) Distribution of the confined (red) and not confined (blue) tracks in *pcrA596* (B) and *pcrA-ssrA* (C) cells in absence of DNA damage (up) or after 60 min incubation with 50 ng/ml MMC (down). Mutant cells containing *pcrA-ssrA* were exposed to 0.2 µM IPTG for 60 min prior to microscope (exponential growth) or to the addition of MMC.

Finally, after incubation with MMC (**Figure 17**B), wt cells did not present changes in RecD2 populations. However, deletion of the helicases AddAB, RecG (**Figure 18**D) or PcrA (**Figure 19**D), produced an increase of the static population by decreasing the fast-dynamic population. In *ΔrecA*, *recF15* and *ΔrarA* cells, slow-dynamic population is increased, while in *ΔrecX* is not only the slow-dynamic, but also the static population, which are increased (**Figure 20**F, G).

We wondered if the location of the RecD2-mVenus bounded to DNA would play a role in its function, so we pooled all tracks in a normalized 3:1 µm cell and sorted the molecules confined and not confined (see Methods, SMTracker). In most of the background studied (**Figure 17**C; **Figure 18**B; **Figure 19** B; **Figure 20**B-D), confined molecules were rare and preferentially presented in 3/4 and centre of the cell. Nevertheless, in the backgrounds were deletion of *recD2* produces an impairment in cell viability, *ΔrecX* (**Figure 20**E) *ΔrecG* (**Figure 18**C) and *PcrA-ssrA* (**Figure 19**C), confined molecules are more abundant and distributed equally in the cell, but after the addition of MMC looked like MMC-induced wt cells (**Figure 17**C; **Figure 20**E; **Figure 18**C; **Figure 19**C).

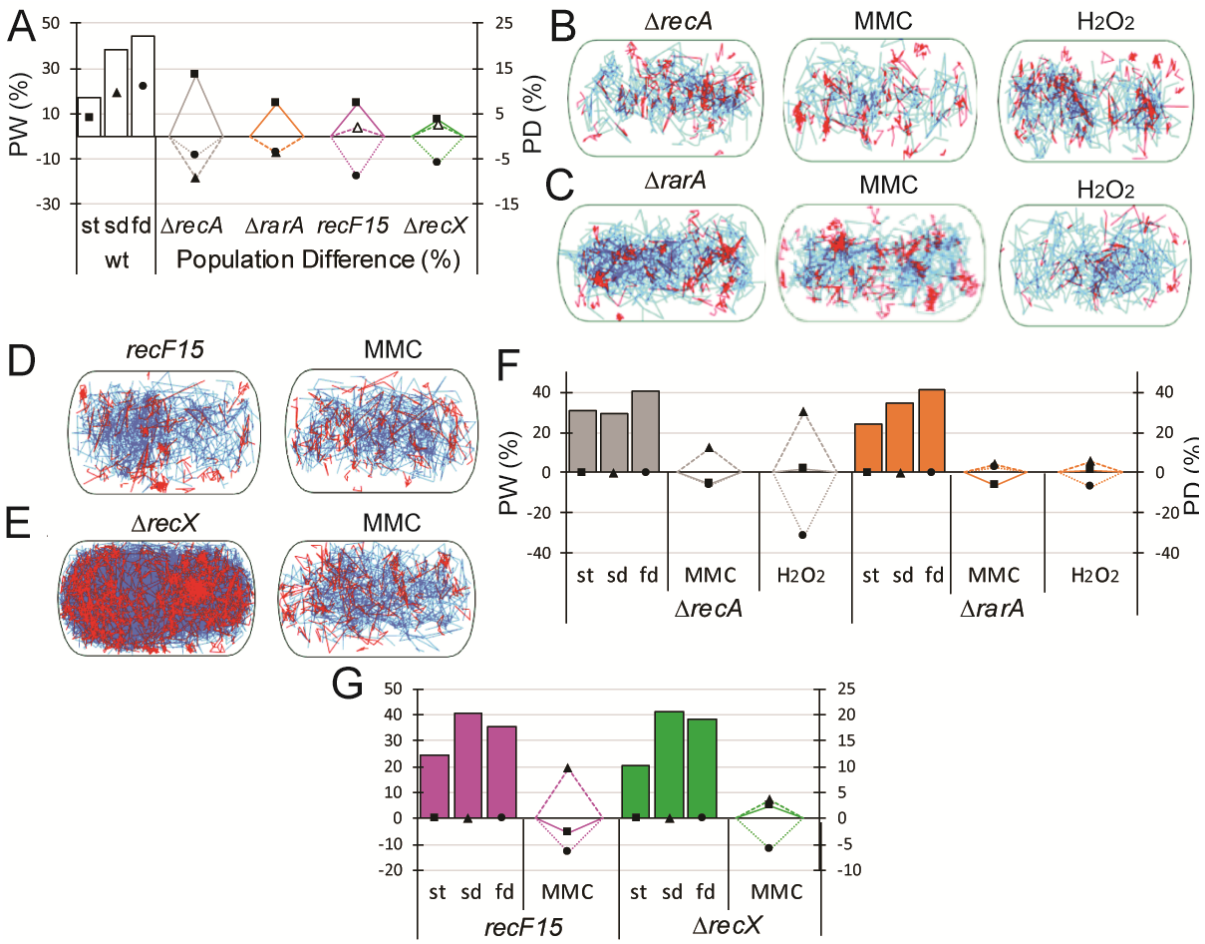

■ st: static; ▲sd: slow-dynamic; ●fd: fast-dynamic; PW: population weight; PD: population difference

Figure 20 RecD2-mVenus dynamics are affected by RecA and its regulatory factors. (A, F, G) Changes in the population distribution in *ΔrecA* (grey), *ΔrarA* (orange), *recF15* (purple) or Δ*recX* (green) cells, considering 0 the population weights (PW) to wt in exponential growth (A) or after 60 min incubation with 50 ng/ml MMC (F, G) or 0.5 mM H_2O_2 (F). For the population difference (PD), population weights (PW) of the same background in absence of damage is considered as 0. Black (■▲●) and white (□○Δ) markers represent significance or not of the population difference (PD) respectively compared to its control in a Z-test (see Methods). (B- E) Distribution of the confined (red) and not confined (blue) tracks in *ΔrecA*

(B), *ΔrarA* (C), *recF15* (D) or *ΔrecX* (E) cells in absence of DNA damage (left) or after 60 min incubation with 50 ng/ml MMC (centre/left) or 0.5 mM H_2O_2 (left).

III.3.4- Influence of PcrA in RarA dynamics

As PcrA and RarA seems to be major interaction partners of RecD2, we wondered if PcrA could also regulate RarA dynamics. For that purpose, we generated a mutant *pcrA-ssrA rarA-mVenus* (**Table 1**).

Degradation of PcrA by induction with 0.2 µM IPTG for 60 min reduced drastically the dynamic population (**Figure 21**A). Indeed, RarA-mVenus population became even more static when after depleting PcrA cells were induced with either H_2O_2 (**Figure 21**C) or MMC (**Figure 21**D).

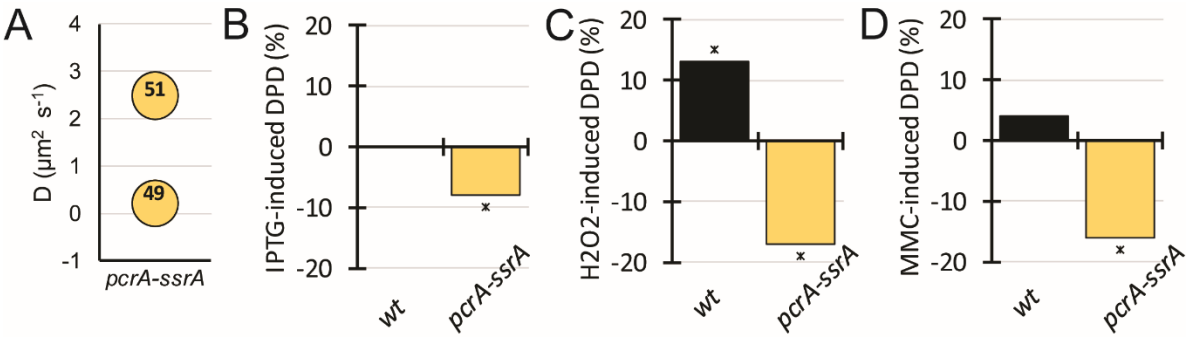

Figure 21. RarA dynamics are affected by deletion of PcrA. (A) Population weights for the static (0.23 µm^2 s^{-1}) and dynamic (2.5 µm^2 s^{-1}) population of RarA in *pcrA-ssrA* 60 min after induction of degradation with 0.2 µM IPTG. (B-D) DPD of RarA-mVenus in IPTG (B), IPTG + 0.5 mM H_2O_2 (C) and IPTG + 50 ng/ml MMC (D). Cells were incubated 60 min in presence of IPTG prior to the addition of either H_2O_2 or MMC. * means significant differences in z-test.

III.3.4- Supplementary Figures

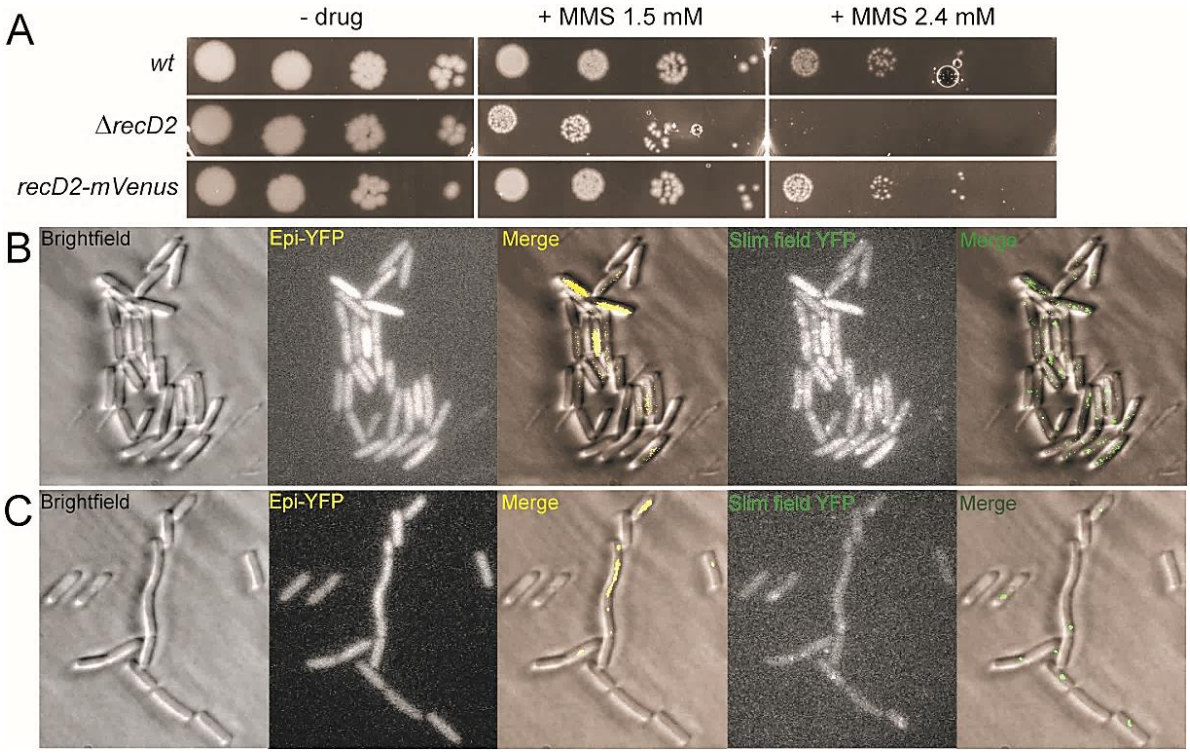

Figure S4. RecD2-mVenus characterization. (A) Chronic viability of RecD2-mVenus cells compared to wt and Δ*recD2* cells. The presence of the m-Venus tag does not affect viability of the strain, which is the same as wt. (B-C) Epifluorescence (Epi-YFP) and slim field (Slim field YFP) pictures of the same cells carrying RecD2-mVenus in exponential growth (B) and after 60 min incubation with 50 ng/ml of MMC (C).

Strain	Condition	D_{STATIC}	$D_{SLOW-DYNAMIC}$	$D_{FAST-DYNAMIC}$
wt	- drug	0.035 (17.0)	0.287 (38.5)	1.735 (44.5)
	H_2O_2	0.034 (14.5)	0.265 (33.9)	1.510 (51.6)
	MMC	0.020 (17.5)	0.191 (38.0)	1.425 (44.6)
ΔaddAB	- drug	0.026 (16.6)	0.190 (36.9)	1.450 (44.5)
	MMC	0.021 (19.0)	0.166 (37.0)	1.435 (44.1)
pcrA596	- drug	0.037 (16.2)	0.285 (51.4)	1.750 (32.4)
	MMC	0.029 (16.8)	0.239 (40.4)	1.540 (42.8)
pcrA-ssrA	- drug (IPTG)	0.019 (13.9)	0.212 (41.1)	1.640 (45.0)
	MMC (IPTG)	0.031 (23.9)	0.263 (40.5)	1.730 (35.7)
ΔrecG	- drug	0.020 (15.4)	0.172 (42.4)	1.110 (42.2)
	MMC	0.016 (21.1)	0.143 (42.0)	1.146 (36.9)
ΔrecA	- drug	0.061 (30.6)	0.364 (29.2)	2.120 (40.2)
	H_2O_2	0.064 (32.4)	0.641 (50.7)	1.880 (16.9)
	MMC	0.028 (24.7)	0.150 (41.5)	1.285 (33.8)
recF15	- drug	0.022 (24.2)	0.153 (40.4)	1.405 (35.4)
	MMC	0.030 (21.3)	0.258 (50.1)	1.615 (28.8)
ΔrecX	- drug	0.030 (20.6)	0.258 (41.1)	1.785 (38.4)
	MMC	0.053 (23.1)	0.335 (44.7)	1.775 (32.2)
ΔrarA	- drug	0.034 (24.3)	0.225 (34.9)	1.240 (40.9)
	H_2O_2	0.044 (25.3)	0.507 (40.7)	2.235 (34.0)
	MMC	0.031 (18.2)	0.266 (38.8)	1.325 (43.1)

Table S4. D values (in $\mu m^2 s^{-1}$) and population weight (in brackets, in %) for all backgrounds in the condition tested, expressed as the mean of two independent experiments.

IV. DISCUSSION

IV.1- Dynamics provides additional information to genetics

In a recent review (Uphoff & Sherrat, 2017), the relevance of SMM for DNA repair and mutagenesis is highlighted, as different *in vitro* approaches can provide useful information, from measuring single DNA lesions to visualize processes such as DSB repair, or which DNA polymerase is present in the fork. In this study, we propose SMM as a method to obtain information from protein interactions. For this purpose, we have analysed the dynamics of fluorescence-tagged RarA and RecD2 in response to drugs that generate DNA damage, H_2O_2 and MMC, in different recombination-, and replication-defective mutants in comparison with wt cells.

Correlation within dynamics and genetics gave four different scenarios: i) changes in dynamics are not correlated with a phenotype when the gene is deleted (silent regulation); ii) changes in dynamics are correlated with a genetic interaction (interaction partners); iii) dynamics are not modified but presented a genetic interaction (functional interaction); iv) no changes are observed neither in dynamics nor in genetics (independent factors).

IV.1.1- Silent regulation

Homologous recombination has been characterized traditionally as a cascade of events (Alonso *et al.*, 2013; Ayora *et al.*, 2011). According to this model, it is reasonable to expect that deletion of factors upstream of the cascade of events is indeed affecting the rest of the process. Until now, genetics suggested the existence of different avenues that are coincident in some key factors. As an example, *B. subtilis* DSB end-processing enzymes AddAB and RecJ-RecQ/S are different avenues that results in a SsbA-coated ssDNA that needs RecO for RecA nucleation (Carrasco *et al.*, 2015). According to this model, deletion of AddAB leads to the use of RecJ-RecQ/S and vice versa, but indeed there is a loss of viability in the process (Carrasco *et al.*, 2015). SMM approach revealed changes in RarA or RecD2 dynamics although deletion of the gene did not produce a different viability phenotype.

RarA was markedly affected by the deletion of one of the DSB-end processing enzymes: i) in exponential growth (**Figure 7**A), deletion of either RecJ or RecS produced a decrease in the dynamic population; ii) after H_2O_2 exposure (**Figure 7**B), deletion of AddAB, RecJ or RecQ suppressed the dynamic response observed in wt

cells, while in absence of RecS this dynamic response is significantly higher than in wt cells; and iii) after MMC exposure (**Figure 7**C), deletion of AddAB reduced the dynamic population while deletion of RecS produced a response equivalent to the H_2O_2-induced dynamic response in wt cells (**Figure 6**D). However, deletion of *rarA* in these backgrounds showed intermediate phenotypes in all double mutants (**Figure 11**B, **Figure S3**B), except for a synergetic recovery of *ΔrarA ΔaddAB* double mutant in H_2O_2 (**Figure 11**B), reflecting a silent regulation of RarA. Most of this silent regulation can be explained as a reduction of the ssDNA surface as a consequence of the deletion of one of the factors (AddAB, RecJ or RecQ), resulting in a smaller SsbA platform. As RarA is part of the SsbA interactome (Costes *et al.*, 2010), this may affect the recruitment to the damaged area. However, absence of RecS regulated RarA in a opposite way as the other factors, with special mention of RecQ, as they share a 36% identity (Fernandez *et al.*, 1998). Previous studies (Fernandez *et al.*, 1998) and our viability assays (**Figure 11**, **Figure 14**, **Figure S3**) failed in establishing a functional difference between the two RecQ-like helicases of *B. subtilis* that has been revealed with our SMM approach. Indeed, the interaction with RecS and RecQ, probably via SsbA (Costes *et al.*, 2010), agrees with the idea that there is a tight relation of RarA with RecQ-like helicases in Evolution (Barbour & Xiao, 2003), and the specificity of RecS and not RecQ is also seen in the eukaryotic homologue of RarA, WRNIP1/WHIP1, that shows specificity to WRN but not to the other RecQ-like helicases in humans (Kawabe *et al.*, 2001).

There is also a silent regulation of RarA in Δ*ruvAB* mutants. In the absence of DNA damage, Δ*ruvAB* cells showed a more static RarA than wt cells (**Figure 7**A), although Δ*ruvAB* Δ*rarA* double mutant did not change viability compared to Δ*ruvAB* (**Figure 11**E). Further experiments are needed to explain this behaviour.

In the case of RecD2, we founded silent regulation in Δ*addAB* mutant cells. MMC induction led to an increase of the static population and a decrease of the cytosol pool (**Figure 18**D). However, genetic assays showed that *recD2* is not epistatic with *addAB* (**Figure 14**). As RecD2 is also part of the SsbA interactome (Costes *et al.*, 2010), the same reasoning as RarA can be followed.

IV.1.2- Interaction partners

SMM method was able to detect several interaction partners for RarA that were lately confirmed by genetic interactions. Indeed, we were able to address the strength of the interaction. In some cases, RarA dynamics are modified in different conditions studied, resulting or not in a phenotype, while in others the interaction is restricted to one special condition.

Main interaction factors for RarA and RecD2

We had shown a clear interaction between RarA and RecD2. RarA dynamics are modified in absence of DNA damage and after MMC induction, but not after H_2O_2 induction (**Figure 7**). In the other hand, deletion of *rarA* drastically modified RecD2 dynamics in a similar way to Δ*recA* for all condition studied (**Figure 20**). Interestingly, Δ*recD2* Δ*rarA* double mutant presented no phenotype in absence of DNA damage (**Figure 11**E), ΔrarA parental phenotype after MMC induction (**Figure S3**D) and Δ*recD2* phenotype after H_2O_2 induction (**Figure 11**D). The interaction of RarA and RecD2 and its implications will be further discussed in the section **IV.4-** RarA and RecD2 are RecA regulators with opposite functions.

RecU is also showing a strong interaction with RarA. Δ*recU* cells have more dynamic RarA in absence of drug (**Figure 7**A) than wt cells, and induction with either H_2O_2 or MMC led to a significant decrease of the dynamic population (**Figure 7**B, C). Nevertheless, we only found a phenotype for H_2O_2 induction, were Δ*recU* Δ*rarA* double mutants presented a synergetic recovery of viability (**Figure 11**D). As RecU has a dual role in HR in *B. subtilis*, as HJ resolvase (Sanchez *et al.*, 2005) homologous to *E. coli* RuvC activity but also as a RecA regulator (Carrasco *et al.*, 2005), we suggest that interactions of RarA and RecU are coming at RecA level.

Finally, PolY1 has been showed also as an important interaction partner although differences were only found after MMC induction. This is explained by the own regulation of PolY1, that does not present basal expression but is induced by MMC (Duigou *et al.*, 2004). In Δ*polY1* mutant cells, RarA became more dynamic after MMC induction (**Figure 7**C), having a similar response to wt H_2O_2 response (**Figure 7**B), and deletion of *rarA* shows a parental Δ*polY1* phenotype. Previous studies in *E. coli* suggest that RarA might recruit other protein to the fork (Sherrat *et al.*, 2004) and interacts with other polymerases (Shibata *et al.*, 2005). Furthermore, RarA homologue

Mgs1 in budding yeast physically interacts with Polδ, a translesion polymerase, and enhances its processivity and fidelity (Barbour & Xiao, 2003).

Correlation of dynamics with genetics was clearer in RecD2 than RarA. Thus, most of the candidates we have explored were showing a dynamic and genetic phenotype. RecD2 has been proved to be an important regulator for RecA by interacting with RecA itself and with RecA-regulatory factors RecF, RecX and RarA. As mentioned above, RecD2 presented similar behaviour in all Δ*recA*, *recF15*, Δ*recX* and Δ*rarA* cells, characterized by an increase in the slow-dynamic fraction after DNA damage (**Figure 20**D). This correlates with recovery of viability by *recD2* deletion in these mutants after DNA damage compared to their respective parental (**Figure 16**B, C). There is also a correlation of loss of viability in absence of DNA damage (**Figure 16**A) with the distribution of the static tracks in the cell in Δ*recX* (**Figure 20**E). As RecF and RecX are opposite regulators of the RecA (Lusetti *et al.*, 2006; Cárdenas *et al.*, 2012), and deletion of RecD2 caused more severe problems in Δ*recX* mutant cells, we suggest that RecD2 is also a negative regulator of the RecA activity.

Then, we founded an interaction partner for RecD2 as an emerging suppressor mutation in *pcrA* gene in Δ*recD2* cells. By SMM, we showed that the suppressor *pcrA596* indeed changed the interaction with RecD2, in absence or presence of DNA damage (**Figure 19**), in a different way that the deletion of the PcrA protein in the mutant *pcrA-ssrA*: while *pcrA596* increased the slow-dynamic and reduced the fast-dynamic fraction in absence of damage, in *pcrA-ssrA* there is a decrease of the static population (**Figure 19**D); and the distribution of the static tracks of RecD2 is more spread in the *pcrA-ssrA* mutant (**Figure 19**C), correlating with a decrease of viability as observed in Δ*recX* (**Figure 20**E). On the other hand, *pcrA596* mutation caused an increase in the sensitivity of the Δ*recD2 pcrA596* to DNA damage compared to the parental strains (**Figure 13**). We can speculate that the growth defect observed on RecD2 is related to its function in the regulation of PcrA, and the mutation *pcrA596* suppresses the need of RecD2, but it also changes the PcrA impact to RecA filament dynamics as a negative regulator by removing RecA molecules from the filaments (Thickman *et al.*, 2002).

Finally, we were able to characterize the interaction of RecD2 with RecG, which opened a new way to study interaction within proteins that are part of an essential process of the cell, and thus generation of double mutants is not possible. This

interaction will be further discussed in the section **IV.3.2-** Deletion of RecD2 increases anomalous chromosomal segregation.

Interactional partners in special conditions

In the case of RarA, we founded two examples of proteins that were showing a dynamic and genetic interaction, but only when cells were induced by H_2O_2: AddAB and RecG.

In Δ*addAB* cells, induction with H_2O_2 did not promote a dynamic response that was characterized for wt cells (**Figure 7**B), and indeed Δ*addAB* Δ*rarA* double mutants presented a synergetic recovery of viability in H_2O_2 near to wt levels (**Figure 11**B). The same absence of dynamic response was observed in Δ*recG* cells (**Figure 7**B), with a smaller synergetic recovery of viability in Δ*recG* Δ*rarA* cells (**Figure 11**C). We can speculate about this factors as a part of an alternative repair process in response to a specific DNA damage generated by H_2O_2 but not by MMC, that could generate toxic intermediates, but further experiments are needed to prove this hypothesis.

IV.1.3- Functional interaction

Despite of the good correlation in other interaction factors, SMM failed in the characterization of two of the main interaction partners of RarA: RecO and RecF. SMM RarA dynamics in Δ*recO* cells were showing no differences to the wt cells in any of the conditions tested (**Figure 7**), while we only found differences in the suppression of the H_2O_2-induced dynamic response of RarA in *recF15* cells (**Figure 7**B). However, deletion of *rarA* caused a severe growth defect in both Δ*recO* and *recF15* cells (**Figure 11**E) and Δ*recO* Δ*rarA* presented a synergetic loss of viability to both H_2O_2 (**Figure 11**A) and MMS (**Figure S3**A). Both Δ*recO* and *recF15* cells were showing a similar phenotype in our epifluorescence approach (**Figure 5**B), with a different intensity and time scale than wt (**Figure 5**A), and opposite to Δ*recX* and Δ*recD2* (**Figure 5**C).

IV.1.4- Independent factors

Finally, we found some factors of the HR cascade that did not show neither dynamic nor genetic interactions with RarA: RecX, RadA and PolY2.

IV.2- RarA has a dual role in replication and recombination repair

Our study has revealed a different behaviour of one repair-related protein, RarA, depending on the source of DNA damage. Then, we can difference different states and functions depending on the DNA: i) in absence of damage and ii) after drug-induced DNA damage.

IV.2.1- Role of RarA in replication

In absence of DNA damage, most of RarA molecules (~80%) were located in or closely related to the replication fork, while ~20% were located in areas not related with the replication fork. This first observation, based on colocalization in both epifluorescence (**Figure 8**) and single-molecule microscopy (**Figure 9**), presenting similar colocalization rates as RecO with DnaX (Costes *et al.*, 2010) and showed a clear difference compared to *E. coli* RarA, which is used as a marker of the replication fork (Sherrat *et al.*, 2004). This preferred location of RarA is due of two different interactions: i) RarA is known to be part of the *B. subtilis* SsbA interactome, and the helicase activity of DnaC in the replication fork provides a suitable ssDNA platform for SsbA (Costes *et al.*, 2010); and ii) interaction with DnaB.

As we showed in this study: non-permissive temperatures in *dnaC30* thermosensitive strain led to a higher dynamic population of RarA, whereas in *dnaB37* was more static (**Figure 8**D) and in fact these dynamics corresponded to a decrease or an increase in the confined molecules merging with the replication fork in *dnaC30* and *dnaB37* respectively (**Figure 9**G). As it is known that DnaC is necessary for the ssDNA platform needed for SsbA to recruit its interactome (Barbour & Xiao, 2003), we propose that RarA is recruited to the replication fork through the normal function of DnaC while DnaB function is the continuous removal of RarA from there. This suggestion could explain the different location behaviour of GFP-DnaB compared to other replication machinery elements (Meile *et al.*, 2006). The presence and removal of RarA evidenced a functional role, as both *dnaC30* and *dnaB37* mutants combined with *ΔrarA* resulted in a more severe loss of viability in semi- and non-permissive temperatures, whereas Δ*rarA* combined with other thermosensitive replication mutants (*dnaE58*, *dnaG20*, *dnaX51* or *dnaF133*) did not show differences to the parental strain (**Figure 12**).

RarA role in replication is also highlighted when *ΔrarA* is combined with other recombination-deficient proteins as *ΔradA*, *ΔrecO*, *recF15* or *ΔrecA* (**Figure 11**E), as double mutants raised a growth defect that was not present in the parental strains (in first three) or exacerbated the growth defect of the parental strain (in the case of *ΔrecA*). In addition, our dynamic study suggested that RarA is silent regulated in absence of other recombinational factors, such as RecD2, RecJ, RecS, RecU and RuvAB, even in absence of DNA damage (**Figure 7**A). Looking to *E. coli*, eYFP-RarA foci disappear when replication is blocked by hydroxyurea or rifampicin (Sherrat *et al.*,

2004), and due to its interaction with RecA it has been proposed to play a role in replication (Shibata *et al.*, 2005). All genes and proteins mentioned to change RarA behaviour in absence of damage, except of RadA, have been characterized in the context of replication fork regression or replication fork restart in previous studies (Courcelle & Hanawalt, 1999; Seigneur *et al.*, 2000; Walsh *et al.*, 2014), including RarA for both prokaryotes (Barre *et al.*, 2001; Lau *et al.*, 2003) and eukaryotes (Barbour & Xiao, 2003).

IV.2.2- Specific response of RarA to DNA damage

Different studies in *E. coli* failed in the search for a clear phenotype in Δ*rarA* mutants considering DNA repair (Barre *et al.*, 2001; Shibata *et al.*, 2005). However, we have shown that *B. subtilis* Δ*rarA* cells were very sensitive to H_2O_2 (**Figure 10**), and it rendered the cells more resistant to MMS or MMC in chronic exposure (**Figure 10**A). Indeed, only H_2O_2 was significantly modifying RarA dynamics, whereas MMC or MMS had either little or no impact (**Figure 6**C, D).

H_2O_2-induced DNA damage not only increased the dynamic population of RarA (**Figure 6**D), but also modified the preferred location of RarA confined molecules from replication fork to other location of the cell (**Figure 9**G), as it has been shown to other proteins such as RecN, RecO and RecF in response to DSB formation (Kidane *et al.*, 2004). As mentioned above, the mobilization is influenced by other recombinational factors, as AddAB, RecJ, RecS, RecQ, RecF, RecU, RecG and RadA (**Figure 7**B), although only Δ*addAB* Δ*rarA*, Δ*recG* Δ*rarA* and Δ*recU* Δ*rarA* double mutants showed a genetic interaction in presence of H_2O_2 (**Figure 11**). The specifity of RarA with H_2O_2 could be related with its influence in the repair of ssDNA gaps that are generated together with the DSB (Prise *et al.*, 1989), as it is known that RarA can provide a suitable substrate to the replicative helicase by creating a flap in the interphase between ssDNA and ds-DNA (Stanage *et al.*, 2017) and avoid recombinational repair.

Although deletion of *rarA* did not result in a severe phenotype for MMC (**Figure 10**), we showed some evidences that points RarA to be involved in MMC-induced DNA damage repair: i) the percentage of cells containing RarA foci was increased after MMC exposure (**Figure 5**A); ii) we showed a recruitment of RarA-mVenus in locations outside of the replication fork influence area (**Figure 8**B); iii) RarA molecules presented higher random movements and less confinement after MMC treatment (**Figure 8**D) ; iv)

RarA recruitment and dynamics are influenced by MMC-induced DNA damage in the absence of other recombinational factors (**Figure 5**, **Figure 7**C). Our results support the idea of DNA repair centres formed outside of the replication forks in *B. subtilis* (Kidane *et al.*, 2004) rather than the absolute need of the presence of a replication fork for homologous recombination (Lenhart *et al.*, 2014).

IV.3- RecD2 has a role in chromosomal segregation and DNA repair

Our study of RecD2 suggested two clearly differentiated functions for the 5'→3' helicase: chromosomal segregation, which can explain the poor growth that characterize Δ*recD2* cells, and as a regulator in the homologous recombination.

IV.3.1- RecD2 presents three populations of molecules considering its D

Our SMM approach revealed the presence of three populations of molecules according to their movement (**Figure 17**A). We determined the D and the weight of the populations by Square Displacement resulting in: i) a static population with D=0.032 $\mu m^2 s^{-1}$, ii) a slow-dynamic fraction with a D=0.254 $\mu m^2 s^{-1}$, and iii) a fast-dynamic population with a D=1.547 ±0.395 $\mu m^2 s^{-1}$ (**Table S4**)

Comparison of this data with other proteins, allowed us to speculate about the subcellular location of each RecD2 fraction. The static population presented a similar D as a DisA fraction tightly bounded to DNA (Gándara *et al.*, 2017). The slow-dynamic D is in the same range at the obtained for different proteins that scan DNA, as SMC (Kleine Borgman *et al.*, 2013) or DisA DNA-scanning fraction (Gándara *et al.*, 2017), and to other DNA-binding proteins as RarA (**Table S2.**). This two populations correspond to two different states of RecD2 in the DNA. We can speculate that the static population is a fraction of RecD2 that is unwinding the DNA according to the passive unwinding model for helicases (Pyle, 2008), while the slow-dynamic could correspond to a scanning fraction of RecD2 searching for the 5'-ssDNA end substrate that needs for the unwinding (Walsh *et al.*, 2014). Finally, the faster population would correspond to the cytosol pool of RecD2.

IV.3.2- Deletion of RecD2 increases anomalous chromosomal segregation

During the generation of the mutants for the genetic characterization of Δ*recD2* we found out that the single mutant exhibited poor growth compared to the wt BG214 parental cells. Indeed, a suppressor located in the *pcrA* gene, *pcrA596*, was founded in two different strains independently: the single mutant Δ*recD2*, and Δ*recD2* Δ*addAB*

double mutant. In addition, we were not able to generate the double mutants Δ*recD2* Δ*recG* and Δ*recD2* Δ*ruvAB*. As Δ*recD2* Δ*recU* was viable, a putative role of RecD2 in HJ-resolution would be insufficient to explain this phenomenon.

We further investigate the effect of Δ*recD2* in chromosomal segregation and confirmed that presented a modest increase in the anucleate cells and unsegregated chromosomes compared to the HJ enzymes Δ*recG*, Δ*ruvAB* or Δ*recU* (**Figure 15**, Carrasco *et al.*, 2004). When we deleted RecD2 using the *recD2-ssrA* degron strategy, we showed an increase of the unsegregated chromosomes, but not the anucleate cells, in Δ*recG* and Δ*ruvAB* cells, but not in Δ*recU* mutants (**Figure 15**), suggesting that the accumulation of unsegregated chromosomes caused the inviability of the double mutants. Interestingly, RecD2 dynamics are slightly modified in the Δ*recG* background compared to wt cells, with a significant increase of the slow-dynamic fraction of RecD2 (**Figure 18**D), that we were considering as DNA scanning fraction. We propose two alternatives to explain this observation: i) RecD2 movement along DNA is enough to remove part of the toxic intermediates that result in unsegregated chromosomes; or ii) RecD2 slow-dynamic fraction correspond to the active helicase activity of RecD2, and then the static fraction correspond to either a stopped helicase activity or a relaxed state of RecD2. Further studies are needed to confirm if one of these alternatives is correct, and if other helicases as RuvB, which also becomes essential in Δ*recG* cells (Sanchez *et al.*, 2007), present similar behavior.

In addition, we found that confined RecD2 molecules are more spread over the cytosol in Δ*recG* cells (**Figure 19**C) than in wt (**Figure 17**C), as was observed in other mutants that showed growth defects.

IV.3.3- RecD2 is involved in DNA repair

We have shown that deletion of Δ*recD2* led to an increase sensitivity to DNA damage caused by different agents (**Figure 13**) and presented genetic interactions with recombinational proteins as PcrA, RecA, RecO, RecF, RecX and RarA (**Figure 13**, **Figure 16**). Indeed, Δ*dinG* Δ*recD2* and *pcrA596* Δ*addAB* Δ*recD2* mutants are depleted of HR repair (**Figure 14**B). Our findings add information of the role of RecD2 to the previous mentioned influence in DNA repair (Walsh *et al.*, 2014).

Genetics of the double mutants combining Δ*recD2* with Δ*recO* or *recF15* resemble to the findings for double mutants of Δ*recX recF15*, suggesting that Δ*recD2*

plays a role as a negative regulator of RecA loading and filament assembly (Cárdenas *et al.*, 2012), maybe in a similar mechanism as the proposed for PcrA (Fagerburg *et al.*, 2012) in the opposite direction (see **Figure 2**).

IV.4- RarA and RecD2 are RecA regulators with opposite functions

In this study, we have highlighted which can be considered as a different role depending on the situation of the cell for both RarA and RecD2. In absence of DNA damage, both proteins have been shown to be important for replication, but in different aspects: RarA can be inferred to play a role in replication fork progression due to its interactions with DnaB, whereas RecD2 could be involved in the elimination of toxic intermediates generated by the homologous recombination machinery. However, after inducing DNA damage by different agents, both RarA and RecD2 are mobilized and show interactions with several recombinational factors, with special importance of RecA and other proteins involved in RecA regulation as RecO, RecF, RecX or PcrA.

Interestingly, deletion of *rarA* or *recD2* in Δ*recA* cells results in an increased growth defect in absence of DNA damage (**Figure 11**E, **Figure 16**A), and a partial suppression after H_2O_2 induction (**Figure 11**A, **Figure 16**C). This growth defect could point to the implication of RarA and RecD2 in a RecA-independent pathway for replication fork progression. Nevertheless, when the relation to the RecA accessory factors is compared, RarA and RecD2 deletions led to opposite phenotypes: In Δ*recO* and *recF15*, deletion of *rarA* led to a high-sensitivity to drugs (**Figure 11**A, **Figure S3**A) while deletion of *recD2* produces a suppression (**Figure 16**C). The antagonic effects of RarA and RecD2 can be continued based on previous studies. *B. subtilis* Δ*recD2* showed increased mutagenesis (Walsh *et al.*, 2014) while is needed to overexpress RarA in *E. coli* for the same purpose (Shibata *et al.*, 2005).

Double mutant Δ*rarA* Δ*recD2* did not present any growth defect (**Figure 16**A), and showed the more resistant parental phenotype for every drug studied: in H_2O_2, it presents a Δ*recD2* phenotype (**Figure 16**C), whereas in MMS showed a Δ*rarA* phenotype (**Figure 16**B). Interestingly, dynamics of RarA are affected by RecD2 in absence of DNA damage (**Figure 7**A) and after MMC induction (**Figure 7**C), but not in H_2O_2-induced DNA damage (**Figure 7**B), whereas RecD2 dynamics are affected in Δ*rarA* cells in all conditions studied in a similar way as the deletion of *recA* (**Figure 18**).

RarA and RecD2 dynamics were modified in presence of DNA damage when PcrA-ssrA degradation was triggered by IPTG induction (**Figure 19**, **Figure 21**). In both cases, absence of PcrA increased the static population, suggesting that PcrA could play a role in the removal of both proteins in the repair centre, probably as a consequence of the RecA depolymerization function of PcrA (Thickman *et al.*, 2002).

We have given strong evidences that point an opposite role of RarA and RecD2 in homologous recombination repair, being RarA a positive and RecD2 a negative regulator of RecA function, with a clear dependence of each other for their function. Altogether, our work adds a new level of regulation of RecA, confirming the existence of a tight control of the cell in this important process that is highly conserved among Evolution.

IV.5- Model

In absence of DNA damage, both RarA and RecD2 are preferentially located in the replication fork and are involved in the restart of a blocked replication fork in a RecA-dependent or independent mechanism, being the RecA-independent minority compared to the RecA-dependent. In RecA-dependent mechanism, RarA can compensate the absence of one of the RecFOR proteins, while RecD2 is able to compensate RecX function. The RecA-independent mechanism might be a marginal way to restart replication involving both factors, and maybe others as RuvAB or RecU. Both RarA and RecD2 seems to be involved in other functions, this time alone: RarA could be implicated in replication fork progression by its interactions with DnaB and DnaC, while RecD2 moving on the DNA is able to resolve some otherwise toxic DNA structures.

In presence of DNA damage, RarA and RecD2 have to be recruited to the repair centre. In the case of RarA, AddAB and RecQ-RecJ have importance in this recruitment, while RecS would act as an inhibitor. Both RarA and RecD2 are part of the RecA regulatory factors: RarA, together with RecO, RecR and RecF, contributes to the extension of RecA filaments, while RecD2, RecX, PcrA and RecU contribute to the disassembly of RecA.

V. CONCLUSIONS

1. Single-molecule microscopy is a powerful method for the *in vivo* characterization of proteins and its interactions, providing valuable additional information to genetics and *in vitro* assays.

2. Homologous recombination is not a lineal but multiway process tightly regulated by many factors involved in the different avenues with partially overlapping functions.

3. Several factors contribute to the specificity of the response to DNA damage based on the kind of damage generated.

4. RarA and RecD2 play a role in both replication and homologous recombination processes, being part of a RecA-independent and RecA-dependent replication fork progression and DNA repair.

5. RarA and RecD2 are antagonistic regulators of RecA filamentation.

6. RarA plays a role during DNA replication through interactions with DnaB.

7. RarA function as a RecA positive regulator in HR is determined by its interaction with RecA, RecO, RecR, RecD2 and RecU, and is regulated mainly by the RecQ-like helicases RecQ and RecS.

8. RecD2 plays a role in chromosomal segregation that becomes essential in the absence of RecG or RuvAB.

9. RecD2 function as a RecA negative regulator in HR is determined by its interaction with RecA, RarA, RecX, RecF and PcrA.

VI. BIBLIOGRAPHY

Ameida K.H. & Sobol R.W (2007) A unified view of base excision repair: lesion-dependent protein complexes regulated by post-translational modification. DNA Repair. 6: 695–711.

Alonso J.C., Cardenas P.P., Sanchez H., Hejna J., Suzuki Y. & Takeyasu K (2013). Early steps of double-strand break in *Bacillus subtilis*. DNA repair. 12: 162-76.

Alonso J.C., Lüder G. & Trautner T.A (1986). Requirements for the formation of plasmid-transducing particles of *Bacillus subtilis* bacteriophage SPP1. EMBO Journal. 5:3723–8.

Alonso J.C., Stiege A.C. & Lüder G (1993). Genetic recombination in *Bacillus subtilis* 168: effect of recN, recF, recH and addAB mutations on DNA repair and recombination. Molecular and General Genetics. 239: 129–36.

Alonso, J.C., Stiege, C.A., Tailor, R.H. & Viret, J.F (1988). Functional analysis of the dna (Ts) mutants of *Bacillus subtilis*: plasmid pUB110 replication as a model system. Molecular and General Genetics. 214: 482-9

Alonso, J.C., Tailor, R.H. and Luder, G (1988). Characterization of recombination-deficient mutants of Bacillus subtilis. Journal of bacteriology. 170: 3001-7.

Amundsen S.K., Taylor A.F., Chaudhury A.M., Smith G.R (1986). recD: the gene for an essential third subunit of exonuclease V. Proceedings of the National Academy of Sciences of the United States of America. 83: 5558–62.

Atkinson J. & McGlynn P (2009). Replication fork reversal and the maintenance of genome stability. Nucleic Acids Research. 37: 3475–92.

Au N., Kuester-Shoeck E., Mandava V., Bothwell L.E., Canny S.P., Chachu K., Colavitto S.A., Fuller S.N., Groban E.S., Hensley L.A., O'Brien T.C., Shah A., Tierney J.T., Tomm L.L., O'Gara T.M., Goranov A.I., Grossman A.D. & Lovett C.M. (2005) Genetic composition of the *Bacillus subtilis* SOS system. Journal of Bacteriology. 187(22): 7655-66.

Ayora S., Carrasco B., Cárdenas P.P., César C.E., Cañas C., Yadav T., Marchisone C. & Alonso J.C (2011). Double-strand break repair in bacteria: a view from *Bacillus subtilis*. FEMS Microbiology Reviews. 35: 1055-81.

Ayora S., Carrasco B., Doncel E., Lurz R. & Alonso J.C (2004). *Bacillus subtilis* RecU protein cleaves Holliday junctions and anneals single-stranded DNA. Proceedings of the National Academy of Sciences of the United States of America. 101: 452–7.

Baharoglu Z., Petranovic M., Flores M.J. & Michel B. RuvAB is essential for replication forks reversal in certain replication mutants. The EMBO Journal. 25: 596-604.

Baker T.A. & Bell S.P (1998). Polymerases and the replisome: machines within machines. Cell. 92(3): 295-305.

Barbour L. & Xiao W (2003). Regulation of alternative replication bypass pathways at stalled replication forks and its effects on genome stability: a yeast model. Mutation Research.532: 137-55.

Barre F.X., Søballe B., Michel B., Aroyo M., Robertson M. & Sherratt D (2001). The replication-recombination-chromosome connection. PNAS. 98(15): 8189-95.

Bell J.C. & Kowalczykowski S.C. (2016) RecA: regulation and mechanism of a molecular search engine. Trends in Biochemical Sciences. 41(6): 491-507.

Berkmen M.B. & Grosmann A.D. (2006) Spatial and temporal organization of the *Bacillus subtilis* replication cycle. Molecular Microbiology. 62(1): 57-71.

Bernard R., Marquis K.A. & Rudner D.Z (2010). Nucleoid occlusion prevents cell division during replication fork arrest in *Bacillus subtilis*. Molecular Microbiology 2010. 78(4): 866-82.

Beyer D.C., Ghoneim M.K. & Spies M (2013). Structure and mechanisms of SF2 DNA helicases. Advances in Experimental Medicine and Biology. 767: 47–73.

Bochman M.L., Judge C.P. & Zakian V.A (2011). The Pif1 family in prokaryotes: what are our helicases doing in your bacteria? Molecular Biology of the Cell. 22: 1955–9.

Bruand C., Farache M., McGovern S., Ehrlich S.D. & Polard P (2001). DnaB, DnaD and DnaI proteins are components of the *Bacillus subtilis* replication restart primosome. Molecular Microbiology. 42(1): 245-55.

Bruand C., Velten M., McGovern S., Marsin S., Serena C., Ehrlich S.D. & Polard P (2005). Functional interplay between the *Bacillus subtilis* DnaD and DnaB proteins essential for initiation and re-initiation of DNA replication. Molecular Microbiology. 55: 1138–50.

Cañas C., Suzuki Y., Marchisone C., Carrasco B., Freire-Beneitez V., Takeyasu K., Alonso J.C. & Ayora S (2014)., Interaction of branch migration translocases with the Holliday junction-resolving enzyme and their implications in Holliday junction resolution. The Journal of Biological Chemistry. 289: 17634–46.

Cárdenas P.P., Carrasco B., Soufo C.D., César C.E., Herr K., Kaufenstein M., Graumann P. & Alonso J.C (2012). RecX facilitates homologous recombination by modulating RecA activities. PLOS Genetics. 8(12): e1003126.

Carrasco B., Ayora S., Lurz R. & Alonso J.C. (2005). *Bacillus subtilis* RecU Holliday-junction resolvase modulates RecA activities. Nucleic Acid Research. 33(12): 3942-52.

Carrasco B., Cozar M.C., Alonso J.C.& Ayora S (2004). Genetic recombination in *Bacillus subtilis* 168: contribution of holliday junction processing functions in chromosome segregation. Journal of Bacteriology. 186(17):5557-66.

Carrasco B., Fernandez S., Petit M.A. & Alonso J.C. (2001). Genetic recombination in *Bacillus subtilis* 168: effect of (helD on DNA repair and homologous recombination. Journal of Bacteriology. 183: 5772–7.

Carrasco B., Yadav T., Serrano E. & Alonso J.C. (2015). *Bacillus subtilis* RecO and SsbA are crucial for RecA-mediated recombinational DNA repair. Nucleic Acid Research. 43(12): 5984-97.

Ceglowski, P., Luder, G. & Alonso, J.C. (1990) Genetic analysis of *recE* activities in *Bacillus subtilis*. Molecular and General Genetics. 222: 4415.

Costes A., Lecointe F., McGovern S., Quevillon-Cherual S. & Polard P. (2010). The C-Terminal domain of the bacterial SSB protein acts as a DNA maintenance hub at active chromosomal replication forks. PLOS Genetics. 6(12): e1001238.

Courcelle J & Hanawalt P.C. (1999) RecQ and RecJ process blocked replication forks prior to the resumption of replication in UV-irradiated *Escherichia coli*. Molecular & General Genetics. 262:543-551.

Cox M.M. (2007) Regulation of bacterial RecA protein function. Critical Reviews in Biochemistry and Molecular Biology. 42(1): 41-63.

Dillingham M.S. (2011). Superfamily I helicases as modular components of DNA-processing machines. Biochemical Society Transactions. 39: 413–23.

Dillingham M.S. & Kowalczykowski S.C. (2008) RecBCD enzyme and the repair of doublestranded DNA breaks. Microbiology and Molecular Biology Reviews. 72: 642–71.

Duigou S., Ehrlich S.D., Noirot P. & Noirot-Gros M.F. (2004) Distinctive genetic features exhibited by the Y-family DNA polymerases in *Bacillus subtilis*. Molecular Microbiology. 54(2): 439-51.

Epshtein V. (2015). UvrD helicase: an old dog with a new trick: how one step backward leads to many steps forward. Bioassays. 37: 12–9.

Epsthtein V., Kamarthaopu V., McGary K., Svetlov V., Ueberheide B., Proshkin A., Mironov A. & Nudler E. (2014). UvrD facilitates DNA repair by pulling RNA polymerase backwards. Nature. 505: 372-7.

Fagerburg M.V., Schauer G.D., Thickman K.R., Bianco P.R., Khan S.A., Leuba S.H. & Anand S.P. (2012). PcrA-mediated disruption of RecA nucleoprotein filaments – essential role of the ATPase activity of RecA. Nucleic Acids Research. 40: 8416–24.

Fairman-Williams M.E., Guenther U.P. & Jankowsky E. (2010). SF1 and SF2 helicases: family matters. Current Opinion in Structural Biology. 20: 313–24.

Fernández S. Ayora S. & Alonso J.C. (2000). *Bacillus subtilis* homologous recombination: genes and products. Research in Microbiology. 151(6): 481-6.

Fernandez S., Kobayashi Y., Ogasawara N. and Alonso J.C. (1999) Analysis of the *Bacillus subtilis recO* gene: RecO forms part of the RecFLOR function. Molecular and General Genetics. 261: 567-73.

Fernández S., Sorokin A. & Alonso J.C. (1988). Genetic recombination in *Bacillus subtilis* 168: effects of recU and recS mutations on DNA repair and homologous recombination. Journal of Bacteriology. 180: 3405–9.

Fu D., Calvo J.A. & Samson L.D. (2012). Balancing repair and tolerance of DNA damage caused by alkylating agents. Nature Reviews Cancer. 12: 104–20.

Gabbai C.B. & Marians K.J. (2010) Recruitment to stalled replication forks of the PriA DNA helicase and replisome-loading activities is essential for survival, DNA Repair. 9: 202–9.

Gándara, C. & Alonso, J.C. (2015). DisA and c-di-AMP act at the intersection between DNA-damage response and stress homeostasis in exponentially growing Bacillus subtilis cells. DNA repair. 27: 1-8

Gándara C., de Lucena D.K.C., Torres R., Serrano E., Altenburger S., Graumann P.L. & Alonso J.C. (2017) Activity and *in vivo* dynamics of *Bacillus subtilis* DisA are affected by RadA/Sms and by Holliday junction-processing proteins. DNA repair. 55: 17-30.

Gilhooly N.S., Gwynn E.J. & Dillingham M.S. (2013). Superfamily 1 helicases. Frontiers of Biosciences (Scholar Edition). 5:206–16.

Griffith K.L. & Grossman A.D. (2008). Inducible protein degradation in *Bacillus subtilis* using heterologous peptide tags and adaptor proteins to target substrates to the protease ClpXP. Molecular Microbiology. 70: 1012–25.

Gupta M.K., Guy C.P., Yeeles J.T., Atkinson J., Bell H., Lloyd R.G., Marians K.J. & McGlynn P. (2013) Protein-DNA complexes are the primary sources of replication fork pausing in Escherichia coli. Proceedings of the National Academy of Sciences of the United States of America. 110: 7252–7.

Guy C.P., Atkinson J., Gupta M.K., Mahdi A.A., Gwynn E.J., Rudolph C.J., Moon P.B., van Knippenberg I.C., Cadman C.J., Dillingham M.S., Lloyd R.G. & McGlynn P. (2009) Rep provides a second motor at the replisome to promote duplication of protein-bound DNA. Molecular Cell. 36: 654-66.

Gwynn E.J., Smith A.J., Guy C.P., Savery N.J., McGlynn P. & Dillingham M.S. (2013) The conserved C-terminus of the PcrA/UvrD helicase interacts directly with RNA polymerase. PLOS One. 8: e78141.

Jameson K.H. & Wilkinson A.J. (2017). Control of initiation of DNA replication in *Bacillus subtilis* and *Escherichia coli*. Genes. 8(22): doi:10.3390.

Kawabe Y.I., Branzeit D., Hayashi T., Suzuki H., Masuko T., Onoda F., Heo S.J., Ikeda H., Shimamoto A., Furuichi Y., Seki M. & Enomoto T. (2001). A novel protein interacts with the Werner's Syndrome gene product physically and functionally. The Journal of Biological Chemistry. 276(23): 20364-9.

Keiler K.C., Waller P.R. & Sauer R.T. (1996). Role of a peptide tagging system in degradation of proteins synthesized from damaged messenger RNA. Science. 271: 990–3.

Kidane D., Carrasco B., Manfredi C., Rothmaier K., Ayora S., Tadesse S., Alonso J.C. & Graumann P.L. (2009) Evidence for different pathways during horizontal gene transfer in competetent *Bacillus subtilis*. PLOS Genetics. 5(9): e1000630.

Kidane D. & Graumann P.L. (2005). Dynamic formation of RecA filament at DNA double strand break repair centers in live cells. The Journal of Cell Biology. 357-66.

Kidane D., Sanchez H., Alonso J.C. & Graumann P.L. (2004). Visualization of DNA double-strand break repair in live bacteria reveals dynamic recruitment of *Bacillus subtilis* RecF, RecO and RecN protein to distinct sites on the nucleoids. Molecular Microbiology. 52(6): 1627-1639.

Kleine Borgman L.A.K., Ries J., Ewers H., Ulbrich M.H. & Graumann P.L. (2013). The bacterial SMC complex displays two distinct modes of interaction with the chromosome. Cell Reports. 3(5) 1483-92.

Kuong K.J. & Kuzminov A. (2010). Stalled replication fork repair and misrepair during thymineless death in *Escherichia coli*. Genes Cells. 15 (6): 619-34.

Kuzminov A. & Stahl F.W. (1999) Double-strand end repair via the RecBC pathway in *Escherichia coli* primes DNA replication. Genes and Development. 13(3): 345-56.

Lau I.F., Filipe S.R., Søballe B., Økstad O.A., Barre F.X. & Sherrat D.J. (2003). Spatial and temporal organization of replication *Escherichia coli* chromosomes. Molecular Microbiology. 49(3): 731-43.

Lecointe F., Serena C., Velten M., Costes A., McGovern S., Meile J.C., Errington J., Ehrlich S.D., Noirot P. & Polard P. (2007). Anticipating chromosomal replication fork arrest: SSB targets repair DNA helicases to active forks. EMBO Journal. 26: 4239–51.

Lenhart J.S., Brandes E.R., Schroeder J.W., Sorenson R.J., Showalter H.D & Simmons L.A. (2014). RecO and RecR are necessary for RecA loading in response to DNA damage and replication fork stress. Journal of Bacteriology. 196(15): 2851-60.

Lenhart J.S, Schroeder J.W., Walsh B.W. & Simmons L.A. (2012). DNA repair and genome manteinance in *Bacillus subtilis*. Microbiology and Molecular Biology Reviews. 76(3): 530-64.

Lestini R. & Michel B. (2007). UvrD control the access of recombination proteins to blocked replication forks. The EMBO Journal. 26(16): 3804-14.

Luise A., Borgman K., Ries J., Ewers H., Ulbrich M.H. & Graumann P.L. (2013). The bacterial SMC complex displays two distinct modes of interaction with the chromosome. Cell Reports. 3(5): 1483-92.

Lusetti S.L., Hobbs M.D., Stohl E.A., Chitteni-Pattu S., Inman R.B., Seifert H.S. & Cox M.M. (2006) The RecF protein antagonizes RecX function *via* direct interaction. Molecular Cell. 21(1): 41-50.

Magner D.B., Blankschien M.D., Lee J.A., Pennington J.M., Lupski J.R. & Rosenberg S.M. (2007) RecQ promotes toxic recombination in cells lacking recombination intermediate-removal proteins. Molecular Cell. 26: 273–86.

McGregor N., Ayora S., Sedelnikova S., Carrasco B., Alonso J.C., Thaw P. & Rafferty J. (2005). The structure of *Bacillus subtilis* RecU Holliday junction resolvase and its role in substrate selection and sequence-specific cleavage. Structural Biology. 13 1341–51.

Meile J.C., Wu L.J., Ehrlich S.D., Errington J. & Noirot P. (2006). Systematic localisation of proteins fused to the green fluorescent protein in *Bacillus subtilis*: identification of new proteins at the DNA replication factory. Proteomics. 6: 2135-46.

Merrikh C.N., Brewer B.J. & Merrikh H. (2015). The *B. subtilis* accessory helicase PcrA facilitates DNA replication through transcription units. PLOS Genetics. 11: e1005289.

Merrikh H., Zhang Y., Grossman A.D. & Wang J.D. (2012). Replication-transcription conflicts in bacteria. Nature Reviews. 10: 449-58.

Michel B., Flores M.J., Viguera E., Grompone G., Seigneur M. & Bidnenko V. (2001). Rescue of arrested replication forks by homologous recombination. Proceedings of the National Academy of Sciences of the United States of America. 98: 8181–8.

Michel B. & Sandler S.J. (2017). Replication restart in Bacteria. Journal of Bacteriology. 199(13): e00102-17.

Migocki M.D., Lewis P.J., Wake R.G. & Harry E.J. The midcell replication factory in *Bacillus subtilis* is highly mobile: implications for coordinating chromosome replication with other cell cycle events. Molecular Microbiology, 2004. 54(2): 452-63.

Mirkin E.V. & Mirkin S.M. (2007). Replication fork stalling at natural impediments, Microbioly and Molecular Biology Reviews. 71: 13–35.

Page A.N., George N.P., Marceau A.H., Cox M.M. & Keck J.L. (2011). Structure and biochemical activities of *Escherichia coli* MgsA The Journal of Biological Chemistry 2011. 286(14) 12075-85.

Park J., Myong S., Niedziela-Majka A., Lee K.S., Yu J., Lohman T.M. & Ha T. (2010). PcrA helicase dismantles RecA filaments by reeling in DNA in uniform steps. Cell. 142: 544–55.

Persky N.S. & Lovett S.T. (2008). Mechanisms of recombination: lessons from *E. coli*. Critical Reviews in Biochemistry and Molecular Biology. 43: 347–70.

Peters J.M., Colavin A., Shi H., Czarny T.L., Larson M.H., Wong S., Hawkins J.S., Lu C.H., Koo B.M., Marta E., Shiver A.L., Whitehead E.H., Weissman J.S., Brown E.D., Qi L.S., Huang K.C. & Gross C.A. (2016). A comprehensive, CRISPR-based functional analysis of essential genes in bacteria. Cell. 165: 1493–506.

Petit M.A., Dervyn E., Rose M., Entian K.-D., McGovern S., Ehrlich S.D. & Bruand C. (1998). PcrA is an essential DNA helicase of *Bacillus subtilis* fulfilling functions both in repair and rolling-circle replication. Molecular Microbiology. 29(1): 261-73.

Petit M.A. & Ehrlich D. (2002). Essential bacterial helicases that counteract the toxicity of recombination proteins. The EMBO Journal. 21(12): 3137-47.

Plank M., Wadhams G.H. & Leake M.C. (2009). Miliseconds timescale slimfield imaging and automated quantification of single fluorescent protein molecules for use in probing complex biological processes. Integrative Biology. 1: 602-12.

Polard P., Marsin S., McGovern S., Velten M., Wigley D.B., Ehrlich S.D. & Bruand C. (2002). Restart of DNA replication in Gram-positive bacteria: a functional characterisation of the *Bacillus subtilis* PriA initiator. Nucleic Acid Research. 30: 1593-605.

Prise K.M., Davies S. & Michael B.D. (1989). Cell killing and DNA damage in Chinese hamster V79 cells. International Journal of Radiation Biology. 55(4): 583-92.

Pyle A.M. (2008) Translocation and unwinding mechanism of RNA and DNA helicases. Annual Reviews in Biophysics. 37: 317-36.

Ragone S., Maman J.D., Furnham N. & Pellegrini L. (2008). Structural basis for inhibition of homologous recombination by the RecX protein. The EMBO Journal. 27(16): 2259-69.

Reardon J.T. & Sancar A. Nucleotide excision repair. (2005) Progress in Nucleic Acid Research and Molecular Biology. 79: 183–235.

Renzette N., Gumlaw N., Nordman J.T., Krieger M., Yeh S.-P., Long E., Centore R., Boonsombat R. & Sandler S.J. (2005) Localization of RecA in *Escherichia coli* K-12 using RecA-GFP. Molecular Microbiology. 57(4): 1074-85.

Rudolph C.J., Upton A.L. & Lloyd R.G. (2008). Maintaining replication fork integrity in UV-irradiated *Escherichia coli* cells. DNA repair. 7: 1589-602.

Saikrishnan K., Powell B., Cook N.J., Webb M.R. & Wigley D.B. (2009). Mechanistic basis of 5'-3' translocation in SF1 B helicases. Cell. 137: 849–59.

Sanchez H., Carrasco B., Ayora S. & Alonso J.C. (2007-A) Homologous recombination in low dC + dG Gram-positive bacteria. Springer Berlin/Heidelberg, Berlin, Heidelberg.

Sanchez H., Carraco B., Cozar M.C. & Alonso J.C. (2007-B). *Bacillus subtilis* RecG branch migration is required for DNA repair and chromosomal seggregation. Molecular Microbiology. 65: 920-35.

Sanchez H., Kidane D., CozarM.C., Graumann P.L. & Alonso J.C. (2007-C) Recruitment of *Bacillus subtilis* RecN to DNA double strand breaks in the absence of DNA end processing. Journal of Bacteriology 2006. 188: 353-60.

Sanchez H., Kidane D., Cozar M.C., Graumann P.L. & Alonso J.C. (2006) Recruitment of *Bacillus subtilis* RecA to DNA double strand breaks in absence of DNA end processing. Journal of Bacteriology. 188: 353-60.

Sanchez H., Kidane D., Reed P., Curtis F.A., Cozar M.C., Graumann P.L, Sharples G.J. & Alonso J.C. (2005). The RuvAB branch migration translocase and RecU

Holliday junction resolvase are required for double-stranded DNA break repair in *Bacillus subtilis*. Genetics. 171: 873-83.

Sanders G.M., Dallman H.G., McHenry C.S. (2010). Reconstitution of the *Bacillus subtilis* replisome with 13 proteins including two distinct replicases. Molecular Cell. 37(2): 273-81.

Sedgwick B. Repairing DNA-methylation damage (2004). Nature Reviews. Moleculerr and Cell Biology. 5: 148–57.

Seigneur M., Bidnenko V., Ehrlich S.D. & Michel B. (1998). RuvAB acts at arrested replication forks. Cell. 95: 419–30.

Seigneur M., Ehrlich S.D. & Michel B. (2000). RuvABC-dependent double-strand breaks in dnaBts mutants require RecA. Molecular Microbiology. 38(3): 565-74.

Septenville A.L., Duigou S., Boubakri H. & Michel B. (2012) Replication fork reversal after replication-transcription collision. PLOS Genetics.8(4): e1002622.

Servinsky M.D. & Julin D.A. (2007). Effect of a recD mutation on DNA damage resistance and transformation in *Deinococcus radiodurans*. Journal of Bacteriology. 189: 5101–7.

Sherrat D., Søballe B., Barre F.X., Filipe S.R., Lau I., Massey T. & Yates J. (2004). Recombination and chromosome segregation. Philosophical transactions of the Royal Society of London. Series B, Biological sciences. 359: 61-9.

Shibata T., Hishida T., Kubota Y., Han Y.W., Iwasaki H. & Shinagawa H. (2005). Functional overlap between RecA and MgsA (RarA) in the rescue of stalled replication forks in Escherichia coli. Genes to Cells. 10: 181-91.

Simmons L.A., Goranov A.I., Kobayashi H. Davies B.W., Yuan D.S., Grossman A.D. & Walker G.C. (2009) Comparison responses to double-strand breaks between *Escherichia coli* and *Bacillus subtilis* reveals different requirements for SOS induction. Journal of bacteriology. 191(4): 1152-61.

Simmons L.A., Grossman A.D. & Walker G.C. (2006). Replication is required for the RecA localization response to DNA damage in *Bacillus subtilis*. PNAS. 104(4): 1360-5.

Singleton M.R., Dillingham M.S. & Wigley D.B. (2007). Structure and mechanism of helicases and nucleic acid translocases. Annual Review of Biochemistry. 76: 23–50.

Smits W.K., Goranov A.I. & Grossman A.D. (2010) Ordered association of helicase loader proteins with the *Bacillus subtilis* origin of replication in vivo. Molecular Microbiology. 75(2): 452-61.

Soultanas P. (2002). A functional interaction between the putative primosomal protein DnaI and the main replicative DNA helicase DnaB in *Bacillus*. Nucleic Acids Research. 30: 966-74.

Stanage T.H., Page A.N., Cox M.N. (2017). DNA flap creation by RarA/MgsA protein of *Escherichia coli*. Nucleic Acid Research. 45(5): 2724-35.

Suzuki Y., Endo M., Canas C., Ayora S., Alonso J.C., Sugiyama H. & Takeyasu K. (2014). Direct analysis of Holliday junction resolving enzyme in a DNA origami nanostructure. Nucleic Acids Research. 42: 7421–8.

Thickman K., Bianco P.R. & Anand S.P. (2002). PcrA-mediated disruption nucleoprotein filaments- essential role of the ATPase activity of RecA. Nucleic Acid Research. 40(17): 8416-24.

Torres R., Romero H., Rodríguez-Cerrato V. & Alonso J.C. (2017). Interplay between *Bacillus subtilis* RecD2 and the RecG or RuvAB helicase in recombinational repair. DNA repair. 55: 40-6.

Uphoff S. & Sherrat D. (2017). Single-molecule analysis of bacterial DNA repair and mutagenesis. Annual Review of Biophysics. 46: 411-32

Veaute X., Delmas S., Selva M., Jeusset J., Le Cam E., Matic I., Fabre F. & Petit M.A. (2005). UvrD helicase unlike Rep helicase, dismantles RecA nucleoprotein filaments in Escherichia coli. EMBO Journal. 24: 180–9.

Velten M., McGovern S., Marin S., Ehrlich S.D., Noirot P. & Polard P. (2003). A two-protein strategy for the functional loading of a cellular replicative DNA-helicase. Molecular Cell. 11: 1009-20.

Vlasic I., Mertens R., Seco E.M., Carrasco B., Ayora S., Reitz G., Commichau F.M., Alonso J.C. & Moeller R. (2014). *Bacillus subtilis* RecA and its accessory factors, RecF RecO, RecR and RecX, are required for spore resistance to DNA double-strand break. Nucleic Acids Research 2014. 42: 2295–307.

Voloshin O.N. & Camerini-Otero R.D. (2007). The DinG protein from Escherichia coli is a structure-specific helicase. Journal of Biological Chemistry. 282: 18437–47.

Walsh B.W., Bolz S.A., Wessel S.R., Schroeder J.W., Keck J.L. & Simmons L.A. (2014). RecD2 helicase limits replication fork stress in *Bacillus subtilis*. Journal of Bacteriology. 196(7): 1359-68.

Wang J. & Julin D.A. (2004). DNA helicase activity of the RecD protein from *Deinococcus radiodurans*. Journal of Biological Chemistry. 279: 52024–32.

West S.C. (1997). Processing of recombination intermediates by the RuvABC proteins. Annual Review Genetics. 31: 213-44.

Wiedermannova J., Sudzinova P., Koval T., Rabatinova A., Sanderova H., Ramaniuk O., Rittich S., Dohnalek J., Fu Z., Halada P., Lewis P. & Krasny L. (2014). Characterization of HelD, an interacting partner of RNA polymerase from *Bacillus subtilis*. Nucleic Acids Research. 42: 5151–63.

Wu L. & Hickson I.D. (2006). DNA helicases required for homologous recombination and repair of damaged replication forks. Annual Review of Genetics. 40: 279–306.

Yadav T., Carrasco B., Myers A.R., George N.P., Keck J.L. & Alonso J.C. (2012). Genetic recombination in *Bacillus subtilis*: a division of labor between two single-strand DNA-binding proteins. Nucleic Acid Research. 40(12): 5546-59.

Yang H., Yung M., Sikavi C. & Miller J.H. (2011). The role of Bacillus anthracis RecD2 helicase in DNA mismatch repair. DNA Repair. 10: 1121–30.

Yasbin R.E., Fields P.I. & Anderson B.J. (1980). Properties of *Bacillus subtilis* derivates freed of their natural prophages. Gene. 12: 155-9.

Yeeles J.T.P & Dillingham M.S. (2010). The processing of double-stranded DNA breaks for recombiantional repair by helicase-nuclease complexes. DNA repair 9: 276-85.

Zhang W. Carneiro M.J., Turner I.J., Allen S., Roberts C.J. & Soultanas P. (2005). The *Bacillus subtilis* DnaD and DnaB proteins exhibit differents DNA remodelling activities. Journal of Molecular Biology. 351: 66-75.

VII. ACKNOWLEDGEMENTS

In every thesis, there are three major factors to consider for a successful experience: a motivational project, a good supervision and funding. In my case, these three factors have become somehow complicated due to the difficult situation in Spain concerning Science, but everything has finally come to a happy end. Because of this, I am very grateful with Juan Carlos Alonso, that was betting on me even in the difficult situation after being rejected in several fellowships and supported me in the very beginning, by giving me this challenging project: characterizing two unknown proteins starting from almost zero; and with Peter Graumann for recruiting me and my project in his lab and demonstrate with his supervision and tips his interest on it. They both have been shown as great supervisors and their knowledge has been a key factor to go through the multiple challenges presented during this work. Then, I am extremely grateful to the FUNDACIÓN MUTUA MADRILEÑA, and its Becas de Posgrado program, for giving me, and many other people, the opportunity to go on in a research career with their fellowships, and especially for the treatment I have received from all the staff and their invaluable help before, during and after the adjudication of the fellowship, with a special mention to Mónica.

In this moment is important to mention that this thesis would not be possible without the support of my family, in special my parents, even when they were 2,000 km from me, and the new family that I have become during my stay in Germany, my wife and my son, for understanding and supporting me in the stressful and difficult moments.

Getting used to work in a new lab, using novel techniques, is a difficult work. I want to appreciate the laboratory team work in both CNB and SYNMIKRO.

En el CNB, quiero agradecer a Chiara Marchisone por enseñarme a dar los primeros pasos en el laboratorio, y por la gran paciencia y dedicación que ha supuesto ayudarme con el *cloning* de todas mis cepas. A Begoña Carrasco, por su dedicación, esfuerzo y sabiduría en la pelea con la larga e infructuosa purificación de RecD2, pero sobre todo por su contagiosa alegría y buen humor. A Carolina Gándara, que allanó el complicado terreno de las pruebas de viabilidad y estaba siempre dispuesta a ayudar en momentos complicados. A Rubén Torres y Mariangela Tabone. Y, finalmente, a Esther Serrano, que ha sido más una amiga que una compañera, por su

gran capacidad para escuchar y su dedicación a la hora de ayudar en los momentos más difíciles.

From SYNMIKRO, I would like to appreciate the former members Felix Dempwolff and especially Stephan Altenburger, their patience and dedication to teach me almost all I know now about microscopes, and be there to help when something was not working; Mathilda Diel for her time and wise discussion; Jad el Andari for being there always for help; and Patty Bedrunka for being there all the time to talk, and helping me in the very difficult moments of writing the thesis. And, of course, the current team of Graummaners: to Julia, for her extremely important assistance not only in the lab but also to “fight” with German bureaucracy; to Daniela, for her great tips, discussions, and cloning experience; to Nina, for her disinterested help in every moment and situation; and all the rest for making every day different than the other. An dieser Stelle möchte ich die Labortechnikerinnen Frauke und Sabrina erwähnen und ihnen für ihre unendliche Geduld mit mir danken, die sie aufbrachten, um mein grässliches Deutsch zu verstehen und es zu verbessern.